1-1-2013

New Approach for Modeling Hybrid Pressure Swing Adsorption-Distillation Processes

Fan Wu
University of South Carolina

NEW APPROACH FOR MODELING HYBRID PRESSURE SWING ADSORPTION-DISTILLATION PROCESSES

by

Fan Wu

Bachelor of Science
Dalian University of Technology, 2008

Submitted in Partial Fulfillment of the Requirements

For the Degree of Doctor of Philosophy in

Chemical Engineering

College of Engineering and Computing

University of South Carolina

2013

Accepted by:

James Ritter, Major Professor

Armin Ebner, Committee Member

Edward Gatzke, Committee Member

John Weidner, Committee Member

Jamil Khan, Committee Member

Lacy Ford, Vice Provost and Dean of Graduate Studies

DEDICATION

To Xueqiang Wu and Yan Dong, my parents for their love and support.

ACKNOWLEDGEMENTS

I would like to express my deepest appreciation to my advisors Dr. Ritter and Dr. Ebner who has given me the opportunity to join their group and to do this wonderful project, also for the knowledge, technology and everything they have taught me and for their patient guidance and mentorship throughout the completion of this degree at University of South Carolina.

I would also like to thank my committee members, Dr. Edward Gatzke, Dr. John Weidner and Dr. Jamil Khan for taking time from their busy schedule to be my committee members and every piece of advice they have given to me during this PhD program including the comprehensive exam, pre-defense exam and final defense exam.

I would like to express my appreciation to Dr. Marjorie Nicholson for her help in the lab and being so nice to me, also Charles Holland for his genius in building experiment systems. I want to acknowledge all present and prior classmates in the research group, Dr. Jan Mangual, Dr. Hai Du, Dr. Amal Mehrotra, Dr. Shubhra Bhadra, Dongxiang Yang, Mohammad Iftekhar Hossain, Anahita Abdollahi, Lutfi Erden, Hanife Erden, Atikur Rahman and Nima Mohammadi for their support and inspiration.

In addition, I would like to appreciate all my friends who have made my life at University of South Carolina filled with happiness. A special thanks goes to my cat

Sesame who has been an alarm clock to wake me up early in the morning and messed up my bedroom with his claws.

Especially, I want to thank my parents, Xueqiang Wu and Yan Dong, for their love and support during my five-year studying aboard. I want to apologize to them for being so away from them for so many years and for not carrying out the obligation as a daughter of them.

Finally, I want to appreciate the funding provided by ExxonMobil and Process Science and Technology Center who has made this dissertation possible.

ABSTRACT

A new methodology for modeling hybrid pressure swing adsorption (PSA)-distillation processes has been developed. Two hybrid systems were simulated as examples. One is for ethanol dehydration, and the other is for propane/propylene separation. Firstly, a distillation process simulator such as Chemsep was used to simulate the distillation process of the hybrid system, in which the PSA unit was treated as a "black box" with an assumed process performance. In this way, a hybrid PSA-distillation process can be analyzed simply by performing mass balances around these units and running Chemsep to determine the possibility of energy saving compared to a reference (commercial) process. Once an energy saving hybrid "black box" PSA-distillation process was found, a rigorous PSA process simulator was used to simulate a "actual" PSA process by designing the operating conditions, cycle scheduling, etc. Then the distillation process was simulated again with the "actual" PSA performance to calculate the distillation operating cost, followed by calculating the total operating cost of the whole hybrid process. According to the results in this dissertation, significant cost saving could be achieved compared with the traditional processes.

The commercial hybrid PSA-distillation uses a simple 2-bed 4-step PSA cycle. It

is surmised that the PSA performance can be improved by designing a more complicated PSA cycle with more beds and steps. In this work, four different PSA cycles were designed and simulated using the dynamic adsorption process simulator (DAPS). The performances of these cycles were put back into the hybrid system to calculate all the costs and compare the results with the 2-bed 4-step commercial hybrid PSA-distillation process. The total operating could be reduced significantly and the distillation capacity could also be increased.

For propane/propylene separation, more energy efficient configurations were designed to compete with the traditional simple distillation process which is a large energy consumer. A hypothetical adsorbent was conceived that has all the desirable and none of the undesirable properties of the commercial adsorbents already tested for this separation. Several PSA cycles configurations that utilize this hypothetical adsorbent under different operating conditions have been investigated via simulation. The results show that a hybrid PSA-distillation process is able to achieve significant energy saving compared to the traditional distillation process.

TABLE OF CONTENTS

LIST OF TABLES

LIST OF FIGURES

LIST OF SYMBOLS

B	flow rate of the bottom product stream from the still (kmol s^{-1})
b	affinity (kPa^{-1})
b_0	affinity (kPa^{-1})
C_1	compressor
C_2	vacuum pump
C_P	thermal capacity of adsorbent (kJ kg^{-1} K^{-1})
C_P^E	constant pressure heat capacity of ethanol (kJ mol^{-1} K^{-1})
C_P^W	constant pressure heat capacity of water (kJ mol^{-1} K^{-1})
C_W	thermal capacity of the wall (kJ kg^{-1} K^{-1})
D	flow rate of the distillate (kmol s^{-1})
D_c	crystal diffusivity (m^2 s^{-1})
D_c^0	limiting diffusivity (m^2 s^{-1})
E_o	distillation column stage efficiency
E_a	activation energy (kJ mol^{-1})
F	flow rate of the feed to the still (kmol s^{-1})
F_1	flow rate of the feed to PSA I of the dual train PSA system (SLPM)

F_2 flow rate of the feed to PSA II of the dual train PSA system (SLPM)

F_F the feed flow rate in feed step of PSA (SLPM)

F_{LR} the feed flow rate in light relux of PSA (SLPM)

F_{PSA} flow rate of the feed to PSA (SLPM)

F_{water} amount of water needs to be removed in PSA process (SLPM)

h heat transfer coefficient (kW m^{-2} K^{-1})

ΔH isosteric heat of adsorption (kJ mol^{-1})

HP flow rate of the heavy product stream from PSA (kmol s^{-1})

ΔH_{vap}^{E} phase change enthalpy of ethanol (kJ mol^{-1})

ΔH_{vap}^{W} phase change enthalpy of water (kJ mol^{-1})

k mass transfer coefficient (s^{-1})

k_{LDF}^{E} ethanol LDF mass transfer resistance (s^{-1})

k_{LDF}^{W} water LDF mass transfer resistance (s^{-1})

L_1 flow rate of partial condenser recycle stream (kmol s^{-1})

L_1 flow rate of partial condenser recycle stream (kmol s^{-1})

LP flow rate of the light product stream (kmol s^{-1})

$\dot{n}$ flow rate of a stream (kmol s^{-1})

n equilibrium amount adsorbed in Toth model (mol kg^{-1})

n_0 Toth parameter

n_s saturated loading in Toth model (mol kg^{-1})

n_t Toth parameter (K)

P flow rate of the light product stream from PSA (kmol s^{-1}) or pressure (kPa)

P_C distillation column pressure (kPa)

P_{CoD} end pressure in concurrent depressurization step of PSA (kPa)

P_e purity of ethanol in the light product from PSA

P_H high pressure in PSA or high pressure for compressor duty calculation (kPa)

P_L low pressure in PSA or low pressure for compressor duty calculation (kPa)

P_M intermediate pressure in equalization step of PSA (kPa)

P_{LPP} pressure in the light product pressurization step of PSA (kPa)

P_w purity of water in the heavy product from PSA

Q_C compressor or vacuum duty (kJ s^{-1})

Q_{DH} distillate heater duty (kJ s^{-1})

Q_{SC1} duty of side stream condenser due to temperature change in gas phase (kJ s^{-1})

Q_{SC2} duty of side stream condenser due to phase change (kJ s^{-1})

q equilibrium loading (mol kg^{-1})

q_B bottom product quality

q_D distillate quality

q_F still feed quality

q_{HP} PSA heavy product quality

q_{LP} PSA light product quality

q_P PSA light product quality

q_S side stream quality

q_s saturation loading (mol kg^{-1})

q_{s0} adsorption isotherm parameter (mol kg^{-1})

q_{st} adsorption isotherm parameter (K^{-1})

R universal gas constant (kPa m^3 mol^{-1} K^{-1})

R_P^E recovery of ethanol in the light product from PSA

R_S^W recovery of water in the side stream (heavy product) from PSA

R_e recovery of ethanol in the light product from PSA

R_H recovery of water from PSA

R_L propane recovery in PSA

R_w recovery of water in the side stream (heavy product) from the PSA unit

r_c crystal radius (m)

r_i inner bed radius (m)

r_o bed outer radius (m)

r_p adsorbent radius (m)

S flow rate of the side stream from the PSA unit to the still (kmol s^{-1})

T temperature (K)

T_B temperature of the bottom product (K)

T_D temperature of the distillate (K)

T_F temperature of the feed to the still (K)

T_{HP} temperature of the heavy product stream from PSA (K)

T_{LP} temperature of the light product stream from PSA (K)

T_{PSA} feed temperature of the PSA unit (K)

T_{TF} temperature of the tray receiving the feed (K)

T_{TS} temperature of the tray receiving the side stream from the PSA unit (K)

T_w temperature of the wall (K)

T^* T_{TF} or T_{TS}

t Toth parameter

t_0 Toth parameter

t_1 Toth parameter (K)

t_F step time of feed (s)

t_{LR} step time of light reflux

t_{cycle} total cycle time (s)

V_2 flow rate of the stream going into the partial condenser (kmol s^{-1})

V_{52} flow rate of the reboiler recycle stream (kmol s^{-1})

V_{bed} bed volume (m^3)

x_B mole fraction of ethanol or propylene in the bottom product stream from the still

x_F mole fraction of ethanol or propylene in the feed to the still

x_S mole fraction of ethanol in the side stream to the still

y_D mole fraction of ethanol or propylene in the distillate

y_{HP} mole fraction of propylene in the heavy product stream from PSA

y_{LP} mole fraction of propylene in the light product stream from PSA

y_P mole fraction of ethanol in the light product stream from PSA

y_S mole fraction of propylene in the heavy product stream from PSA

Z bed length (m)

Greek Letters

ε_b bed porosity

ε_p adsorbent porosity

γ isentropic constant

η compressor or vacuum pump efficiency

θ_F throughput of the F step

θ_F throughput of the feed step

θ_{LR} throughput of light reflux

ρ_p adsorbent density (kg m^{-3})

ρ_w wall density (kg m^{-3})

LIST OF ABBREVIATIONS

CnD ..... countercurrent depressurization

CoD ..... concurrent depressurization

DAPS ..... dynamic adsorption process simulator

DH ..... distillate heater

E ..... ethanol

EQ ..... equalization step

F ..... feed step

HP ..... heavy product

I ..... Idle step

LDF ..... linear driving force

LR ..... light reflux

LP ..... light product

LPP ..... light product pressurization

P ..... purity

PC ..... partial condenser

PSA ..... pressure swing adsorption

R ..... recovery

SC..... side stream condenser

SLPM ..... standard litter per minute

W.....water

CHAPTER 1: METHODOLOGY FOR MODELING HYBRID PSA-DISTILLATION PROCESSES WITH ETHANOL DEHYDRATION AS AN EXAMPLE

1.1 Summary

A new methodology for modeling hybrid pressure swing adsorption (PSA)-distillation processes has been developed. This new approach involves two parts. Part I determines if energy savings are possible. It can be done easily with sufficient knowledge of distillation process design, but with only minimal knowledge of PSA process design. Part I is carried out using a distillation process simulator like Chemsep™ to model a distillation column connected to a PSA unit that is treated as a "black box" with an assumed process performance. In this way, a hybrid PSA-distillation process can be analyzed simply by performing mass balances around these units and running Chemsep™ to determine if energy savings are possible compared to a reference (commercial) process. Once an energy savings hybrid "black box" PSA-distillation process is found in Part I, Part II determines if an "actual" PSA process exists that mimics its performance. Part II is carried out using a rigorous PSA process simulator like Adsim from AspenTech; thus, it requires significant knowledge of PSA process design. The outcome of Part II is a hybrid PSA-distillation process that has the potential to be more energy efficient than the reference process. This new approach was successfully

demonstrated using the commercial hybrid PSA-distillation process developed for fuel grade ethanol production as the reference case. This two-part analysis found several, more energy efficient designs than the reference case. All of them with proportionately reduced internal vapor and liquid flows in the distillation column, a direct effect of reducing condenser or reboiler duty. These results illustrated that the new methodology should be very useful for quickly accessing the utility of hybrid PSA-distillation processes for a variety of other applications, with many possibilities for achieving significant energy savings and/or throughput debottlenecking.

1.2 Introduction

The refining industry, both petroleum and chemical, is one of the largest consumers of energy in the United States.[1-3] It utilizes approximately 35% of the total energy used in manufacturing, with 60% of it in separations, almost entirely in distillation processes. To date there are about 40,000 distillation columns operating in over 200 processes.[4] In other words, a considerable fraction of the refining products, around 10%, are currently being burned to keep refineries moving (distillation columns operating), while producing enormous amounts of carbon dioxide. In fact, as far back as 20 years ago Humphrey et al.[5] reported that 2.4 quads (2,400 trillion Btu/yr) of energy were being consumed by distillation in the United States and it was growing. To make matters worse, the replacement of existing distillation columns with new technologies is not going to happen any time soon, because distillation is a simple and proven technology. So, it

appears that the only way to substantially reduce the current use of energy by distillation in the refining industry is through the use of hybrid separation processes.

Humphrey et al.[5] further stated that a distillation-adsorption hybrid system could save 16% of the energy consumed per installation, which corresponded to the United States saving 0.06 quads of energy per year (60 trillion Btu/yr) after 15 years. This energy savings also averts 5 to 10 trillion tons/yr of CO_2 when the reboiler and condenser duties come from steam produced from coal fired power plants. That was over 20 years ago. More recently the same relative numbers (but of course larger) were reported by Robinson and Jubin[6] in 2005, with hybrid separation systems again mentioned as a way to save tremendous amounts of energy.

If the implementation of hybrid processes can save so much energy, especially distillation-adsorption hybrid schemes, what has delayed there widespread implementation throughout the chemical and petrochemical industries? The answer to this question is simple but surprising. A major problem with the implementation of hybrid separation schemes is the paucity of information available for the design and development of integrated unit operations. This point was made very clearly by numerous separations engineers from the leading chemical and petrochemical companies at a 2005 U.S. Department of Energy workshop.[7]

Therefore, the objective of this work is to introduce a new, relatively simple, two part approach for modeling hybrid pressure swing adsorption (PSA)-distillation processes.

The first part utilizes readily available distillation process design software, like Chemsep™, to model a distillation column connected to a PSA unit that is treated as a "black box" with an assumed process performance. This part determines if energy savings are possible compared to a reference (commercial) process for different "black box" PSA process performances. If a hybrid PSA-distillation process is found in Part I that saves energy, Part II utilizes a rigorous PSA process simulator, like Adsim (AspenTech), to determine if an "actual" PSA process exists that mimics the performance of the best "black box" PSA process. This new approach is illustrated with the reference case based on the commercial hybrid PSA-distillation process developed for fuel grade ethanol production.[8]

1.3 Hybrid Process Concept

A hybrid process consists of two or more unit operations such as adsorption, membrane or distillation integrated in such a way that the performance of the process is better than either of its unit operations operating independently. Although the term "hybrid" has been widely used, it has not always been used properly. Sometimes it has been applied to processes that merely constitute a simple sequence of unit operations.[9-11] The difference between a hybrid process and a simple sequence of unit operations is illustrated in Figure 1.1.

In a simple sequence of unit operations, the performance of a unit operation located upstream is not influenced by the performance of a unit operation located

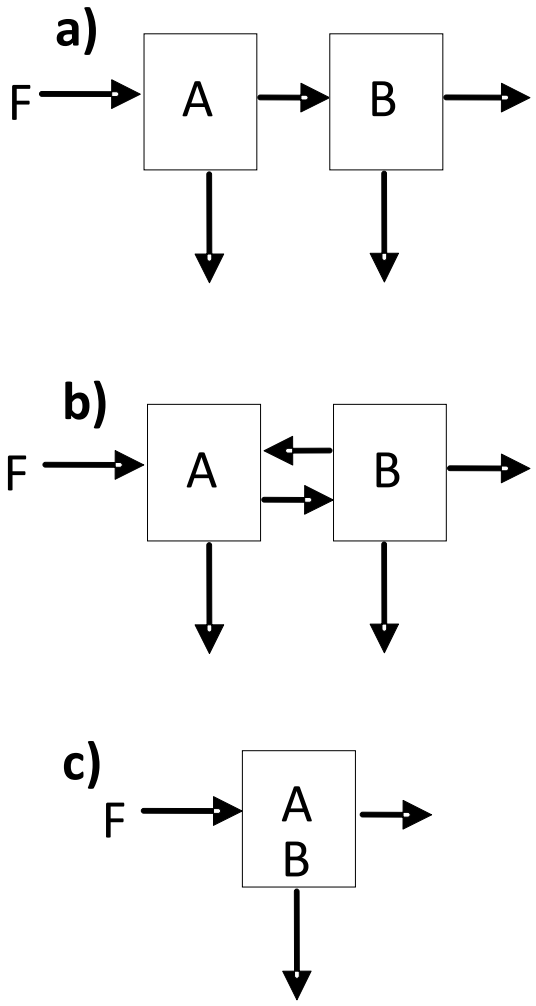

Figure 1.1 Depictions of a) a sequence of separations units, where the performance of B does not affect the performance of A (not a hybrid process); b) a sequence of separations units, where the performance of B does affect the performance of A (a hybrid process); c) the separations units, A and B, residing in the same vessel (a hybrid process).

downstream, as depicted in Figure 1.1a. In contrast, for a hybrid process the performance of any unit operation in the process is affected by the performance of any other unit operation in the process, as depicted in Figures 1.1b and 1.1c. In addition, a hybrid process may have its individual unit operations operating in separate units (Figure 1.1b) or in one unit (Figure 1.1c).

The hybrid process concept is not new and practically all combinations of distillation, membrane and adsorption hybrid processes can be found in the literature: distillation-membrane systems in multiple units,[10-24] with pervaporation[12-19] being the most well-known and already commercial; distillation-membrane systems in single units or membrane distillation;[25,26] distillation-adsorption systems (typically PSA) in multiple units,[27-37] with the separation of ethanol from water being commercial and popular in the corn industry;[27-30] distillation-adsorption systems (typically PSA) in a single unit or adsorptive distillation;[37-39] membrane-adsorption systems in multiple units;[40-42] and membrane-adsorption systems in a single unit, e.g., pressure swing permeation.[43,44]

1.4 Hybrid PSA-Distillation Process Configurations

Figure 1.2 shows a few examples of hybrid PSA-distillation process configurations with the PSA unit being fed with still end streams, depending on whether the feed is supplied to the still (Figure 1.2a to 1.2d) or the PSA unit (Figure 1.2e and 1.2f). For the case where the feed is supplied to the still, the hybrid processes vary depending on whether the PSA unit is located on the light product (Figure 1.2a and 1.2b) or heavy product (Figure

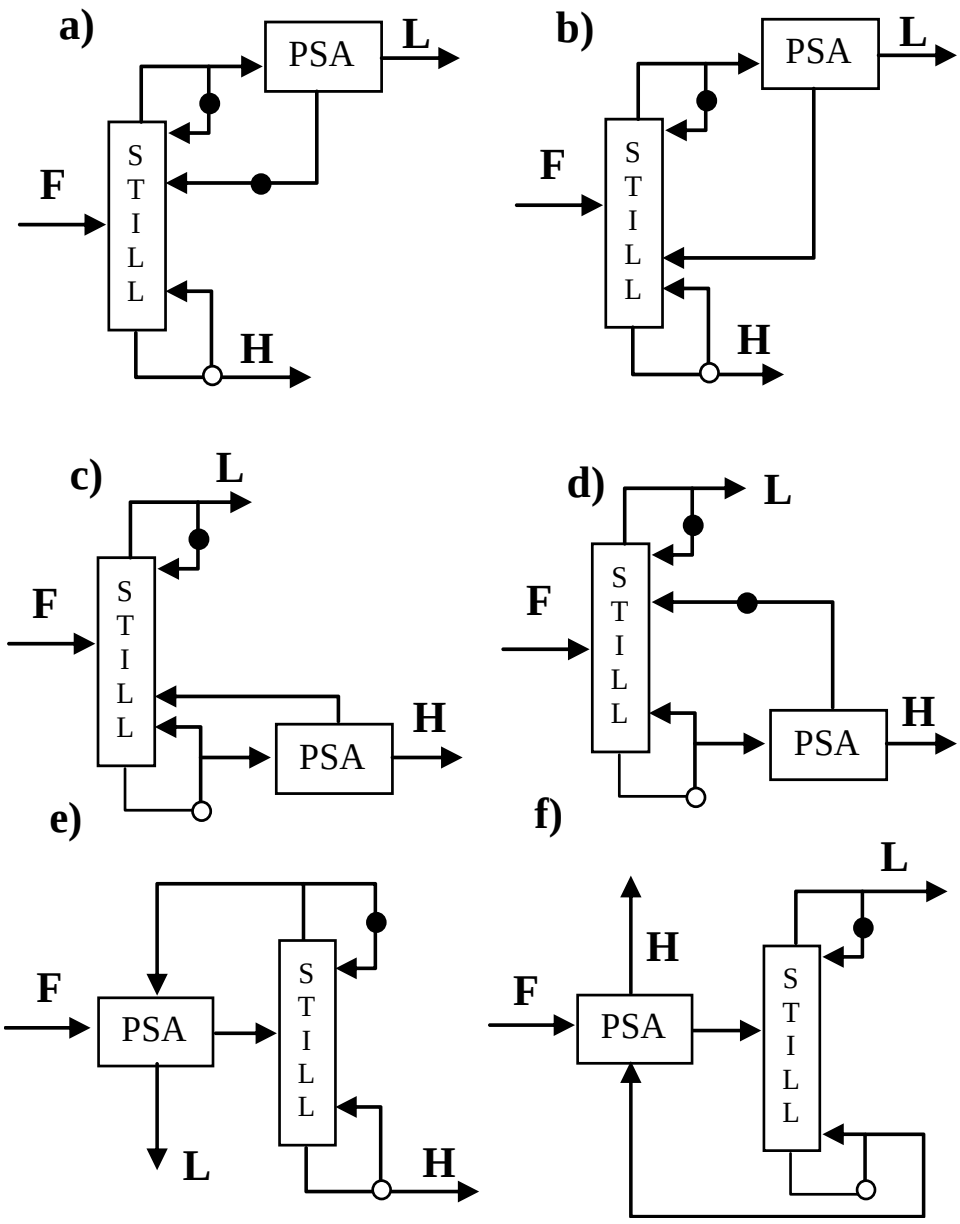

Figure 1.2 Different hybrid PSA-distillation configurations with the PSA unit fed with still end streams, depending on whether the feed is supplied to the still (a, b, c and d) or the PSA unit (e and f). F: feed; L: light product, H: heavy product; solid circles: condenser; open circles: reboiler.

1.2c and 1.2d) end of the still, or whether one of the PSA products is returned back to either the rectification (Figure 1.2a and 1.2d) or stripping (Figure 1.2b and 1.2c) section of the still. For the case where the feed is supplied to the PSA unit, the hybrid processes vary depending on whether the light (Figure 1.2e) or heavy (Figure 1.2f) product of the still is returned back to the PSA unit.

Figure 1.3 shows a few more examples of hybrid PSA-distillation process configurations with the PSA unit being fed with still side streams, depending on whether the feed is supplied to the still (Figure 1.3a to 1.3d) or the PSA unit (Figure 1.3e and 1.3f). For the case where the feed is supplied to the still, the hybrid processes vary depending on whether the PSA unit is located on the rectification side (Figure 1.3a and 1.3b) or stripping (Figure 1.3c and 1.3d) side of the still, or whether both (Figure 1.3a and 1.3c) or one (Figure 1.3b and 1.3d) PSA product stream is returned back to one side of the feed (Figure 1.3a and 1.3c). For the case where the feed is supplied to the PSA unit, the hybrid processes vary depending on whether a side stream from the rectification (Figure 1.3e) or stripping (Figure 1.3f) side of the still is returned back to the PSA unit.

There are many other possible hybrid PSA-distillation process configurations other than those shown in Figures 1.2 and 1.3. For example, in Figure 1.2a there is at least one other option for the origin of the light reflux stream going to the still. As an alternative to using the fraction split off from the light product stream of the still prior to the feed of the PSA unit, a fraction can be split off instead from the light product stream of the PSA unit.

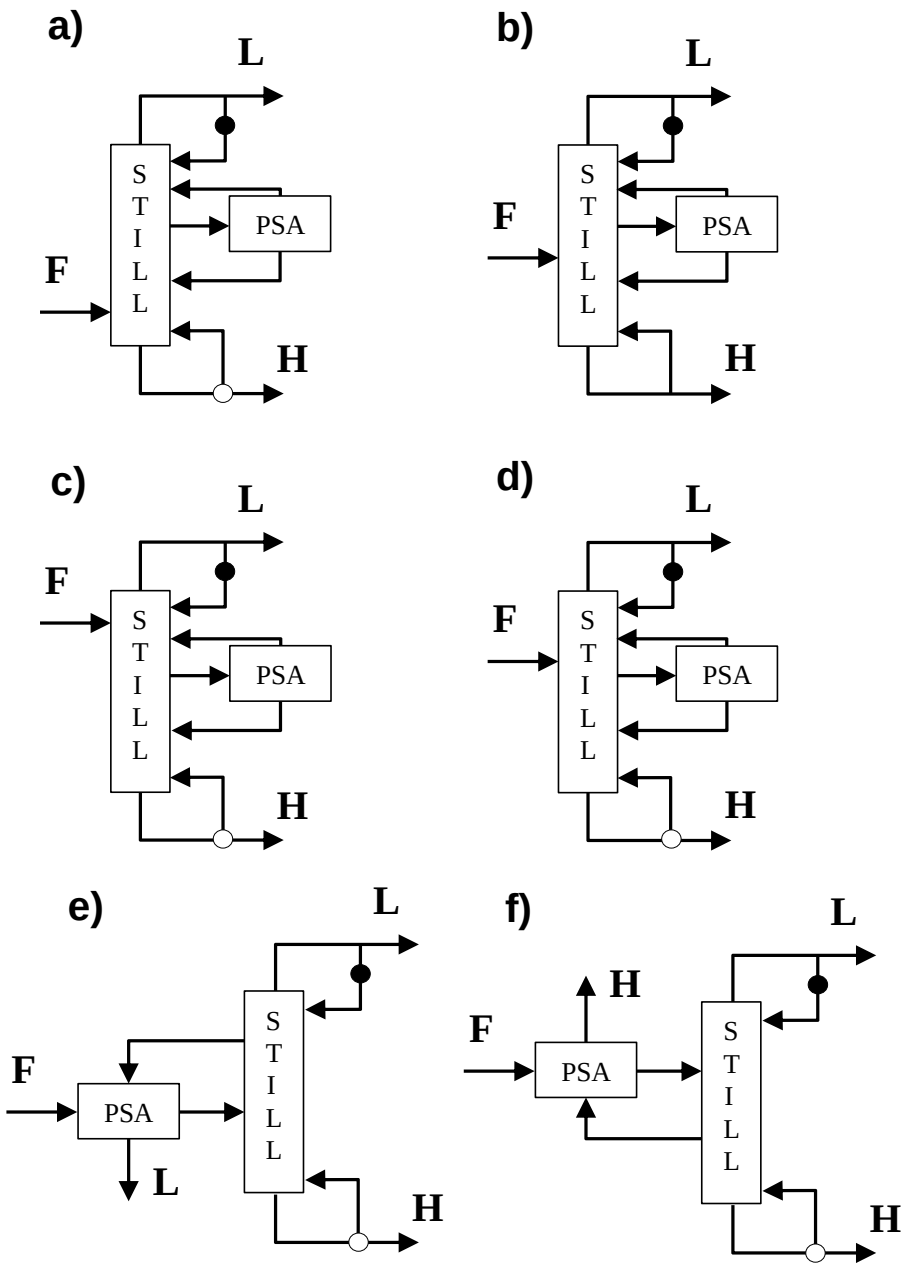

Figure 1.3 Different hybrid PSA-distillation configurations with the PSA unit fed with still side streams, depending on whether the feed is supplied to the still (a, b, c and d) or the PSA unit (e and f). F: feed; L: light product, H: heavy product; solid circles: condenser; open circles: reboiler.

Clearly, the number of configurations is seemingly endless.

1.5 Reference and New Hybrid PSA-Distillation Process Flow Sheets

First, a reference process must be selected for comparison with the new hybrid process. In this illustration, the reference process was the commercial hybrid PSA-distillation process for fuel grade ethanol production.[8] However, in general, it would simply be a non-hybrid, standalone, commercial, distillation process. The flow sheet for the reference hybrid PSA-distillation process is shown in Figure 1.4a.[8] The distillation column contains 50 stages plus a partial condenser, which is stage 1 and a reboiler, which is stage 52. A feed stream of saturated liquid (F) containing 40 mol% ethanol (x_F) is fed into stage 36. A 98.7 mol% ethanol stream leaves the PSA unit as the light product (y_P), and a 99.5 mol% water stream leaves the bottom of the distillation column as the bottoms product (1-x_B). The distillate contains 81.8 mol% ethanol (y_D). This stream is compressed, heated and sent to the PSA unit as feed. A 47.7 mol% ethanol stream (y_S) is produced in the PSA unit as the heavy product through a vacuum pump with a discharge pressure of essentially 1 atm (thus, the PSA unit experiences a pressure swing from super-atmospheric pressure to sub-atmospheric pressure). This side stream is then condensed and recycled to feed stage 36 in the distillation column. For scaling purposes all the flows are evaluated relative to the feed flow F, i.e., B/F, P/F, S/F, and D/F.

The flow sheet for the new hybrid PSA-distillation process is shown in Figure 1.4b. Again, the same distillation column feed (F and x_F) and the same products are

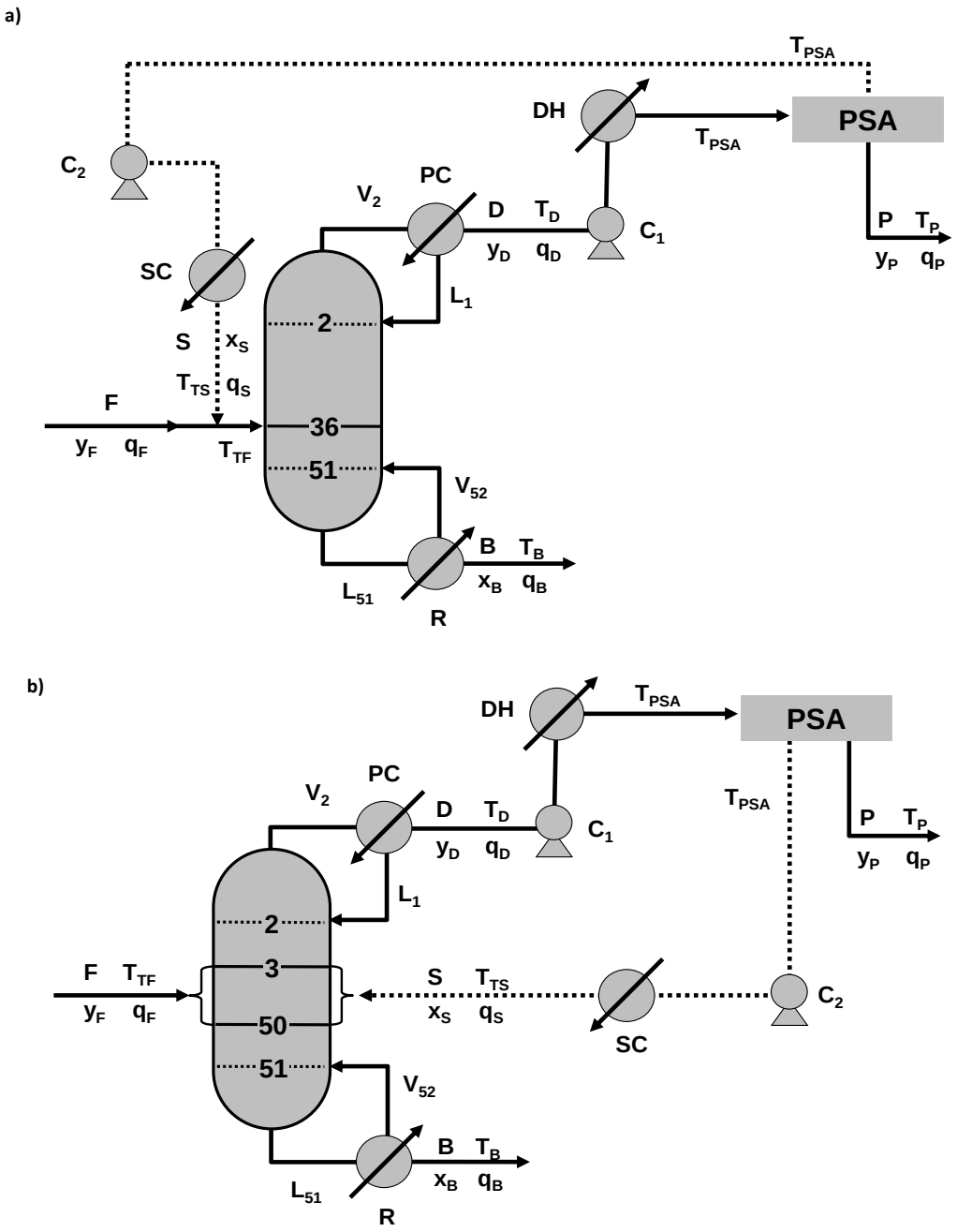

Figure 1.4 Hybrid PSA-distillation fuel grade ethanol production systems: a) commercial reference system,[8] with S and F both fed to still stage 36. (b) new system with S and F fed to different, optimum still stages anywhere between stages 2 and 51. F: still feed; P: light (ethanol) product from PSA unit; D: feed to PSA unit (still distillate); B: bottoms (water) product from still; S: side stream from PSA unit; PC: partial condenser; R: reboiler; SC: side stream total condenser; DH: distillate heater; C_1: compressor 1; C_2: vacuum pump 2.

produced from the light product of the PSA unit (P and y_P) and the bottoms product of the distillation column (B and x_B), i.e, F, x_F, B, x_B, P and y_P remain the same for both hybrid systems. The relative flow rate (S/F) and concentration of the side stream from the PSA unit to the still (x_S) are now considered variables with specified ranges. Moreover, the side stream is sent back to the optimum stage based on its flow rate and concentration, instead of the feed stage as in the reference case.

It is noteworthy that fixing F, x_F, B, x_B, P and y_P in both the reference and new cases creates an internal loop between the still and the PSA unit, resulting in S, x_S, D, y_D, and the still internal vapor and liquid flows as the only variables. A change in either S or x_S changes the distillate flow (D) or its concentration (y_D), as dictated by overall and component balances around the PSA unit. This necessarily produces changes in the internal vapor and liquid flows in the still. These changes are determined through mass balances around various units in the flow sheets, as illustrated below.

1.6 Simulation Approaches

1.6.1 Part I. Hybrid "Black Box" PSA-Chemsep™ Distillation

Part I utilized Chemsep™ to simulate the distillation process. However, any suitable distillation process simulator could be used for this purpose, e.g., like that available through AspenTech. The PSA unit was considered to be a "black box", with its performance defined either *a priori* as an input or determined by overall and component balances around it. This "black box" PSA approach greatly simplified the analysis by

reducing it to solving algebraic expressions in a spreadsheet and running Chemsep™. The overall approach allows those with significant distillation process design experience, but only minimal PSA process design experience, to carry out Part I. A simple algorithm delineating this Part I analysis is shown in Figure 1.5.

In short, for the reference hybrid process, mass balances were carried out algebraically around both the PSA and distillation units using information available for all the input and output streams. This determined all the flow rates and concentrations of the streams around the distillation unit. With these flow rates and concentrations known, and with the number of trays and feed tray location specified, Chemsep™ was run. The output from Chemsep™ was the flow rates and concentrations of the internal vapor and liquid streams in the still, the temperatures of the distillate and feed tray, as well as the energy duties of the reboiler and partial condenser. Finally, the energy duties incurred by the PSA feed compressor, PSA vacuum pump, and heaters external to the still were calculated.

For the new hybrid process, the analysis was carried out essentially in the same manner, except for the flow rate and concentration of the side stream from the "black box" PSA unit into the still now being defined and the optimum tray locations of both the feed and side streams being determined. These optimum tray locations were determined by minimizing the condenser and reboiler duties via Chemsep™ for each set of assumed "black box" PSA process conditions and performance. In addition, the temperature of the

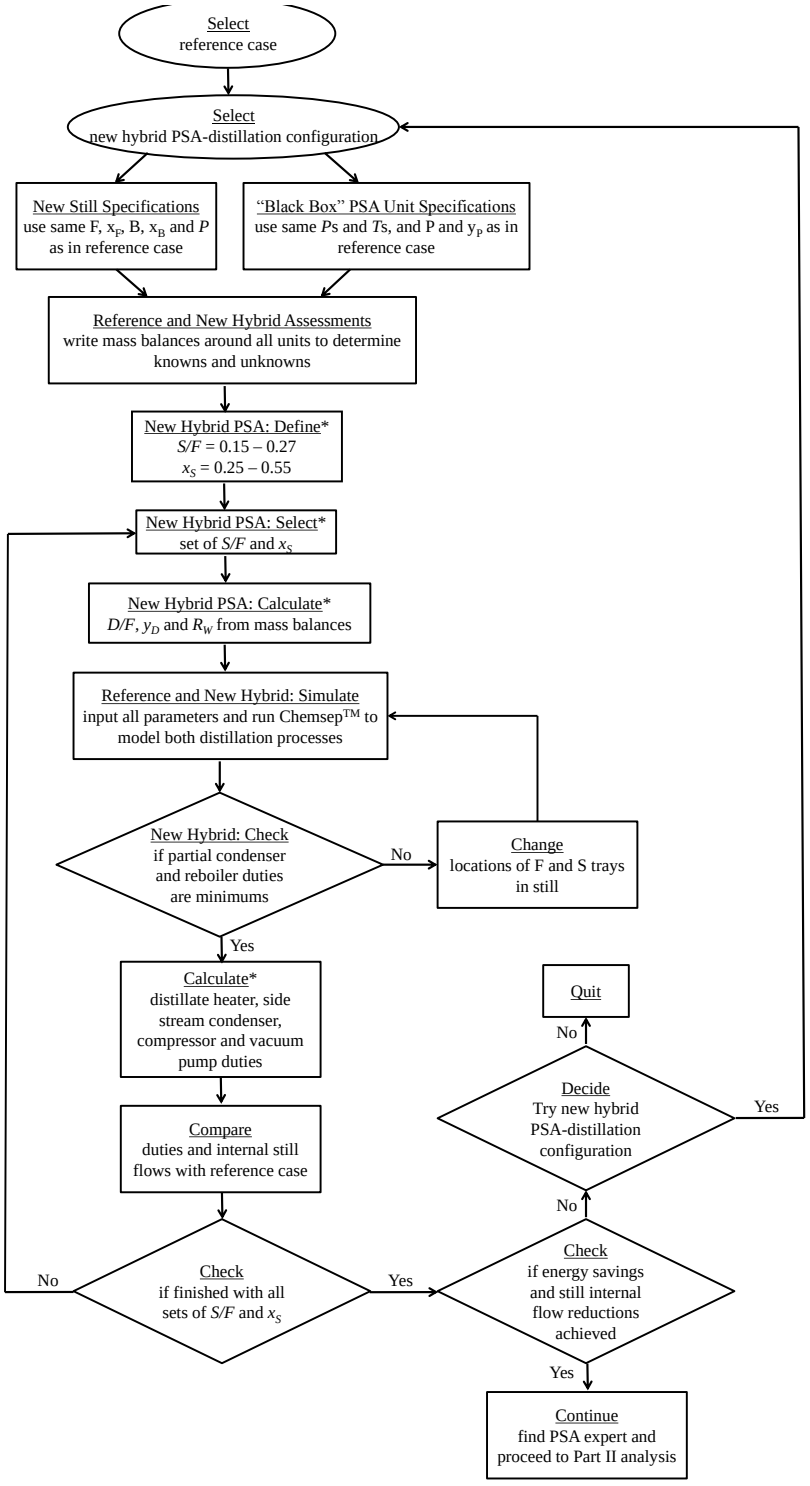

Figure 1.5 Example algorithm for the Part I hybrid "black box" PSA-Chemsep™ simulations, based on the case study of the commercial hybrid PSA-distillation process for ethanol production;[8] modifications may be required for other case studies, especially in the boxes denoted with an asterisk.

tray for the side stream was also required for determining the energy duty of the side stream condenser. The total energy duty of the new hybrid process and the internal flows of the distillation unit were then compared with those of the reference case. This procedure was repeated for the range of specified side stream flow rates and concentrations. All the mass balance relationships required for this Part I analysis are derived below.

The flow rates and concentrations of the external streams were calculated from overall and component (relative to ethanol) mass balances around both units as a whole. These were expressed as

$$F = P + B \tag{1}$$

$$x_F F = y_P P + x_B B \tag{2}$$

With F, x_F, y_P and x_B known for both hybrid systems, combining Eqs. 1 and 2 led to

$$\frac{P}{F} = \frac{x_F - x_B}{y_P - x_B} \tag{3}$$

$$\frac{B}{F} = \frac{y_P - x_F}{y_P - x_B} \tag{4}$$

The overall and component mass balances around the PSA unit were given by

$$D = P + S \tag{5}$$

$$y_D D = y_P P + x_S S \tag{6}$$

For the reference case, in which the side stream and distillate concentrations (x_S and y_D) were known, Eqs. 5 and 6 were combined to provide the relative side stream flow as

$$\frac{S}{F} = \frac{P}{F}\frac{y_P - y_D}{y_D - x_S} \tag{7}$$

For the new case, in which S and x_S were known, Eqs. 5 and 6 were alternatively combined to provide the concentration of the distillate as

$$y_D = \frac{y_P P/F + x_S S/F}{P/F + S/F} \tag{8}$$

In either case, the flow rate of the distillate D was obtained directly from Eq. 6. The performance of the PSA unit, defined in terms of water recovery in the side stream, was calculated from

$$R_S^W = \frac{S/F(1-x_S)}{D/F(1-y_D)} \tag{9}$$

The condenser and reboiler duties, as well as all the still internal vapor and liquid flows, were obtained from Chemsep^{TM} using a reference feed flow rate F and relative flow rates and concentrations x_F, B/F, x_B, S/F, x_S, D/F *and* y_D defined and calculated from the above equations.

A compressor (C_1) and a vacuum pump (C_2), as shown in Figures 1.4a and 1.4b, were needed to bring a stream from P_L (lower pressure) to P_H (higher pressure). C_1 was used to bring the distillate from the distillation column pressure to the feed pressure of the PSA unit. C_2 was used to bring the side stream (heavy product) from the low vacuum pressure of the PSA unit to the distillation column pressure. The compressor or vacuum pump duty was calculated from

$$Q_C = \frac{\gamma}{\gamma-1} RT \left[\left(\frac{P_H}{P_L} \right)^{\frac{\gamma}{\gamma-1}} - 1 \right] \frac{1}{\eta} \dot{n} \tag{10}$$

where γ is the isentropic constant, η is the assumed efficiency of the unit, $\dot{n}$ is the flow

rate of a stream, and T is the temperature of a stream. A distillate heater was used after the compressor to increase the distillate temperature to the feed temperature of the PSA unit T_{PSA}, a defined quantity. The distillate heater (DH) duty was calculated from

$$Q_{DH} = D \int_{T_D}^{T_{PSA}} [y_D C_P^E + (1 - y_D) C_P^W] dT \tag{11}$$

where T_D is the distillate temperature, and C_P^E and C_P^W are the constant pressure heat capacities of ethanol and water, respectively. A side stream condenser (SC) was used after the vacuum pump to change the phase of the side stream from gas to liquid and to decrease the temperature from T_{PSA} to that of the feed tray (T_{TF}) for the reference hybrid process or the temperature of the side stream tray (T_{TS}) for the new hybrid process. This duty was calculated by separating it into two parts: one due to the temperature change in the gas phase:

$$Q_{SC_1} = S \int_{T_{PSA}}^{T^*} [x_S C_P^E + (1 - x_S) C_P^W] dT \qquad \text{with } T^* = T_{TF} \text{ or } T_{TS} \tag{12}$$

and the other due to the phase change at constant temperature, which was determined from

$$Q_{SC_2} = S\left[x_S \Delta H_{vap}^E + (1 - x_S) \Delta H_{vap}^W\right] \tag{13}$$

ΔH_{vap}^E and ΔH_{vap}^W are respectively the phase change enthalpies of ethanol and water at the side stream (heavy product) temperature of the PSA unit.

The resulting duties of the reboiler, partial condenser, compressor, vacuum pump, distillate heater and side stream condenser were calculated for all the cases, in both the reference and new cases, relative to the flow of the ethanol product, i.e.,

$$Q_i^* = \frac{Q_i}{P} \quad (14)$$

The results from the new cases were compared with those of the reference case to determine if any energy savings were incurred with commensurate decreases in the internal flows in the still. When energy savings were realized, Part II was carried out to determine if an "actual" PSA process could be developed that mimicked the performance of the best "black box" PSA process, as outlined below.

1.6.2 Part II. Hybrid "Actual" PSA-Chemsep™ Distillation

Part II utilized the dynamic adsorption process simulator (DAPS) developed and validated by Ritter and co-workers[45] to develop an "actual" PSA process. DAPS imposes the following assumptions: ideal gas behavior; plug flow; no axial dispersion; no film mass transfer resistance (i.e., identical concentrations in both the bulk gas and within the pores of the pellet); linear driving force (LDF) mass transfer resistance between the gas and adsorbed phases; no heat transfer resistance between the gas phase, solid phase (i.e., pellet) and wall; adiabatic condition between the wall and exterior; and no axial thermal conduction.

Adsim from AspenTech[46] could also be used for this Part II analysis. However, it must be emphasized that since Adsim and DAPS are very rigorous adsorption process simulators that can model the most complex multi-bed multi-step PSA processes in commercial operation, their use requires someone with significant PSA process design experience to ensure that a potential PSA process design is not overlooked. In other

words, the "actual" PSA process might need a very complex PSA cycle schedule[47] to mimic the performance of the "black box" PSA process. This is a non-trivial exercise in PSA process development, with the recommendation that it should be carried out only by qualified experts in the field.

In this illustration, the PSA cycle utilized in the commercial reference case[48] was the 2-bed 4-step PSA cycle shown in Figure 1.6. The four steps were feed (F), countercurrent depressurization (CnD), light reflux (LR), and light product pressurization (LPP). In the F step, the distillate from the still was fed to the bottom of the bed in the PSA unit at the higher pressure. The light product (enriched ethanol) was collected from the top of the bed, part of which was sent to the top of the other bed for LR and LPP. The heavy product (enriched water) was withdrawn from the bottom of the bed during the CnD and LR steps. LR was carried out at the lower pressure under vacuum by using a small fraction of the light product produced during the F step as purge or reflux. The bed was then pressurized from the lower to the higher pressure during the LPP step using a fraction of the light product produced during the F step.

Because this Part II analysis was based on modifying a commercial PSA cycle,[48] based on experience, it was decided that only the flow rate and concentration of the feed stream to the PSA unit (i.e., D and y_D) and the LR step time had to be varied. This would not be the case in a grassroots PSA process design effort, which is why significant PSA process design experience is required in this Part II analysis. It was also decided to keep

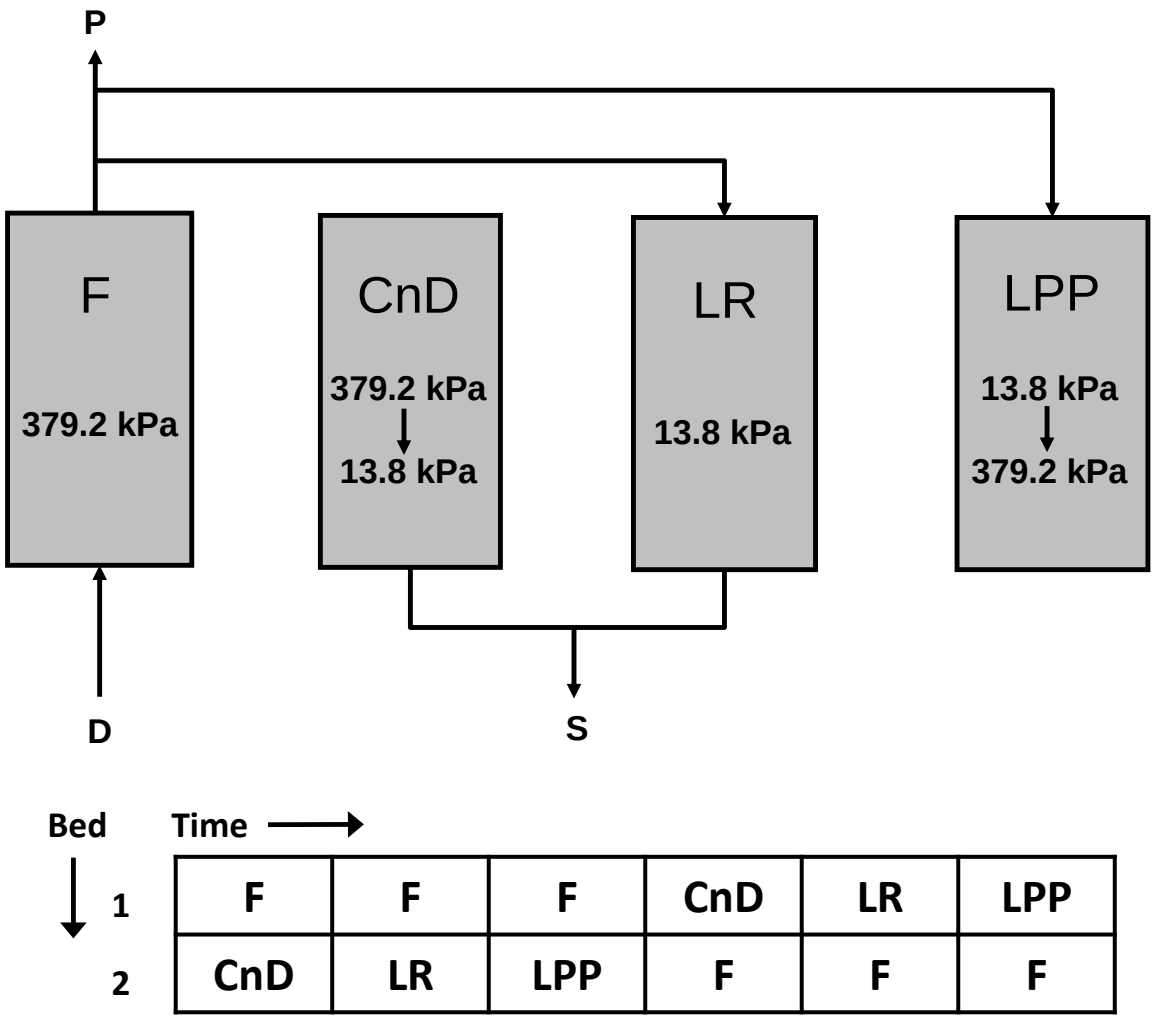

Figure 1.6 2-bed 4-step PSA cycle schematic and schedule.[48] F: feed step; CnD: countercurrent depressurization step; LR: light reflux step; LPP: light product pressurization step; D: PSA feed from distillate still; P: light (ethonal) product; S: side stream to still (heavy product). The times indicate the length of each step: 345 s for F; 225 s for CnD plus LR; 120 s for LPP.

the sum of the CnD and LR step times constant. So, when the LR step time increased, the CnD step time decreased, accordingly. The remaining PSA process parameters were fixed and kept the same as those in the commercial PSA cycle.[48]

The reference PSA unit also used 3A zeolite as the adsorbent.[48] 3A zeolite only adsorbs water; ethanol is too large to fit in its pores.[48] The adsorption isotherms for water vapor on 3A zeolite[48] were fitted to the following Toth model:

$$n = \frac{n_s b P}{(1+(bP)^t)^{1/t}} \tag{15a}$$

$$n_s = n_0 + n_1 T \tag{15b}$$

$$b = b_0 \exp(\frac{-\Delta H}{RT}) \tag{15c}$$

$$t = t_0 + t_1 \frac{1}{T} \tag{15d}$$

Now, with T_{PSA}, D and y_D necessarily provided as inputs to DAPS, at the periodic state, it returned values of P, y_P, S and x_S for a given set of PSA process conditions. Recall that in the "black box" PSA process P and y_P were fixed while D and y_D varied as a result of varying S and x_S; however, in the "actual" PSA process D and y_D were fixed while P and y_P, and hence S and x_S, varied. This was the case because it was impossible to *a priori* fix P and y_P in DAPS. Thus, to ensure that the "actual" and "black box" PSA process performances were essentially equivalent, "actual" PSA process conditions had to be found that resulted in similar ranges of P/D and y_P for both the "actual" and "black box" PSA processes. To this end, several simulations were carried out while varying PSA process conditions such as bed size, cycle time, step times and feed flow rate. When a set

of “actual” PSA process conditions produced values of P/D and y_P in the respective acceptable ranges, the resulting y_P was utilized in the mass balance relationships developed in Part I to calculate P/F from Eq. 3. P/F was then used together with the resulting x_S from the simulations to calculate D/F and S/F from Eqs. 5 and 7. Recall that in these calculations, B/F and x_B were the same as in Part I. All these results were scaled to the reference flow F and then input to Chemsep™ to obtain the corresponding duties of the partial condenser and reboiler, and still internal vapor and liquid flows. The remaining duties were calculated using the same methodology as previously described in Part I. Finally, all the results from Part II were compared with the reference case to determine if the energy savings and still internal flow reductions were similar to the hybrid PSA-distillation process obtained in Part I based on the best “black box” PSA process. Clearly, some trial and error was necessary to achieve an “actual” PSA process that provided the same performance as the best “black box” PSA processes.

1.7 Results and Discussion

1.7.1 Part I. Hybrid “Black Box” PSA-Chemsep™ Simulations

Based on the Part I algorithm (Figure 1.5), 42 hybrid “black box” PSA-Chemsep™ distillation simulations were carried out at seven different ratios of the side stream to still feed flow rates (S/F) and six different concentrations of ethanol in the side stream (x_s). This resulted in 42 different “black box” PSA process performances in terms of water purity and water recovery in the side stream (heavy product) of the PSA

unit. All the conditions utilized in the hybrid "black box" PSA-Chemsep^{TM} distillation simulations are summarized in Table 1.1 for both the reference and new cases. The individual energy duties are discussed first, followed by the total energy duties and distillation column internal flow changes. Finally, the energy savings regions along with the corresponding "black box" PSA conditions that resulted in energy savings and commensurate still internal flow reductions are discussed.

Partial Condenser and Reboiler Energy Duties

Figures 1.7a and 1.7b respectively show the duties for the partial condenser and reboiler versus *S/F* for different x_s. These duties both decreased as *S/F* increased and x_s decreased; and both *S/F* and x_s had marked and comparable effects on both of them. For constant *S/F*, a smaller value of x_s meant the side stream (heavy product) from the PSA unit was more enriched in water. This translated into more separations work being done by the PSA unit. For constant x_s, a larger value of *S/F* meant that the PSA unit was processing more water. This also translated into more separations work being done by the PSA unit. The net effect was that the partial condenser and reboiler duties both decreased with larger *S/F* and smaller x_s, eventually resulting in energy savings.

Figures 1.7c and 1.7d show the corresponding energy savings relative to the reference case. In both duties, energy savings resulted with increasing *S/F* and decreasing x_s. For the partial condenser, a maximum of 49.4 kJ/mol of ethanol was saved, which corresponded to a 71.1% energy savings over the reference case. This occurred for the

Table 1.1 Process parameters and conditions used in the hybrid "black-box" PSA process simulations in Part I, and all Chemsep^{TM} simulations for Parts I and II.

Fixed Conditions	***Reference and New***	
distillation column pressure, P_c (kPa)	101.3	
distillation column stage efficiency, E_o	0.75	
distillation column feed flow rate, F (kmol/s)	1.0	
ethanol mole fraction in feed, x_F	0.40	
ethanol mole fraction in bottoms product, x_B	0.005	
feed quality, q_F	1	
side stream quality, q_S	1	
distillate quality, q_D	0	
bottom product quality, q_B	1	
PSA light product quality, q_P	0	
PSA high pressure, P_H (kPa)	379.2	
PSA low pressure, P_L (kPa)	13.8	
PSA feed temperature, T_{PSA} (K)	440	
PSA compressor or vacuum pump efficiency, η	0.8	
isentropic constant, γ	1.4	
Varied Conditions	***Reference***	***New***
relative side stream flow rate, *S/F*	0.20	0.15 to 0.27
ethanol mole fraction in side stream, x_S	0.477	0.25 to 0.55
ethanol mole fraction in distillate product, y_D	0.818	depended on *S/F* and x_S

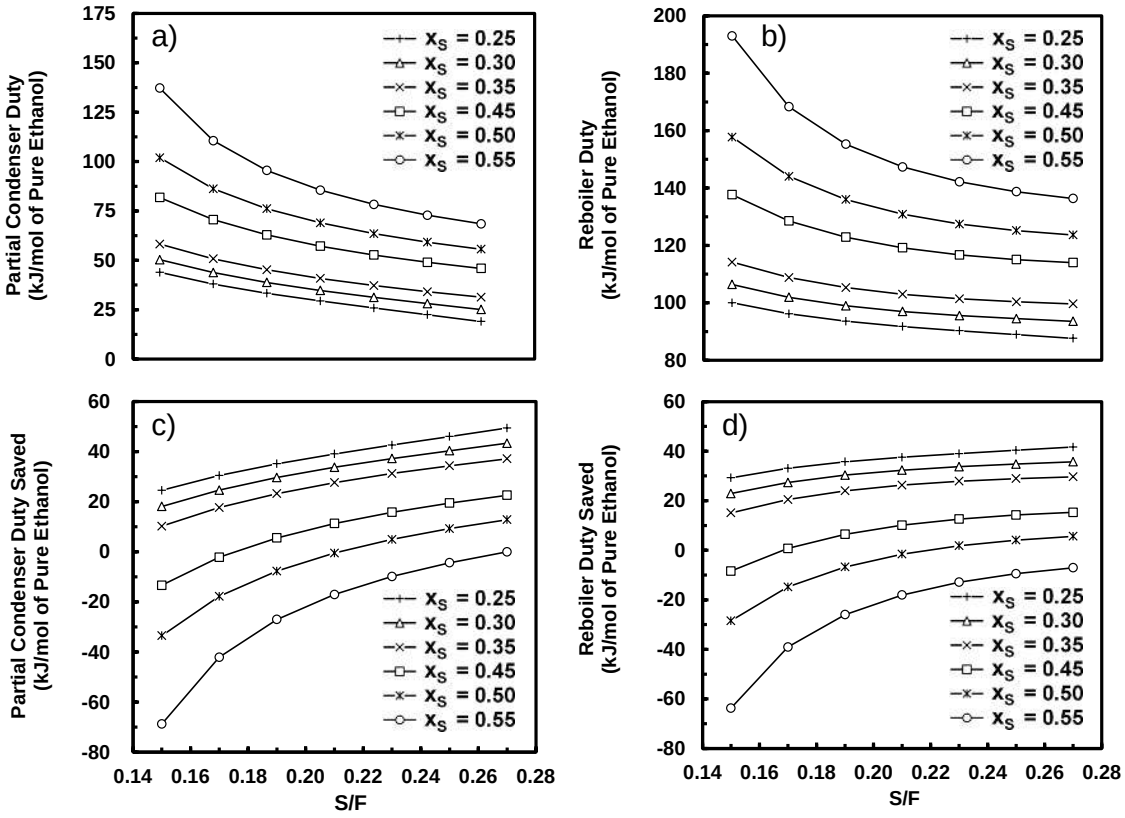

Figure 1.7 Hybrid "black-box" PSA-Chemsep^{TM} simulations: partial condenser and reboiler duties, and corresponding energy savings relative to the reference case, with *S/F* = 0.207 and x_s = 0.447.

largest *S/F* and smallest x_s. Similarly, for the reboiler, a maximum of 42.4 kJ/mol of ethanol was saved under the same conditions, which corresponded to a 32.3% energy savings over the reference case. Moreover, as long as x_s was less than about 0.35 both duties exhibited energy savings for all values of *S/F*. For these cases the optimum side stream stage of the still was always below the feed stage.

Distillate Heater and Side Stream Condenser Energy Duties

Figures 1.8a and 1.8b respectively show the duties of the distillate heater and side stream condenser versus *S/F* for different x_s. The distillate heater duty increased with *S/F* and x_s both increasing. However, the effect was more pronounced for changes in *S/F*. For constant *S/F*, since the distillate contained more ethanol with increasing x_s and water has a much smaller heat capacity than ethanol, more heater duty was required when more ethanol was in the distillate. For constant x_s, and with *F*, *B* and R_D constant, a larger *S/F* necessarily resulted in a larger *D*, which in turn required a greater heater duty. Since the effect of x_s on the distillate heater duty was small, it was neglected.

In contrast, the side stream condenser duty increased only with increasing *S/F*; it did not change with changing x_s. The effect of *S/F* on the side stream condenser duty was also much greater than that on the distillate heater duty. More than 88% of the side stream condenser duty was due to changing its phase at constant temperature, which increased significantly with increasing *S/F* (eq 13). Since water and ethanol have similar phase change enthalpies, there was no effect of x_s on this duty.

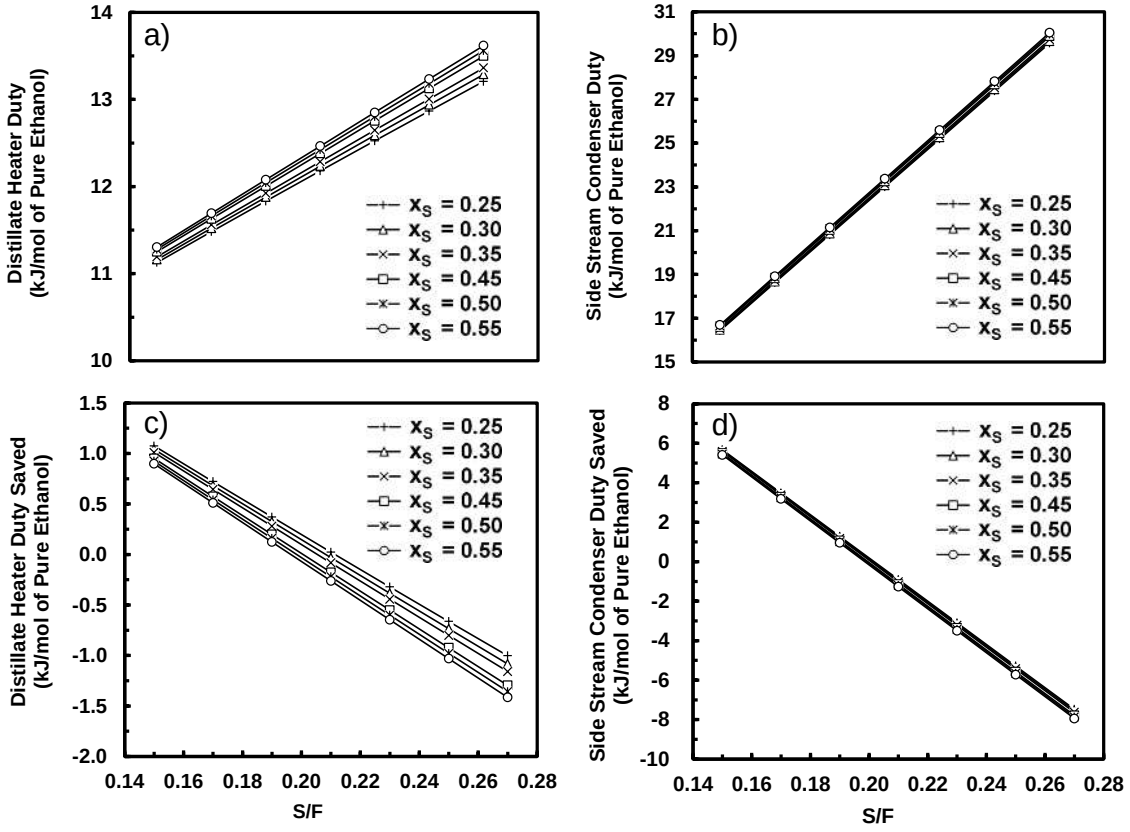

Figure 1.8 Hybrid "black-box" PSA-Chemsep™ simulations: distillate heater and side stream condenser duties, and corresponding energy savings relative to the reference case, with S/F = 0.207 and x_S = 0.447.

Figures 1.8c and 1.8d show the corresponding energy savings relative to the reference case. For the distillate heater duty, more energy was saved with both *S/F* and x_s decreasing. However, the savings were markedly more significant with changes in S/F than x_s. For the side stream condenser duty, more energy was saved only with S/F decreasing; no energy savings were incurred by changing x_s. The energy savings were five to six times greater for the side stream condenser duty than the distillate heater duty.

Compressor and Vacuum Pump Energy Duties

Figures 1.9a and 1.9b show respectively the combined duties for the compressor and vacuum pump and the corresponding energy savings relative to the reference case, both versus *S/F* for different x_s. There was no effect of x_s on the combined compressor and vacuum pump duty and it increased with increasing *S/F*. Correspondingly, there was no effect of x_s on the energy savings, and it decreased with increasing *S/F*. The compressor and vacuum pump duties are proportional to *S/F* according to eq 10, and do not depend on concentration, just flow. Clearly, a larger value of *S/F* corresponded to both the compressor and vacuum pump facing larger flows, which in turn, required more energy.

Total Energy Duty

The total duty was calculated by adding all the duties together, which included the duties of the partial condenser, reboiler, distillate heater, side stream condenser, compressor and vacuum pump. Figures 1.10a, 10b and 10c respectively show the total

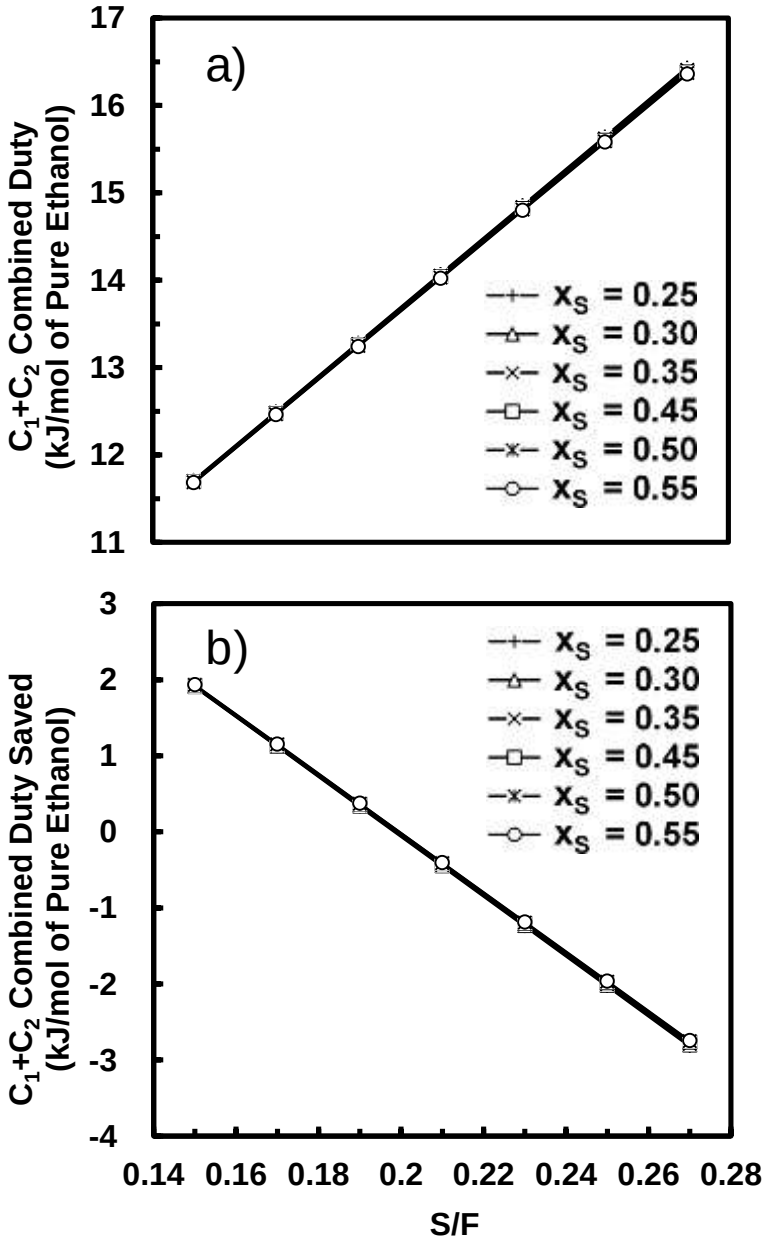

Figure 1.9 Hybrid "black-box" PSA-Chemsep^{TM} simulations: PSA compressor (C_1) and PSA vacuum pump (C_2) combined duty, and corresponding energy savings relative to the reference case, with S/F = 0.207 and x_S = 0.447.

duty, the total energy savings relative to the reference case and the percent total energy savings relative to the reference case, all versus *S/F* for different x_s. The results in Figures 1.7 to 1.9 showed that the partial condenser and reboiler duties both overwhelmed the other duties by an order of magnitude or more. This made the trends in Figure 1.10 very similar to those exhibited by the partial condenser and reboiler (Figure 1.7). Thus, energy savings were incurred for larger *S/F* and smaller x_s, with a maximum total energy savings of 32.5% compared to the reference case; and again, energy savings resulted for all values of *S/F* as long as x_s was less than 0.35.

It is worth reiterating that since energy savings always improved by increasing *S/F* or decreasing x_s, this meant that the energy efficiency of the hybrid process improved relative to the reference case as the PSA unit did more of the separations work. For example, for constant *S/F*, a smaller value of x_s corresponded to a higher enrichment of water in the side stream, and for constant x_s, a larger value of *S/F* corresponded to more water being processed in the PSA unit. Both of these trends corresponded to more separations work being done by the PSA unit, thereby reducing both the partial condenser and reboiler duties of the still. However, since the effect of *S/F* was not as pronounced when the side stream was enriched with more water (i.e., smaller x_s), the enrichment or purity of water produced in the PSA unit was much more important in saving energy than the amount of water processed by the PSA unit. This was an informative, unexpected outcome from this simple hybrid "black box" PSA-distillation process analysis.

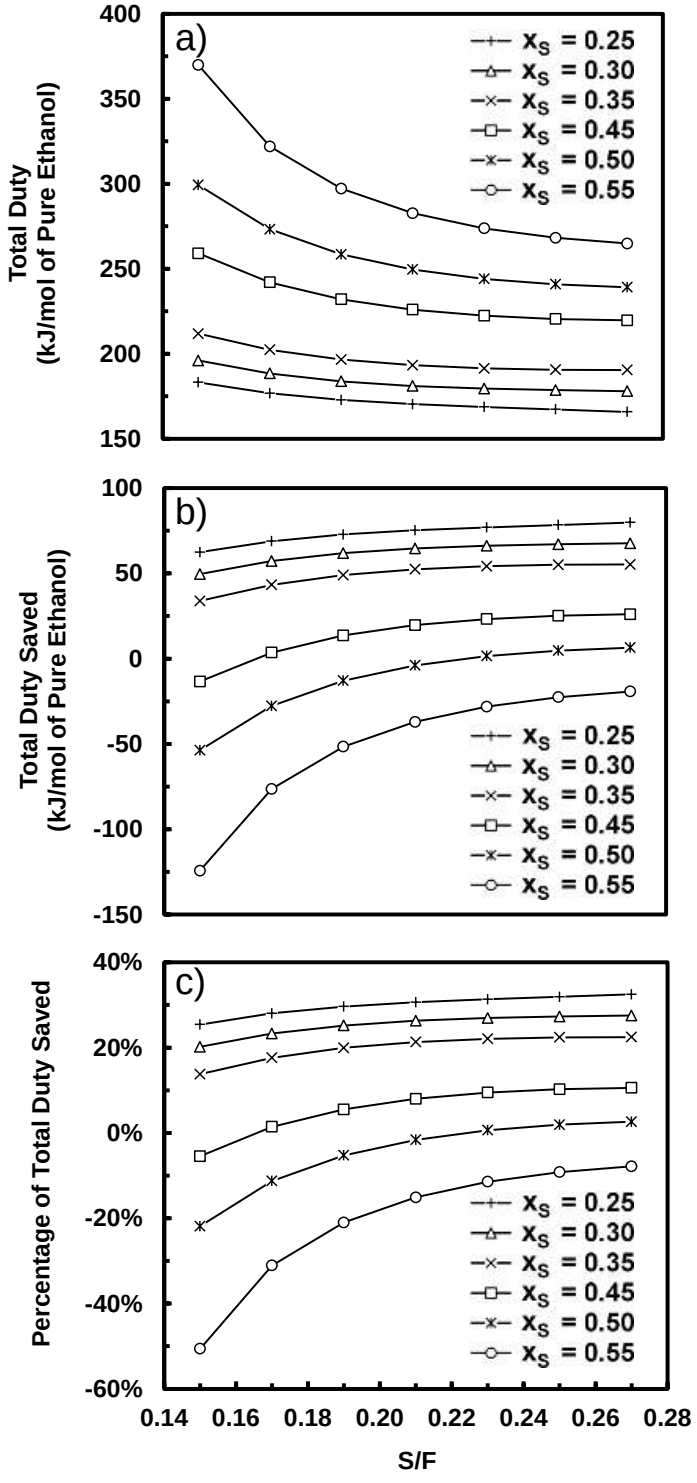

Figure 1.10 Hybrid "black-box" PSA-Chemsep^{TM} simulations: total duty, and corresponding energy savings and percent energy savings, both relative to the reference case, with S/F = 0.207 and x_S = 0.447.

Distillation Column Internal Flow Changes

The results just discussed showed that the partial condenser and reboiler duties changed considerably, depending on the concentration x_S and flow rate S of the side stream (heavy product) from the PSA unit. The only way these duties could change was by having commensurate changes in the internal vapor and liquid flows within the distillation column. As shown in Figure 1.4, V_2 is the vapor phase flow from the 2nd stage which is going into the partial condenser; L_{51} is the liquid phase flow from the 51st stage which is going into the reboiler. ΔV_2 and ΔL_{51} represent the difference of flows in the reference and new cases, which are defined as V_2 (reference case) - V_2 (new case) and L_{51} (reference case) - L_{51} (new case) respectively. These internal still flow changes are shown in Figure 1.11, where Figures 1.11a and 1.11b show the difference between the internal vapor (V_2) and liquid (L_{51}) flows in the new and reference cases and Figures 1.11c and 1.11d show the corresponding percent reductions in those two flows compared to the reference case. A larger *S/F* always resulted in smaller internal flows; and when x_S was less than 0.35, the internal flows of the new cases were always smaller than those of the reference case for all values of *S/F*. A reduction of either internal flow meant less mass had to be condensed or evaporated, resulting in a significant reduction in the partial condenser or reboiler duty. Most importantly, even when energy savings are not a major concern, e.g., because of heat integration, a reduction in the internal still flows necessarily implies that the throughput or capacity of the distillation column can be

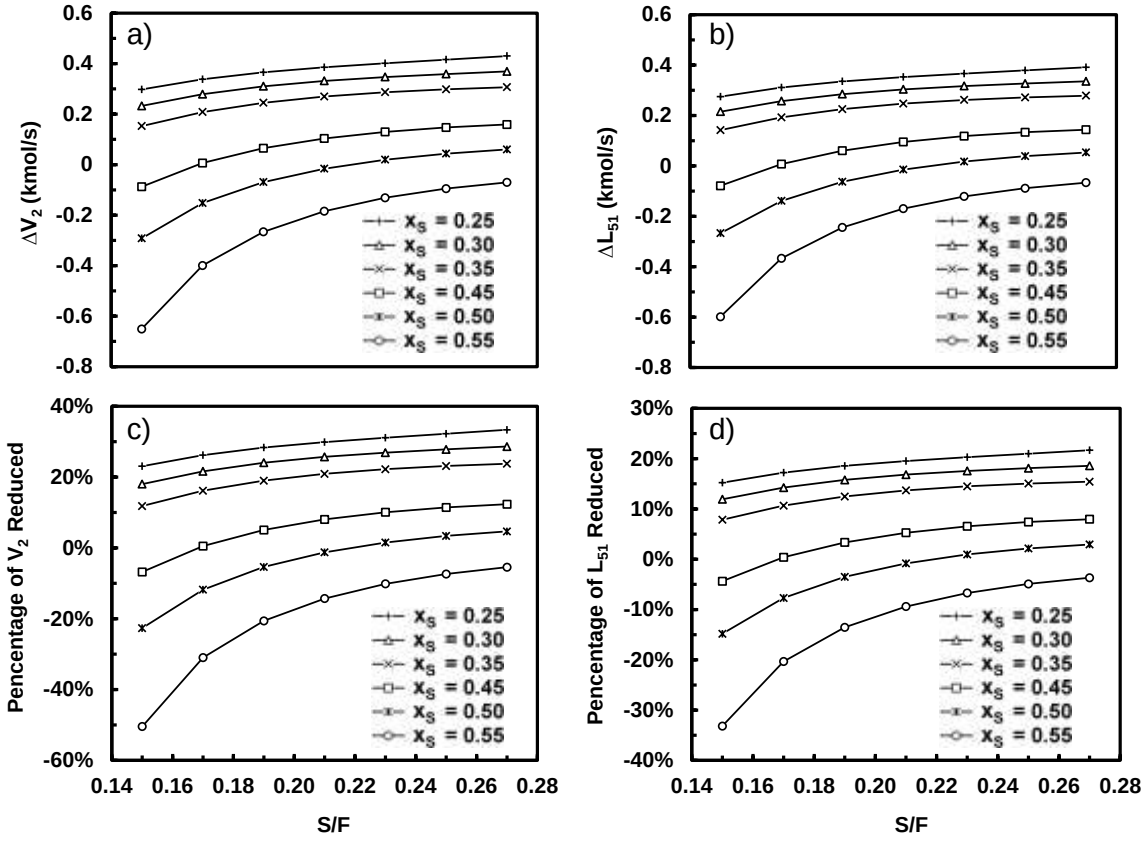

Figure 1.11 Hybrid "black-box" PSA-Chemsep^{TM} simulations: still internal vapor (V) and liquid (L) flow changes and corresponding percent changes relative to the reference case.

proportionately increased. This was a key finding of this Part I analysis, although it is now an intuitively obvious outcome.

Energy Savings Regions and "Black Box" PSA Conditions and Performance

The Chemsep^{TM} results were analyzed to determine the "black box" PSA unit operating conditions that resulted in energy savings. Figure 1.12a shows the corresponding performance of the "black box" PSA unit for all the new cases, in terms of water recovery (eq 9) and water purity $(1-x_S)$ in the side stream, with *S/F* and x_S varying as shown. According to these "black box" PSA performance curves, to save energy the purity of water produced in the side stream from the PSA unit had to be greater than 65 mol%, and the recovery of water in this stream had to be greater than 95%. So, the goal was to design an "actual" PSA process that exhibited a performance lying somewhere in the upper right hand corner of Figure 1.12a, i.e., the energy savings region indicated by the acute angle formed by the two dotted lines.

When the results in Figure 1.12a were plotted in a slightly different manner, i.e., in terms of the "black box" PSA process performance based on *P/D* and y_D instead of *S/F* and x_S, the curves in Figure 1.12b resulted. Recall that *P/D* and y_D were important for making sure similar performances would be obtained for the "actual" and "black box" PSA processes, because of the different sets of parameters that were fixed during the respective simulations. Since, these "black box" PSA performance curves revealed the ranges of *P/D* and y_D that the "actual" PSA process had to fall into to be similar to the

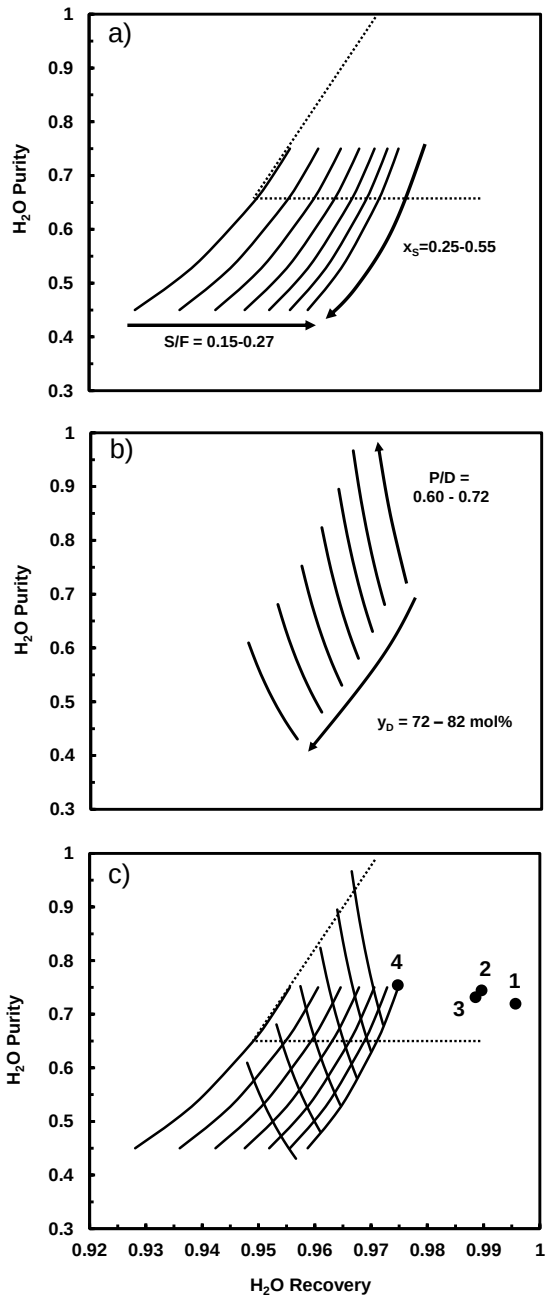

Figure 1.12 a) "Black box" PSA process performance curves in terms of *S/F* and x_S, with the energy savings region indicated by the acute angle formed by two dotted lines. b) Same "black box" PSA process performance curves but in terms of *P/D* and y_D. c) Overlay of "black box" PSA process performance curves in (a) and (b), with the energy savings region indicated by the acute angle formed by two dotted lines and the "actual" PSA process performances indicated by the solid symbols labeled 1 to 4.

"black box" PSA processes, the energy savings region for the "actual" PSA process was revealed by overlaying them with the curves in Figure 1.12a. This plot is shown in Figure 1.12c. These combined performance curves revealed that a lower y_D was better for achieving energy savings at some intermediate *P/D*. However, to avoid an overly large PSA unit, a y_D of 79 to 80 mol% was chosen and used as input to the rigorous PSA process simulations discussed next.

1.7.2 Part II. Hybrid "Actual" PSA-Chemsep™ Simulations

A number of simulations were carried out using DAPS with the PSA cycle depicted in Figure 1.6. All the process parameters and conditions used in DAPS are listed in Tables 1.2. This "actual" PSA process was essentially the same one reported in the literature for ethanol production.[48] However, as stated earlier, slightly different feed concentrations (y_D), feed flow rates (D) and LR times (t_{LR}) were investigated. The results from four "actual" PSA process simulations are provided in Table 1.3, with their corresponding process performances plotted in Figure 1.12c, along with the "black box" PSA process performances.

The results in Table 1.3 showed that y_P was always greater in the "actual" PSA processes than in the "black box" PSA processes (0.993 to 0.999 compared to 0.987, respectively). This indicated that the "actual" PSA process columns were oversized. A higher y_P also necessarily resulted in a higher water recovery for the "actual" PSA process. This was why three of the four points deviated from the performance curves

Table 1.2 Process parameters and conditions used in DAPS for the "Actual" PSA process simulations in Part II.

3A Zeolite-Water Toth Isotherm Parameters:	
n_0 (mol/kg)	16.26
n_1 (K^{-1})	-1.9×10^{-2}
b_0 (kPa^{-1})	1.6×10^{-8}
t_0	1.14
t_1 (K)	-56.42
ΔH (kJ/mol)	-57.95
3A Zeolite LDF Mass Transfer Resistance:	
k_{LDF}^{E} (s^{-1})	1.0×10^{-3}
k_{LDF}^{W} (s^{-1})	8.0×10^{-3}
Bed Properties	
length, Z (m)	7.5
outer radius, r_o (m)	1.25
inner radius, r_i (m)	1.2246
porosity, ε_b	0.31
Wall Properties	
density, ρ_w (kg/m^3)	8000
thermal capacity, C_w (kJ/kg/K)	0.5
heat transfer coefficient, h ($kW/m^2/K$)	0.0
temperature, T_w (K)	440
Operating Conditions	
PSA feed Temperature, T_{PSA} (K)	440
high pressure, P_H (kPa)	379.2
low pressure, P_L (kPa)	13.8
feed flow rate F_{PSA} (SLPM)	150,000 or 200,000
mole fraction ethanol in feed, y_D	0.79 or 0.80
3A Zeolite Adsorbent Properties	
radius, r_p (m)	0.005
density, ρ_p (kg/m^3)	1116
porosity, ε_p	0.54
thermal capacity, C_p (kJ/kg/K)	1.045

Table 1.3 “Actual” PSA process performances obtained with DAPS in the Part II analysis: PSA unit water purity and recovery in the side stream and PSA unit ethanol purity and recovery in the light product.

Run	y_D	D (SLPM)	t_{LR} (s)	$(1-y_S)$	R_S^W(%)	y_P	R_P^E (%)
1	0.80	150000	100	0.7197	99.57	0.9992	90.34
2	0.80	150000	75	0.7316	98.86	0.9972	90.96
3	0.80	200000	100	0.7445	98.96	0.9974	91.52
4	0.79	150000	50	0.7542	97.48	0.9932	91.58

exhibited by the “black box” PSA processes, even though all four points fell within an energy savings region, as shown in Figure 1.12c. Thus, all four “actual” PSA processes resulted in significant energy savings with commensurate still internal flow reductions, as shown in Table 1.4. Typically, 20 to 25% energy savings were achieved based on the new hybrid PSA-distillation configuration (Figure 1.4b) compared to the commercial (reference) one (Figure 1.4a). This energy savings corresponded to still internal flow reductions of 18 to 22% for the vapor flows and 12 to 15% for the liquid flows. Since energy savings and flow reductions are concomitant, energy savings, throughput debottlenecking, or both could be the outcome of this two-part analysis for other distillation processes, just like it was here for the commercial hybrid PSA-distillation process for ethanol production.

1.8 Conclusions

A new methodology for modeling hybrid PSA-distillation processes was developed. This new approach involves two parts. Part I determines if energy savings are possible. It can be done easily with sufficient knowledge of distillation process design and only minimal knowledge of PSA process design. Part I is carried out using Chemsep^{TM} to model a distillation column connected to a PSA unit that is treated as a “black box” with an assumed process performance. In this way, a hybrid PSA-distillation process can be analyzed simply by performing mass balances around these units and running Chemsep^{TM} to determine if energy savings are possible compared to a reference

Table 1.4 “Actual” PSA processes performances obtained from DAPS in the Part II analysis: energy savings and still internal flow reductions.

Run	Total Duty (kJ/mol)	Total Duty Saved (%)	ΔV_2 kmol/s	ΔL_{51} kmol/s	V_2 Reduced (%)	L_{51} Reduced (%)
Reference	245.6	-	-	-	-	-
Simulation 1	195.1	20.6	0.2395	0.2167	18.57	12.01
Simulation 2	192.9	21.5	0.2468	0.2243	19.14	12.43
Simulation 3	191.3	22.1	0.2534	0.2304	19.65	12.77
Simulation 4	183.6	25.2	0.2894	0.2648	22.44	14.67

(commercial) process for different “black box” PSA process performances.

Once an energy savings hybrid PSA-distillation process is found in Part I, Part II determines if an “actual” PSA process exists that mimics the performance of the best “black box” PSA processes. Part II is carried out using a rigorous PSA process simulator like Adsim from AspenTech; thus, it requires significant knowledge of PSA process design. The outcome of this two-part analysis is a hybrid PSA-distillation process that has the potential to be more energy efficient than the reference process with a commensurate reduction in the internal flows within the distillation column.

This new approach was successfully demonstrated using a commercial hybrid PSA-distillation process as the reference case that is in use for fuel grade ethanol production. Part I of this two-part analysis found several, more energy efficient designs than the reference case with proportionately reduced internal flows within the still. Compared to the reference case, which mixes the side stream recycled from the PSA unit with the feed to the still, better designs were obtained using the “black box” PSA process when the locations of the feed and side stream stages were optimized for different PSA process conditions. These new hybrid systems exhibited energy savings and still internal flow reductions when the ethanol concentration in the side stream was smaller than that in the feed to the still and the side stream was sent back to a stage lower than the feed stage, and then for larger feed to side stream flow rate ratios or lower ethanol (higher water) concentrations in the side stream. Also, the purity of water produced in the PSA

unit was much more important in saving energy than the amount of water produced in the PSA unit.

Based on the Part I results, Part II of this analysis found several “actual” PSA processes using the in-house developed dynamic adsorption process simulator (DAPS) that provided nearly the same performance, energy savings and internal still flow reductions as the best “black box” PSA processes. These “actual” PSA processes exhibited typical energy savings of 25%, with a corresponding decrease in the vapor and liquid flow rates in the still of 22% and 15%, respectively. Overall, these results illustrated that this new methodology should be very useful for quickly accessing the utility of hybrid PSA-distillation processes for a variety of other applications, with many possibilities for achieving significant energy savings and/or throughput debottlenecking.

REFERENCES

1. Kumins, L, Parker L.; Yacobucci, B. Refining capacity-challenges and opportunities facing the U.S. industry. Report, Petroleum Industry Research Foundation, Inc," 2004.
2. http://tonto.eia.doe.gov/dnav/pet/pet_pnp_top.asp: Data, Energy Information Administration.
3. http://www.eia.doe.gov/pub/oil_gas/petroleum/analysis_publications/oil_market_basics/refining_text.htm: Refining, Annual Energy Review.
4. Eldridge R. B.; Seibert A. F.; Robinson S. Hybrid Separations/Distillation Technology Research Opportunities For Energy and Emissions Reduction. Report prepared for Industrial, DOE, *Energy Efficiency and Renewable Energy*, 2005.
5. Humphrey, J. L.; Koort, R.; Seibert, A. F. Separation Technologies-Advances and Priorities. Work Performed Under Contract No. AC07-90ID12920, U.S. Department of Energy, DOE Report, February 1991.
6. Robinson, S.; Jubin, R. Materials for Separation Technologies: Energy and Emission Reduction Opportunities. Work Performed Under Contract No. DE-AC05-00OR22725, U.S. Department of Energy, DOE Report, May 2005.
7. Eldridge, R. B.; Seibert, A. F.; Robinson, S. Hybrid Separations/Distillation

Technology: Research Opportunities for Energy and Emissions Reduction. Work Performed Under Contract, U.S. Department of Energy, DOE Report, April 2005.

8. Quintero, J. A.; Montoya, M. I.; Sanchez, O. J.; Giraldo, O. H.; Cardona, C. A. Fuel Ethanol Production from Sugarcane and Corn: Comparative Analysis for a Columbian Case. *Energy* **2008**, *33*, 383-399.
9. Kumar, R.; Golden, T.C.; White, T.R.; Rokicki, A. Novel Adsorption Distillation Hybrid Scheme for Propane Propylene Separation. *Sep. Sci. Technol.* **1992,** *27*, 2157-2170.
10. Bryan, P. F. Removal of Propylene from Fuel-Grade Propane. *Sep. Purif. Rev.* **2004,** *33*, 157-182.
11. Eldridge, R. B. Olefin Paraffin Separation Technology: A Review. *Ind. Eng. Chem. Res.* **1993,** *32*, 2208-2212.
12. Van Hoof, V.; Dotremont, C.; Buekenhoudt, A. Performance of Mitsui NaA Type Zeolite Membranes for the Dehydration of Organic Solvents in Comparison with Commercial Polymeric Pervaporation Membranes. *Sep. Purif. Technol.* **2006,** *48*, 304-309.
13. Van Hoof, V.; Van den Abeele, L.; Buekenhoudt, A.; Dortemont, C.; Leysen, R. Economic Comparison Between Azeotropic Distillation and Different Hybrid Systems Combining Distillation with Pervaporation for the Dehydration of Isopropanol. *Sep. Purif. Technol.* **2004,** *37*, 33-49.

14. Szitkai, Z.; Lelkes, Z.; Rev, E.; Fonyo, Z. Optimization of Hybrid Ethanol Dehydration Systems. *Chem. Eng. Process.* **2002,** *41*, 631-646.

15. Qariouh, H.; Schue, R.; Schue, F.; Bailly, C. Sorption, Diffusion and Pervaporation of Water/Ethanol Mixtures in Polyetherimide Membranes. *Polym. Inter.* **1999,** *48*, 171-180.

16. Nomura, M.; Yamaguchi, T.; Nakao, S. Ethanol/Water Transport through Silicalite Membranes. *J. Mem. Sci.* **1998,** *144*, 161-171.

17. Sano, T.; Yanagishita, H.; Kiyozumi, Y.; Mizukami, F.; Haraya, K. Separation of Ethanol-Water Mixture by Silicalite Membrane on Pervaporation. *J. Mem. Sci.* **1994**, *95*, 221-228.

18. Huang, Z.; Shi, Y.; Wen, R.; Guo, Y. H.; Su, J. F.; Matsuura, T. Multilayer Poly(Vinyl Alcohol)-Zeolite 4A Composite Membranes for Ethanol Dehydration by Means of Pervaporation. *Sep. Purif. Technol.* **2006,** *51*, 126-136.

19. Smitha, B.; Suhanya, D.; Sridhar, S.; and Ramakrishna M. Separation of Organic-Organic Mixtures by Pervaporation – A Review. *J. Mem. Sci.* **2004,** *241*, 1-21.

20. Suk, D. E.; and Matsuura, T. Membrane-Based Hybrid Processes: A Review. *Sep. Sci. Technol.* **2006**, *41*, 595-626.

21. Pressly, T. G.; and Ng, K. M. A Break-Even Analysis of Distillation-Membrane Hybrids. *AIChE J.* **1998**, *44*, 93-105.

22. Pettersen, T.; Argo, A.; Noble, R. D.; Koval, C. A. Design of Combined Membrane and

Distillation Processes. *Sep. Technol.* **1996**, *6*, 175-187.

23. Parthan, W.; Noble, R. D.; Koval, C. A. Design Methodology for a Membrane Distillation Column Hybrid Process. *J. Mem. Sci.* **1995**, *99*, 259-272.
24. Moganti, S.; Noble, R. D.; Koval, C. A. Analysis of a Membrane Distillation Column Hybrid Process. *J. Mem. Sci.* **1994**, *93*, 31-44.
25. Lee, C. H.; and Hong, W. H. Effect of Operating Variables on the Flux and Selectivity in Sweep Gas Membrane Distillation for Dilute Aqueous Isopropanol. *J. Mem. Sci.* **2001**, *188*, 79-86.
26. El-Bourawi, M. S.; Ding, Z.; and Ma, R.; Khayel, M. A Framework for Better Understanding Membrane Distillation Separation Process. *J. Mem. Sci.* **2006**, *285*, 4-29.
27. Ausitakis, J. P.; Garg, D. R. Adsorption Separation Cycle. U. S. Patent **1983,** 4,373,935 .
28. Skarstrom, C. W. Combination Process Comprising Distillation Operation in Conjunction with a Heatless Fractionator. U. S. Patent **1964**, 3,122,486.
29. Ginder, W. F. Method of Removing Water from Ethanol. U. S. Patent **1983,** 4,407,662.
30. Fan, Z. L.; Lynd L. R. Conversion of Paper Sludge to Ethanol, II: Process Design and Economic Analysis. *Biopro. Biosyst. Eng.* **2007**, *30*, 35-45.
31. Westphal.; K. G. G. Combined Adsorption-Rectification Method for Separating a Liquid Mixtures. International Patent. DE3 **2007**, 712,291.

32. Krishnamurthy R.; Maclean, D. L. Method and Apparatus of Producing Carbon Dioxide in High Yields from Low Concentration Carbon Dioxide Feeds. U. S. Patent **1990**, 4,952,223.

33. Nguyen, T. C.; Baksh, M. S. A.; Bonaquist, D. P.; Weber, J. A. Cryogenic Hybrid System for Producing High Purity Argon. U. S. Patent **1998**, 5,730,003.

34. Ramachandran R.; Dao L. H. Method of Producing Unsaturated Hydrocarbons and Separating the Same from Saturated Hydrocarbons. U. S. Patent **1994**, 5,365,011.

35. Kumar R.; Kleinberg W. T. Integrated Adsorption/Cryogenic Distillation Process for the Separation of an Air Feed. *U. S. Patent* **1995**, 5,463,869.

36. Ghosh, T. K.; Lin, H. D.; Hines, A. l. Hybrid Adsorption Distillation Process for Separating Propane and Propylene. *Ind. Eng. Chem. Res.* **1993**, *32*, 2390-2399.

37. Mujiburohman, M.; Sediawan, W. B.; Sulistyo, H. A Preliminary STudy: Distillation of Isopropanol-Water Mixture Using Fixed Adsorptive Distillation Method. *Sep. Purif. Technol.* **2006**, *48*, 85-92.

38. Fukada, S. Tritium Isotope Separation by Water Distillation Column Packed with Silica-Gel Beads. *J. Nuclear Sci. Technol.* **2004**, *41*, 619-623.

39. Lei, Z. G.; Li, C. Y.; Chen, B. H. Extractive Distillation: A Review. *Sep. Purif. Rev.* **2003**, *32*, 121-213.

40. Knaebel, K. S.; Reinhold, H. E. Landfill Gas: From Rubbish to Resource. *Adsorption-J. Inter. Adsorption Soc.* **2003**, *9*, 87-94.

41. Esteves, I. A. A. C.; Mota, J. P. B. Simulation of a New Hybrid Membrane/Pressure Swing Adsorption Process for Gas Separation. *Desalination* **2002**, *148*, 275-280.

42. Sircar, S.; Waldron, W.E.; Rao, M. B.; Anand, M. Hydrogen Production by Hybrid SMR-PSA-SSF Membrane System. *Sep. Purif. Technol.* **1999**, *17*, 11-20.

43. Feng, X. S.; Pan, C. Y.; Ivory, J. Pressure Swing Permeation: Novel Process for Gas Separation by Membranes. *AIChE J.* **2000**, *46*, 724-733.

44. Feng, X. S.; Pan, C. Y.; Ivory, J.; Ghosh, D. Integrated Membrane/Adsorption Process for Gas Separation. *Chem. Eng. Sci.* **1998**, *53*, 1689-1698.

45. Reynolds, S. P.; Ebner, A.D.; Ritter, J.A. Stripping PSA Cycles for CO_2 Recovery from Flue Gas at High Temperature Using a HTlc Adsorbent. *Ind. Eng. Chem. Res.* **2006**, *45*, 4278-4294.

46. Aspen Adsim 2004.1; Adsorption Reference Guide; Aspen Technology: Cambridge, MA, 2005.

47. Mehrotra, A.; Ebner, A. D.; Ritter, J. A. Arithmetic Approach for Complex PSA Cycle Scheduling. *Adsorption*, **2010**, 16, 113-116.

48. Simo, M.; Brown, C. J.; Hlavacek, H. Simulation of Pressure Swing Adsorption in Fuel Ethanol Production Process. *Comp. Chem. Eng.* **2008**, *32*, 1635-1649

CHAPTER 2: IMPROVED PSA CYCLES OF HYBRID PRESSURE SWING ADSORPTION-DISTILLATION PROCESS FOR ETHANOL DEHYDRATION

2.1 Summary

This work aims to design new PSA cycles with improved PSA performance in the hybrid PSA-distillation system for ethanol-water separation. The commercial hybrid PSA-distillation uses a simple 2-bed 4-step PSA cycle. It is surmised that the PSA performance can be improved by designing a more complicated PSA cycle with more beds and steps.

In this work, four different PSA cycles were designed and simulated using the dynamic adsorption process simulator (DAPS). The performances of these cycles were put back into the hybrid system to calculate all the costs and compare the results with the 2-bed 4-step commercial hybrid PSA-distillation process.

2.2 Introduction

The fuel ethanol, whose concentration is about 98.7 mol%, is used as a gasoline alternative. It is getting wide popularity and application, because it is less poisonous and better to the environment. Anhydrous ethanol can be blended with gasoline as a car fuel additive and most modern gasoline engines will operate well with mixtures of 10 volume%

ethanol. The production of fuel ethanol is increasing fast these years. The North and Central America, South America and Brazil were the major ethanol producers who were together responsible for more than 80% of global fuel ethanol production in 2011.[1] Fermentation of the carbon based feedstocks, such as sugar cane, switch grass and corn, typically results in a mixture containing 3-5 mol% ethanol.[2, 3] Then this mixture is sent to a beer stripper to be enriched into 40 mol%[4], and the product is fed into the second distillation column for further dehydration. Ethanol and water forms an azeotrope with a boiling point about 351K at 1 atm, so the concentration of ethanol produced in a simple distillation cannot be higher than 89.5 mole%. Azeotropic distillation is usually applied after the traditional distillation to produce pure ethanol. However, it has a high consumption of energy. Thus some other separation alternatives have been developed, such as novel distillations, adsorption, liquid-liquid extraction, pervaporation and vapor permeation.[5-7] Hybrid processes[8-10] are also developed to obtain a better performance with less energy consumption. Bausa and Marquardt (2000)[8] presented the shortcut method for designing hybrid membrane/distillation processes for multicomponent mixtures separation. Ethanol purification was studied as an example in their work. Hoch and Espinosa (2008)[9] proposed a methodology to design and simulated the hybrid distillation-pervaporation process for bio-ethanol purification. Operation costs were calculated and show that the hybrid process is economically attractive. Pressure swing adsorption (PSA) is attractive for final ethanol dehydration because of its low energy

requirement. Several adsorbents study and PSA processes for ethanol dehydration have been done by others, and the results show that 3A zeolite is the promising adsorbent.[10-18] In this study, four PSA cycles were designed and simulated using the dynamic adsorption process simulator (DAPS) to improve PSA performance with 3A zeolite being used as adsorbent. Then the PSA unit was connected to the distillation column to build a new hybrid system to calculate all the costs and compare the results with the commercial hybrid PSA-distillation process, in which a simple 2-bed 4-step PSA cycle is applied.

2.3 Modeling

In the commercial hybrid PSA-distillation system for ethanol dehydration, as shown in Figure 1.4a, the distillation column contains 52 stages. The partial condenser on the top is considered as stage 1, and the reboiler at the bottom is considered as stage 52. The saturated liquid stream containing 40 mol% ethanol is fed into the 36^{th} stage. 81.8 mol% ethanol is produced from distillation as distillate, and is sent into a PSA unit, in which fuel ethanol is produced as light product and 47.7 mol% water is produced as heavy product. Usually, the heavy product stream from PSA unit is recycled and mixed with the feed to distillation. 99.5 mol% water is produced as bottom product in distillation. In the PSA unit, a simple 2-bed 4-step cycle is applied, which is shown in Figure 2.2. This is the reference case in this study. In the new hybrid system, as shown in Figure 1.4b, instead of mixing with the feed to distillation, the heavy product stream from PSA is sent into the optimum stage in distillation which was determined by minimizing

the partial condenser and reboiler duties using Chemsep™. The procedure developed to design and study hybrid PSA-distillation processes and all the other details were reported in previous work[19]. Four different PSA cycles, including the simple cycle used in the reference case, were used to simulate the PSA process and were compared.

In the PSA unit, 3A zeolite is used as adsorbent, which is inert to ethanol. So only water is adsorbed in 3A zeolite and ethanol is left in the gas phase. Ethanol is produced as a light product, and water is produced as a heavy product. Figure 2.1 shows the isotherm of water vapor on 3A zeolite at four different temperatures. The experiment data (circles)[15] were fitted to the Toth model (lines), which is given by

$$n = \frac{n_s b P}{(1+(bP)^t)^{1/t}} \quad (1)$$

$$n_s = n_0 + n_1 T \quad (2)$$

$$b = b_0 \exp(\frac{-\Delta H}{RT}) \quad (3)$$

$$t = t_0 + t_1 \frac{1}{T} \quad (4)$$

where q is the equilibrium loading (mol/kg), ΔH is the isosteric heat of adsorption (= -59.56 kJ/mol), and the other parameter values are: q_{s0} = 16.26 mol/kg, q_{st} = -1.9×10^{-2} 1/K, b_0 = 1.6×10^{-8} 1/Pa, n_0 = 1.14 and n_t = -56.42 K.

In this work, four different PSA cycles were simulated and studied, as shown in Figure 2.2-2.5. Case I is a 2-bed 4-step cycle, as shown in Figure 2.2. The steps are feed (F), countercurrent depressurization (CnD), light reflux (LR) and light product pressurization (LPP). During F step, the gas mixture is sent into the bed at constant

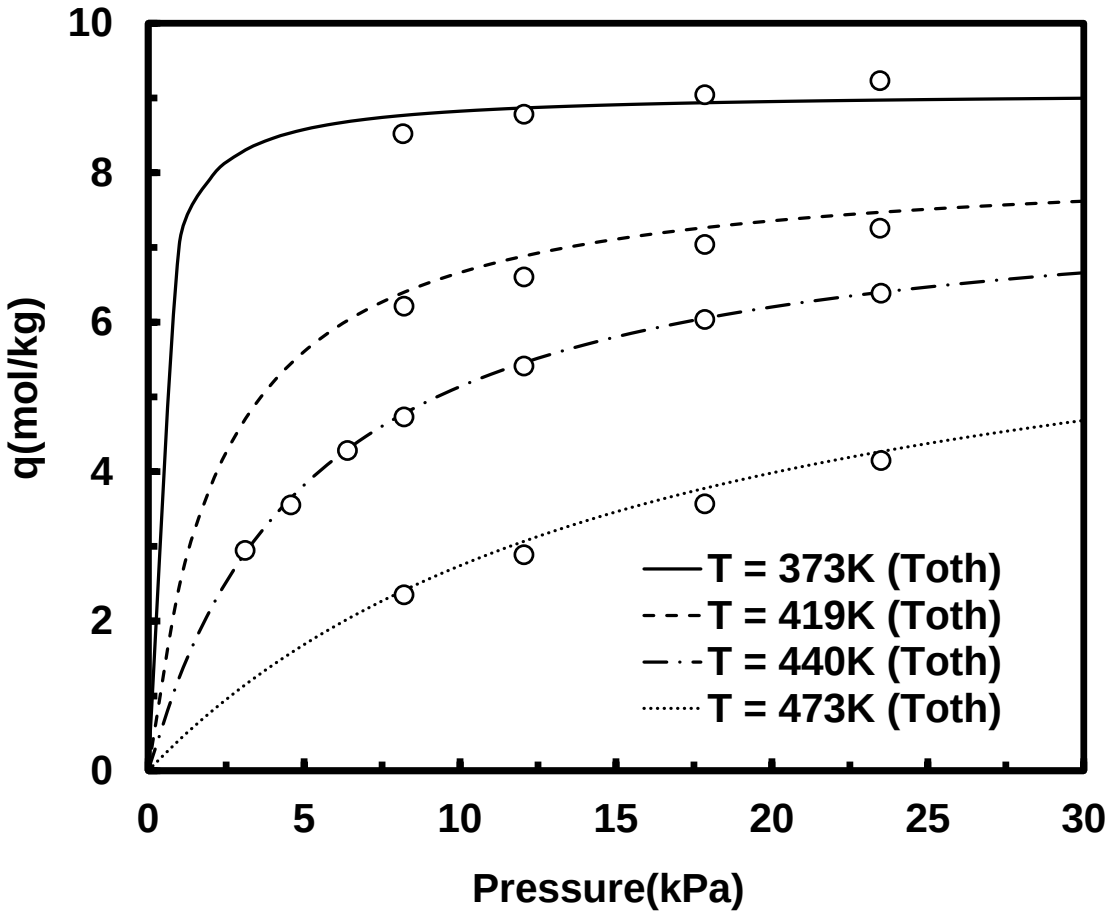

Figure 2.1 Adsorption isotherms for water vapor on 3A zeolite at four different temperatures: 373, 419, 440 and 473 K. Circles are experimental data; lines are the Toth model.

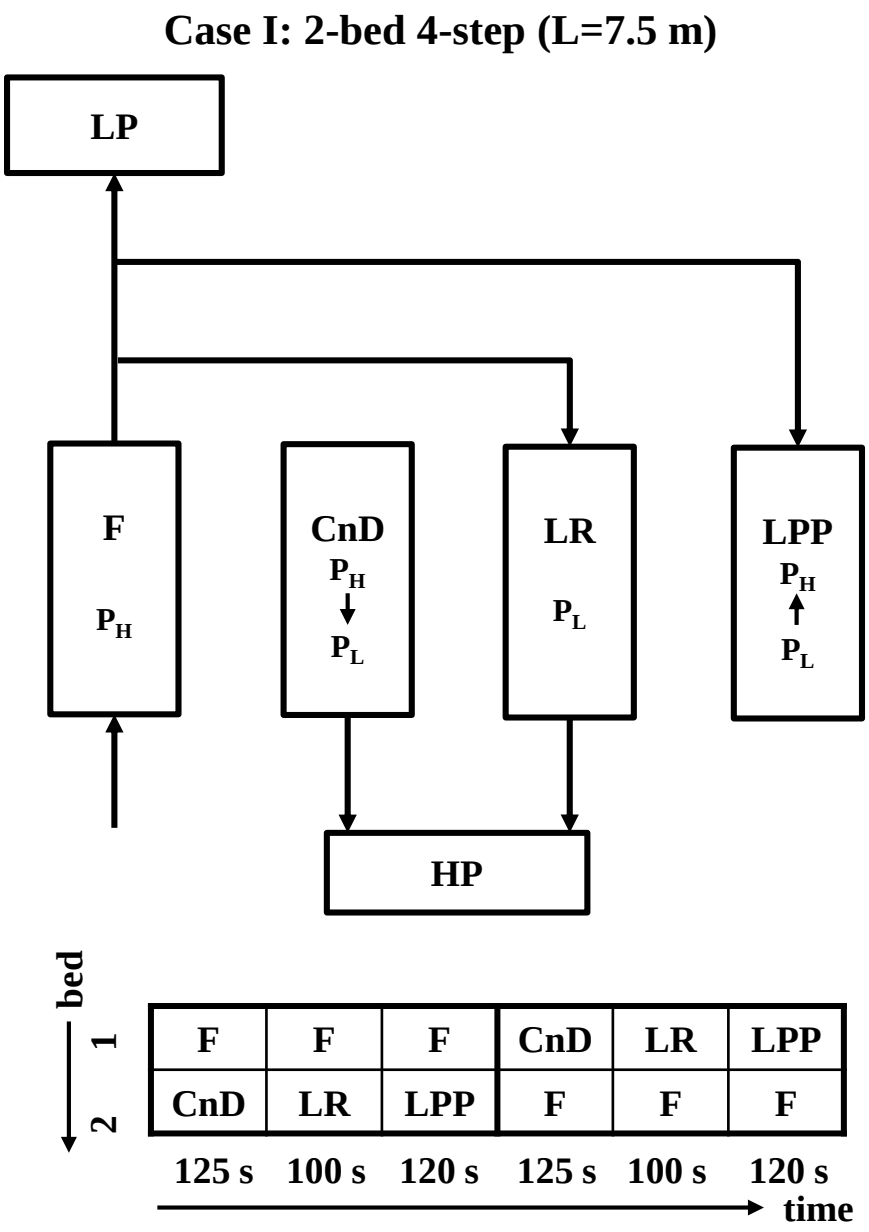

Figure 2.2 2-bed 4-step cycle schematic and schedule for ethanol-water separation.[14] F: feed step; CnD: countercurrent depressurization step; LR: light reflux step; LPP: light product pressurization step. The times indicates the length of each step.

Case II: 3-bed 6-step (L=5.0 m)

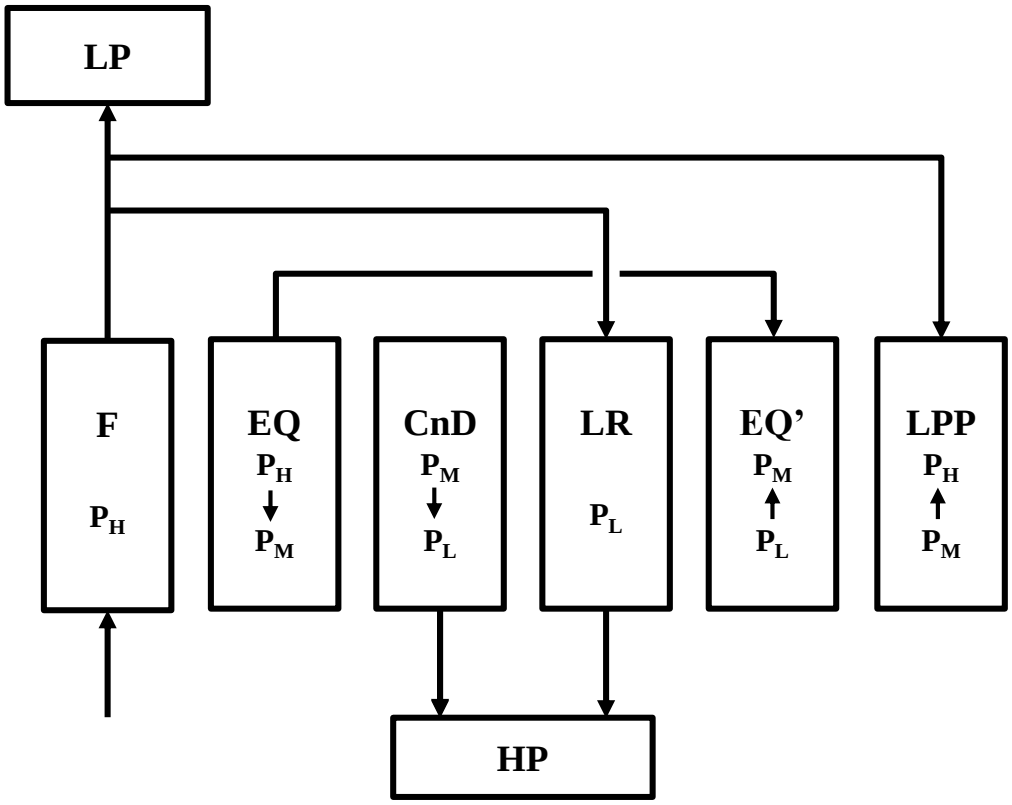

bed									
1	F	F	F	EQ	CnD	LR	EQ'	LPP	LPP
2	EQ	CnD	LR	EQ'	LPP	LPP	F	F	F
3	EQ'	LPP	LPP	F	F	F	EQ	CnD	LR
	110 s	53.3 s	66.7 s	110 s	53.3 s	66.7 s	110 s	53.3 s	66.7 s

time

Figure 2.3 3-bed 6-step cycle schematic and schedule for ethanol-water separation. F: feed step; EQ: cocurrent equalization; CnD: countercurrent depressurization step; LR: light reflux step; EQ': countercurrent equalization; LPP: light product pressurization step. The times indicate the length of each step.

Case III: 4-bed 9-step (L=3.75 m)

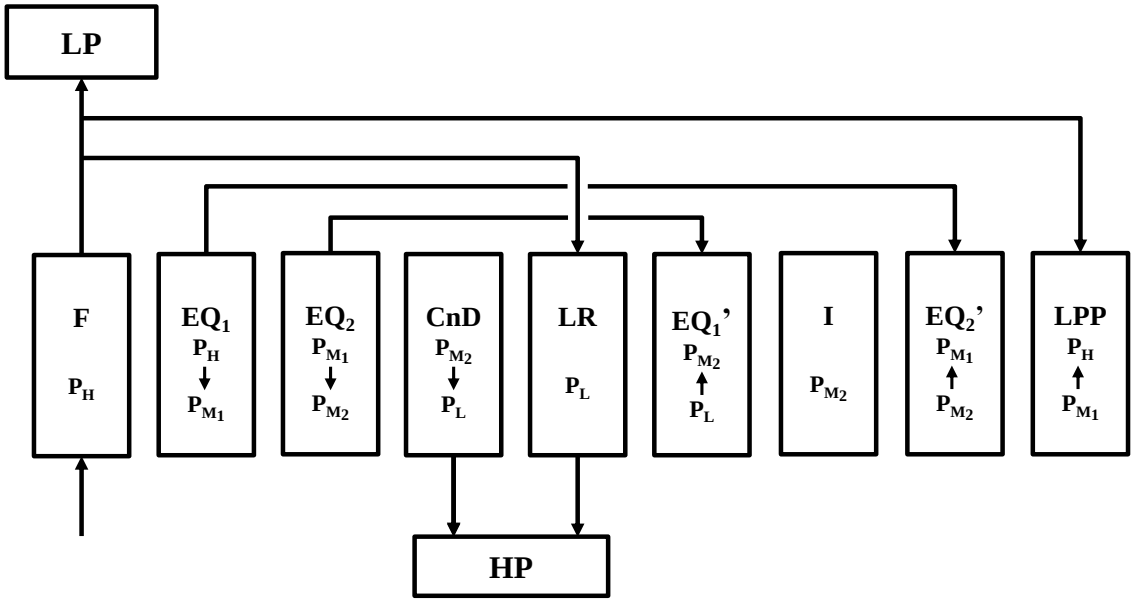

bed												
1	F	F	F	EQ_1	EQ_2	CnD	LR	EQ_2'	I	EQ_1'	LPP	LPP
2	EQ_1	EQ_2	CnD	LR	EQ_2'	I	EQ_1'	LPP	LPP	F	F	F
3	LR	EQ_2'	I	EQ_1'	LPP	LPP	F	F	F	EQ_1	EQ_2	CnD
	EQ_1'	LPP	LPP	F	F	F	EQ_1	EQ_2	CnD	LR	EQ_2'	I
	50 s	61.25 s	61.25 s	50 s	61.25 s	61.25 s	50 s	61.25 s	61.25 s	50 s	61.25 s	61.25 s

time

Figure 2.4 4-bed 9-step cycle schematic and schedule for ethanol-water separation. F: feed step; EQ: cocurrent equalization; CnD: countercurrent depressurization step; LR: light reflux step; EQ': countercurrent equalization; I: idle; LPP: light product pressurization step. The times indicate the length of each step.

Case IV: 4-bed 7-step (L=3.75 m)

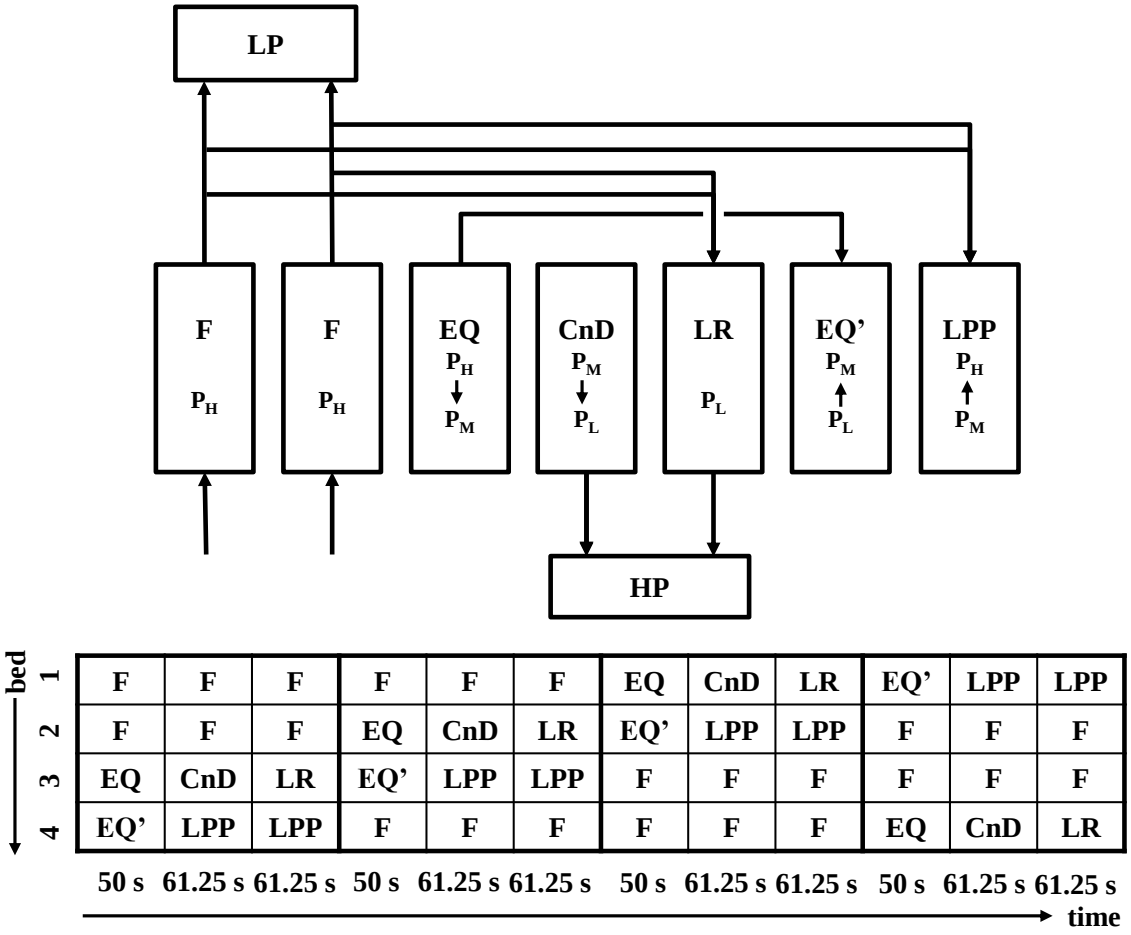

Figure 2.5 4-bed 7-step cycle schematic and schedule for ethanol-water separation. F: feed step; EQ: cocurrent equalization; CnD: countercurrent depressurization step; LR: light reflux step; EQ': countercurrent equalization; LPP: light product pressurization step. The times indicate the length of each step.

pressure, which is the high operating pressure of PSA. Then the bed is depressurized into the low operating pressure during CnD step. Part of the gas in the downstream of F is recycled. Some is sent into the bed as the purge gas at constant pressure during LR step; the rest is sent used to pressurize the bed from the low pressure to the high pressure. Light product (ethanol enriched stream) is collected from the downstream of F step, and heavy product (water enriched stream) is collected from CnD and LR. The time of F step is 345s, and the sum of the time of the other three steps is also 345s. So when one bed is operating the F step, the other bed is operating the other three steps in sequence. Then continuous feeding is obtained. It is the simple PSA cycle used in the reference hybrid system. Case II is a 3-bed 6-step cycle, as shown in Figure 2.3. This cycle is generated by adding one pair of equalization steps (EQ) in Case I. During the equalization steps, two beds are connected at the light ends until the pressures in these two beds are equalized at the intermediate pressure. The pressure in one bed decreases from the high pressure to the intermediate pressure. At the same time, the pressure in the other bed increases from the low pressure to the intermediate pressure. Case III is a 4-bed 9-step cycle, as shown in Figure 2.4. Two pairs of equalization steps are used. In EQ_1, one bed is connected to another one with lower pressure to release some gas, and then connected the other one to release more gas in EQ_2. Thus the beds are connected twice to match the pressures and there are two intermediate pressures. Idle step (I) is used to fulfill the schedule designing, in which all the valves are closed and the pressure is constant. Case IV is a 4-bed 7-step

cycle, as shown in Figure 2.5, similar with Case II, also having one pair of equalization steps. However, there are two feed steps, and two beds are fed at the same time. The purpose of having two feed steps is to have smaller feed flow rate but longer feeding time, so the total mass of feed is the same as that in the other three cases.

The total bed volume in the whole PSA unit was the same for all four cases. So if the bed length in Case I, which has two beds, was 7.5 m, it was 5.0 m in Case II since there were three beds. Similarly, the bed length in Case III and Case IV was 3.75 since there were four beds in both cases. The step time was adjusted proportionally for each case to keep the total cycle time the same.

These four cycles were studied and compared by changing the flow rates of the feed to PSA. For each feed flow rate, all the cases had the same flow rate except Case IV, in which the flow rate was one-half of the others because the feed time was doubled. In this way, the throughput of feed (F) and light reflux (LR) of these four cases were all the same. The throughputs for Case I are given by the following equations

$$\theta_{F,I} = \frac{F_{F,I} t_{F,I}}{M_{bed,I} t_{cycle,I}} \tag{5}$$

$$\theta_{LR,I} = \frac{F_{LR,I} t_{LR,I}}{M_{bed,I} t_{cycle,I}} \tag{6}$$

where $\theta_{F,I}$ is the throughput of the F; $\theta_{LR,I}$ is the throughput of LR; $F_{F,I}$ is the flow rate in F; $F_{LR,I}$ is the flow rate in LR; $t_{F,I}$ is the step time of F; $t_{LR,I}$ is the step time of LR; $M_{bed,I}$ is the mass of adsorbent in each bed; $t_{cycle,I}$ is the total cycle time. Then the throughputs of the other three cases are given by

$$\theta_{F,II} = \frac{F_{F,II}\frac{2}{3}t_{F,II}}{\frac{2}{3}M_{bed,II}t_{cycle,II}} \quad (7)$$

$$\theta_{LR,II} = \frac{F_{LR,II}\frac{2}{3}t_{LR,II}}{\frac{2}{3}M_{bed,II}t_{cycle,II}} \quad (8)$$

$$\theta_{F,III} = \frac{F_{F,III}\frac{1}{2}t_{F,III}}{\frac{1}{2}M_{bed,III}t_{cycle,III}} \quad (9)$$

$$\theta_{LR,III} = \frac{F_{LR,III}\frac{1}{2}t_{LR,III}}{\frac{1}{2}M_{bed,III}t_{cycle,III}} \quad (10)$$

$$\theta_{F,IV} = \frac{\frac{1}{2}F_{F,IV}t_{F,IV}}{\frac{1}{2}M_{bed,IV}t_{cycle,IV}} \quad (11)$$

$$\theta_{LR,IV} = \frac{F_{LR,IV}\frac{1}{2}t_{LR,IV}}{\frac{1}{2}M_{bed,IV}t_{cycle,IV}} \quad (12)$$

The flow rates of feed in Case I, II and III were the same. In Case IV, the flow rate of feed was not the same any more, but one-half of that of the others. However, the step time of feed was twice as that in Case III which also has four beds. That is the step time of feed in Case IV was the same as Case I. So the mass of feed in Case IV was still the same as the other three cases. When canceling the numbers in Eqs. 7, 9 and 11, these equations become the same as Eq. 5. Similarly, it can be shown by the same analysis that the throughput of LR was same in these four cases. The difference is that in case IV, the feed flow rate in LR was the same as that in case I; however, the step time of LR was half of that of case I. So, the throughput was still the same. The bed properties, adsorbent properties and operating conditions of these four PSA cycles were all the same and were summarized in Table 2.1.

All the simulating runs were compared and the qualified ones were picked out to connect with the distillation column to build a hybrid system. The distillation process was simulated using Chemsep™ to get the duties in the reboiler and the partial

condenser, and the other values. The all the duties and costs were compared with the reference case to see which one gave the best saving.

2.4 Results and Discussion

Table 2.2 shows the ethanol recovery and purity for the four different PSA cycles with feed flow rates (F_F) ranging from 50000 to 150000 SLPM. Figure 2.6a and 2.6b also show the simulation results, including water recovery and purity in heavy product and ethanol recovery and purity in light product. The wide arrows in both figures show the direction of feed flow rate decreasing. As shown in Figure 2.6a, water recovery always goes up along with decreasing feed flow rate for all the cases. However, water purity reaches a maximum and then goes down except for case IV. With the same water recovery, the highest water purity is always obtained in case III. Figure 2.6b shows the corresponding ethanol recovery and purity, and higher purity and lower recovery is obtained along with decreasing feed flow rate. The arrow shows the required purity of fuel ethanol, which is 98.7 mol%. So among all the simulation results, those PSA units whose performances in Figure 2.6b are above the arrow satisfy the goal of this study by making fuel grade ethanol. The reference case, which is the commercial hybrid PSA-distillation system, is marked by a dot and the letter "R". The performances of the other satisfactory PSA units are marked from left to right with I1 (Case I with 70000 SLPM (F_F)), I2 (Case I with 80000 SLPM (F_F)), I3 (Case I with 90000 SLPM (F_F)), IV (Case IV with 80000 SLPM (F_F)), II (Case II with 60000 SLPM (F_F)) and III (Case III

Table 2.1 PSA process parameters and conditions used in the DAPS.

3A Zeolite-Ethanol Toth Isotherm Parameters:	
n_0 (mol/kg)	16.26
n_1 (K^{-1})	-1.9×10^{-2}
b_0 (kPa^{-1})	1.6×10^{-8}
t_0	1.14
t_1 (K)	-56.42
ΔH (kJ/mol)	57.95
3A Zeolite LDF Mass Transfer Resistance:	
k_{LDF}^{E} (s^{-1})	1.0×10^{-7}
k_{LDF}^{W} (s^{-1})	1.2×10^{-3}
Bed Properties	
length, Z (m)	7.5 or 5.0 or 3.75
outer radius, r_o (m)	1.25
inner radius, r_i (m)	1.2246
porosity, ε_b	0.31
Wall Properties	
density, ρ_w (kg/m^3)	8000
thermal capacity, C_w (kJ/kg/K)	0.5
heat transfer coefficient, h ($kW/m^2/K$)	0.0 (adiabatic)
temperature, T_w (K)	440.15
Operating Conditions	
PSA feed Temperature, T_{PSA} (K)	440.15
high pressure, P_H (kPa)	379.2
low pressure, P_L (kPa)	13.8
feed flow rate (SLPM)	50,000 or 150,000
mole fraction ethanol in feed, y_D	0.80
3A Zeolite Adsorbent Properties	
radius, r_p (m)	0.005
density, ρ_p (kg/m^3)	1116
porosity, ε_p	0.54
thermal capacity, C_p (kJ/kg/K)	1.045

Table 2.2 PSA performance for four different cycles with feed flow rates from 50000 to 150000 SLPM

Ethanol Case I Case II Case III Case IV(F is half)								
F_F (SLPM)	**Recovery (%)**	**Purity (%)**	**Recovery (%)**	**Purity (%)**	**Recovery (%)**	**Purity (%)**	**Recovery (%)**	**Purity (%)**
150000	89.98	93.39	94.15	91.76	95.47	88.75	89.14	91.27
140000	89.63	94.27	-	-	-	-	-	-
120000	88.71	96.25	93.54	94.51	95.08	90.80	89.34	94.00
100000	87.35	98.29	-	-	-	-	-	-
90000	86.41	99.12	-	-	-	-	-	-
80000	85.22	99.66	91.72	96.62	93.94	95.27	88.36	98.82
70000	83.62	99.91	90.90	98.17	93.41	96.72	-	-
60000	-	-	89.80	99.37	92.68	98.17	-	-
50000	-	-	-	-	91.66	99.22	-	-

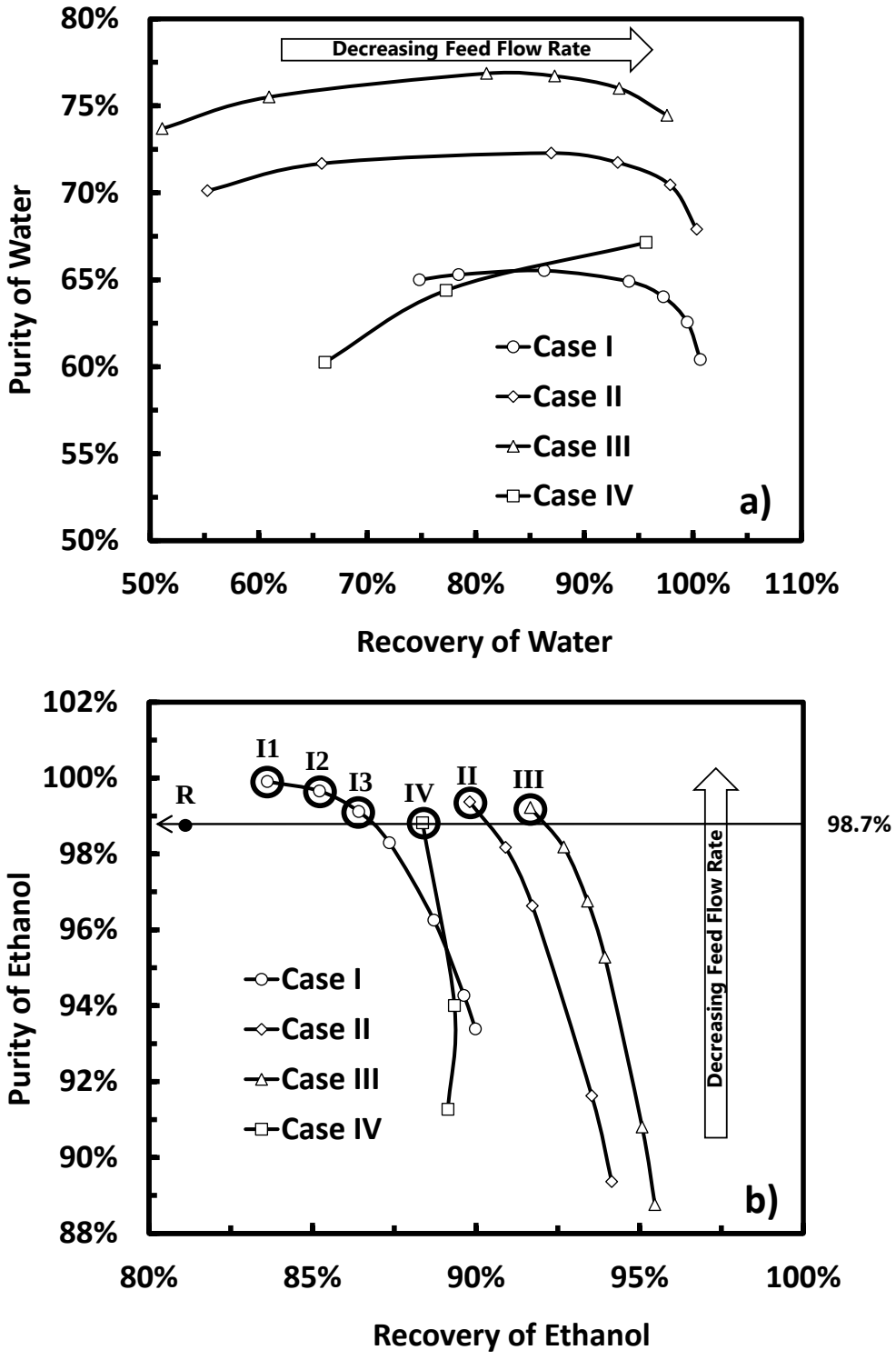

Figure 2.6 PSA performance of four PSA cycles with different feed flow rates.

with 50000 SLPM (F_F)). If these cycles are used to replace the 2-bed 4-step PSA cycle, the PSA performance would improve.

Next, these favorable PSA units were connected to the distillation column to build the hybrid system, and the distillation column was simulated using Chemsep™ to calculate the partial condenser and reboiler costs. The other costs were also calculated and added together to obtain the total operating cost to compare with the reference case. The method of calculating other costs were introduced in the previous work.[19]

Figure 2.7 shows all the duties in the partial condenser, reboiler, distillate heater, side stream condenser and compressors. The duty was calculated as kJ/mol of fuel ethanol finally produced. Each column of points represents each case, and they are marked with the names introduced in Figure 2.6b. As shown in Figure 2.7, most duty is due to the partial condenser and reboiler in the distillation part, and the duties are much lower in the distillate heater, side stream condenser and compressor. The reference case, which is marked with "R", requires more energy than the others in which new PSA cycles are used. Among all the PSA units, the unit with the case III cycle, which is marked by the square, always shows the lowest duty. So the least energy is required in case III, which has two Eq steps in the cycle. Then the total operating cost was calculated according to the duties and the utility prices summarized in Table 2.3. Figure 2.8a shows the total operating cost, which was calculated as dollars of mega mole of fuel ethanol finally produced. Each point represents each case, including the reference case. As shown

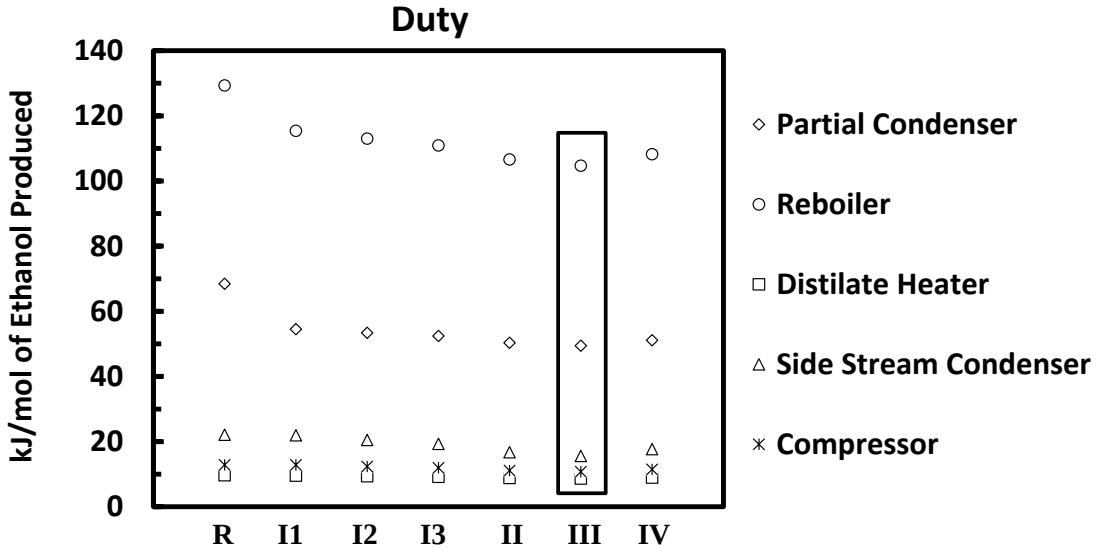

Figure 2.7 Duties in the partial condenser, reboiler, distillate heater, side stream condenser and compressors.

in the figure, the reference case requires more total operating cost than the others, and the hybrid system with a case III PSA unit requires the list cost, which is marked by label "III". Figure 2.8b shows the percentage of total operating cost savings compared with the reference case (for the reference the savings are thus 0%). As shown in this figure, the total operating cost can be reduced with these new PSA units, with a maximum savings of 17.82% if a case III PSA unit is used in the hybrid system. The improved PSA process performance stems from the use of Eq steps in the PSA cycle.

Not only do the operating costs decrease, but also the internal flows in the distillation column decrease. These results are shown in Figure 2.9a and 10b. V_2 is the vapor phase flow from the 2nd stage which is going into the partial condenser (Figure 2.10a), and L_{51} is the liquid phase flow from the 51st stage which is going into the reboiler (Figure 2.9b). ΔV_2 and ΔL_{51} represent the difference of flows in the reference and new cases, which are defined as [V_2 (reference case) - V_2 (new case)] and [L_{51} (reference case) - L_{51} (new case)] respectively. These figures show the percentage reduction in these two flows compared to the reference case. The largest reduction was 12.98%, which was obtained by adding two Eq steps to the PSA cycle. Any reduction implies less mass is sent into the partial condenser and reboiler, which is why the operating cost of the partial condenser and reboiler are both reduced. It also means the throughput or capacity of the distillation column can be increased.

2.5 Conclusions

Table 2.3 Utility Prices

Utility	**Prices (¢/kWh)**
Steam (200 psig)	1.083
Cooling Water	1.7×10^{-7}
Compression (Electricity)	5

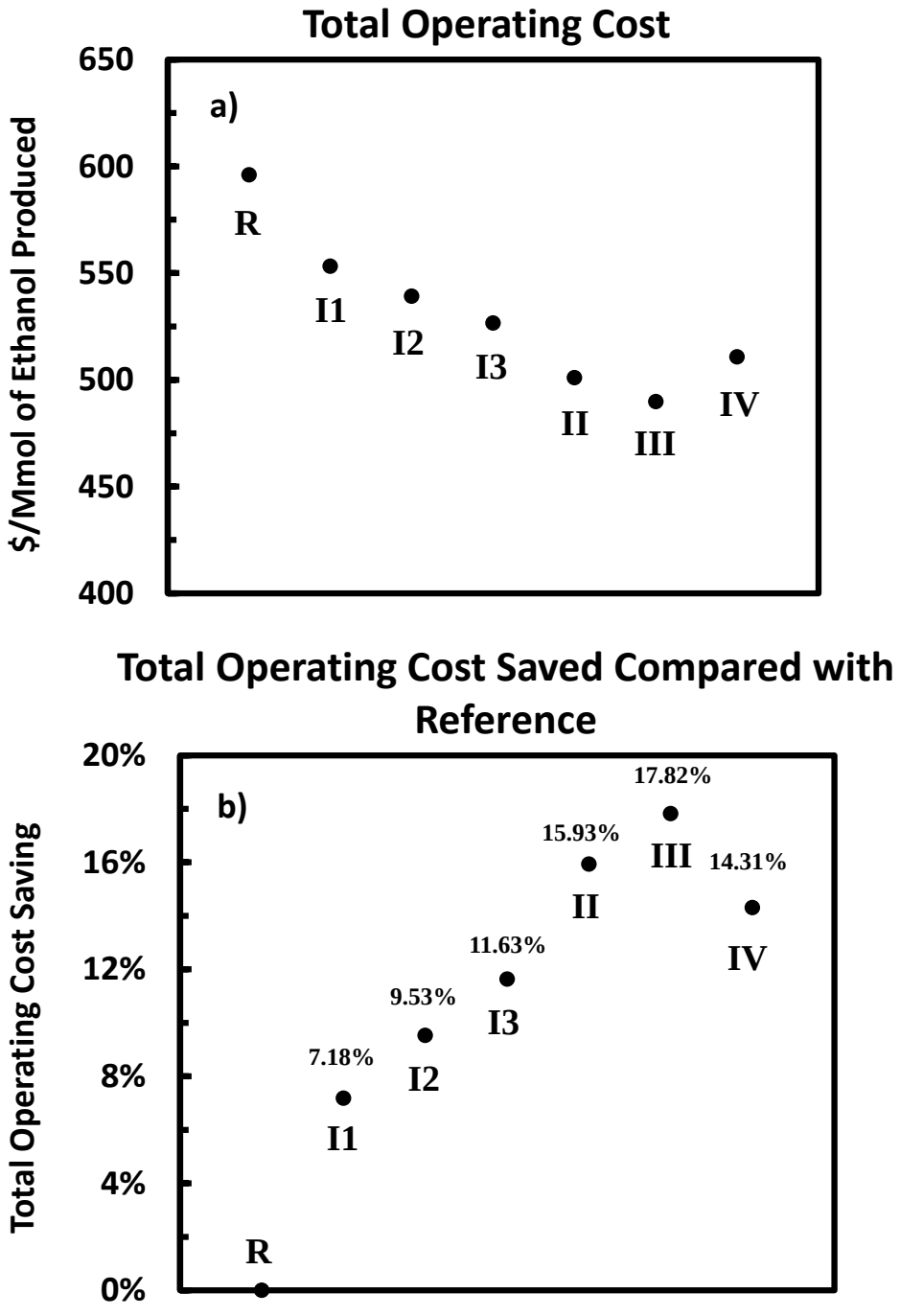

Figure 2.8 Total operating cost and savings of the new hybrid systems compared with the reference case.

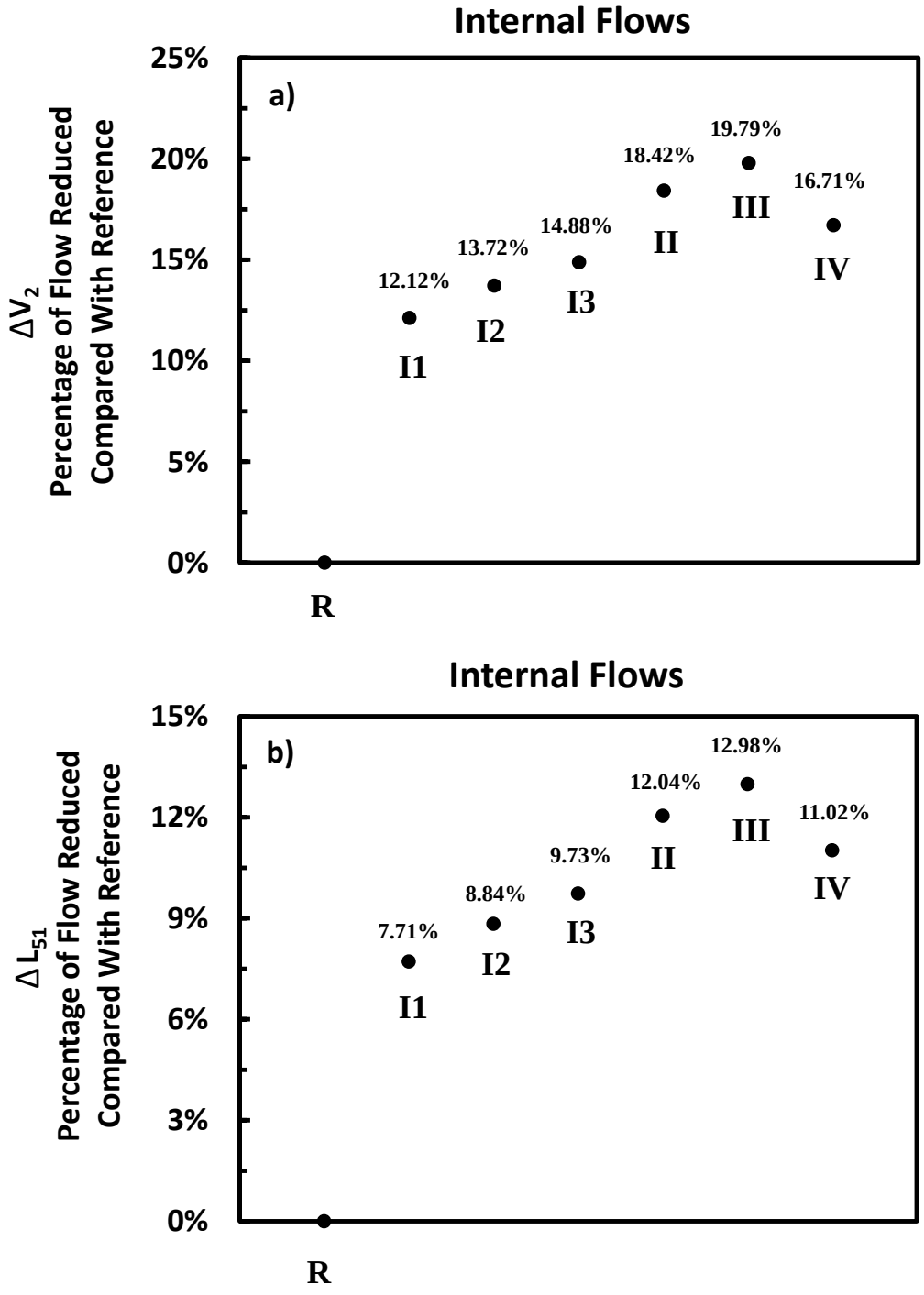

Figure 2.9 Percentage reduction of the internal flows in the distillation column of the new hybrid systems compared with the reference case.

In this work, four different "actual" PSA cycles were simulated and studied. These cycles were tested by keeping the same feed and light reflux throughput and by changing the feed flow rate to the PSA unit. Six cases, which could produce fuel grade ethanol, were picked out and marked with different labels. Then the flow rates and concentrations of all the streams in the hybrid process were calculated based on both the overall mass balance and units' mass balance. The distillation process was simulated in Chemsep^{TM} to obtain the duties in the reboiler and partial condenser. The tray locations of the feed and the side stream were optimized by minimizing the duties in the reboiler and the partial condenser. All the other duties, which are in the side stream total condenser, distillate heater and compressors, were also calculated. Then the operating costs were calculated based on the utility prices, and compared with the reference case. The results show that the PSA performance can be improved by adding equalization steps in the PSA cycle. Less duty was required in the six favorable hybrid PSA systems than in the reference system, and the system with case III cycle required the least duty. Similar results were obtained for the total operating cost calculation. Based on the comparison between the reference and the improved cases, the maximum saving in total operating cost was obtained by using a PSA cycle with two equalization steps, which is about 18%. The flow rates of the internal flows in the distillation column were given by Chemsep^{TM} simulations. According to the comparison, the internal flows in the distillation column can be reduced in the new hybrid systems, and the maximum saving

was obtained in the hybrid system with a case III PSA cycle. It also means the distillation capacity can be increased by the same factor. Thus, equalization steps can improve the performance in the PSA unit, and reduce the total operating cost of the hybrid systems.

REFERENCES

1. http://www.ethanolrfa.org/pages/annual-industry-outlook: RFA's 2012 Ethanol Industry Outlook.
2. Madson, P. W.; Monceaux, D. A. Fuel Ethanol Production. *KATZEN International, Inc.* **2003**.
3. Collura, M. A.; Luyben, W. L. Energy-Saving Distillation Designs in Ethanol Production. *Ind. Eng. Chem. Res.* **1988**, *27*, 1686-1696.
4. Quintero, J. A.; Montoya, M. I.; Sanchez, O. J.; Giraldo, O. H.; Cardona, C. A. Fuel Ethanol Production from Sugarcane and Corn: Comparative Analysis for a Columbian Case. *Energy* **2008**, *33*, 383-399
5. Vane, L. M. Separation Technologies for the Recovery and Dehydration of Alcohols from Fermentation Broths. *Biofuels, Bioprod. Bioref.* **2008**, *2*, 553-588.
6. Collura, M. A.; Luyben, W. L. Energy-Saving Distillation Designs in Ethanol Production. *Ind. Eng. Chem. Res.* **1988**, *27*, 1686-1696.
7. Haelssig, J. B.; Tremblay, A. Y.; Thibault, J. Technical and Economic Considerations for Various Recovery Schemes in Ethanol Production by Fermentation. **2008**, *47*, 6185-6191.

8. Bausa, J.; Marquardt, W. Shortcut Design Methods for Hybrid Membrane/Distillation Processes for the Separation of Nonideal Multicomponent Mixtures. *Ind. Eng. Chem. Res.* **2000**, *39*, 1658-1672.
9. Hoch, P. M.; Espinosa, J. Design of a Hybrid Distillation-Pervaporation Bio-Ethanol Purification Process Using Conceptual Design and Rigorous Simulation Tools. *AIChE Annual Meeting* **2008**, 316a.
10. Quintero, J. A.; Montoya, M. I.; Sanchez, O. J; Giraldo, O. H.; Cardona, C. A. Fuel Ethanol Production from Sugarcane and Corn: Comparative Analysis for a Colombian Case. *Energy*, **2008**, *33*, 385-399.
11. Carmo, M. J.; Gubulin, J. C. Ethanol-Water Separation in the PSA Process. *Adsorption* **2002**, *8*, 235-248.
12. Guan, J.; Hu, X. Simulation and Analysis of Pressure Swing Adsorption: Ethanol Drying Processes by the Electrical Analogue. *Separation and Purification Technology* **2003**, *31*, 31-35.
13. Caputo, D.; Iucolano, F.; Pepe, F.; Colella, C. Modeling of Water and Ethanol Adsorption Data on a Commercial Zeolite-Rich Tuff and Prediction of the Relevant Binary Isotherms. *Microporous and Mesoporous Materials*, **2007**, *105*, 260-267.
14. Simo, M.; Brown, C. J.; Hlavacek, V. Simulation of Pressure Swing Adsorption in Fuel Ethanol Production Process. *Computers and Chemical Engineering* **2008**, *32*, 1635-1649.

15. Simo, M.; Sivashanmugam, S. Brown, C. J.; Hlavacek, V. Adsorption/Desorption of Water and Ethanol on 3A Zeolite in Near-Adiabatic Fixed Bed. **2009**, *48*, 9247-9260.
16. Jeong, J. S.; Jang, B. U.; Kim, Y. R.; Chung, B. W.; Choi, G. W. Production of Dehydrated Fuel Ethanol by Pressure Swing Adsorption Process in the Pilot Plant. *Korean J. Chem. Eng.* **2009**, *26*, 1308-1312.
17. Pruksathorn, P.; Vitidsant, T. Production of Pure Ethanol from Azeotropic Solution by Pressure Swing Adsorption. *American J. of Engineering and Applied Sciences* **2009**, *2*, 1-7.
18. Boonfung, C.; Rattanaphanee, P. Pressure Swing Adsorption with Cassava Adsorbent for Dehydration of Ethanol Vapor. *World Academy of Science, Engineering and Technology* **2010**, *71*, 637-640.
19. Ritter, J. A.; Wu, F.; Ebner, A. D. New Approach for Modeling Hybrid PSA-Distillation Processes. *Ind. Eng. Chem. Res.* **2012,** *51*, 9343-9355

CHAPTER 3: SINGLE PSA SYSTEM AND DUAL TRAIN PSA SYSTEM FOR ETHANOL DEHYDRATION

3.1 Summary

In Chapter 2, several new hybrid PSA-distillation processes with four different PSA cycles were designed, simulated and compared with the commercial hybrid process. The results show that the PSA performance can be improved by adding equalization steps in the cycle and about 18% of total operating cost can be saved. The cost was cut down due to the reduced energy use in the distillation process, so new processes with no distillation may be more energy efficient.

Two new systems with only PSA units were designed to replace the hybrid PSA-Distillation system. One is the single PSA system, and the other is the dual train PSA system. These two systems were simulated using the dynamic adsorption process simulator (DAPS) with different PSA cycles under different operating conditions. The PSA performance was compared and the total operating cost was estimated. Unfortunately, the single PSA system cannot satisfy the product recovery requirement and more total operating cost is required in the dual train PSA system due to high compression cost.

3.2 Introduction

As a gasoline alternative, the fuel ethanol production has been a very popular topic[1] and more energy efficient processes are needed. In order to produce dehydrated ethanol, an additional process is applied which is usually azeotropic distillation. However, it has been supplanted by other less energy consuming processes, such as adsorption, liquid-liquid extraction, pervaporation and vapor permeation.[2-4] Hybrid processes have also been developed and utilized commercially in industry.[5-7] In the previous work, a new methodology of modeling hybrid PSA-distillation process was developed and improved PSA cycles were designed for ethanol dehydration.[8-9] Results show that significant cost saving could be obtained by using the improved hybrid systems compared with the commercial hybrid system. Figure 3.1 shows the costs in the reboiler, compressors, and distillate heater the hybrid system. Cooling cost is negligible because cooling water is very cheap. Based on the calculation, more than 60% of the cost is consumed in partial condenser and reboiler. The cost is reduced by adding a high performance PSA unit in the system because the PSA unit is doing some separation work.

A new system was proposed to let the PSA unit take more separation work and make the cost in distillation as low as possible. It is a single PSA system, in which distillation column was removed and the feed to distillation is sent into the PSA unit directly. The high purity ethanol is produced as light product and water is produced as heavy product. Based on the results and cost calculation, more cost was required in this

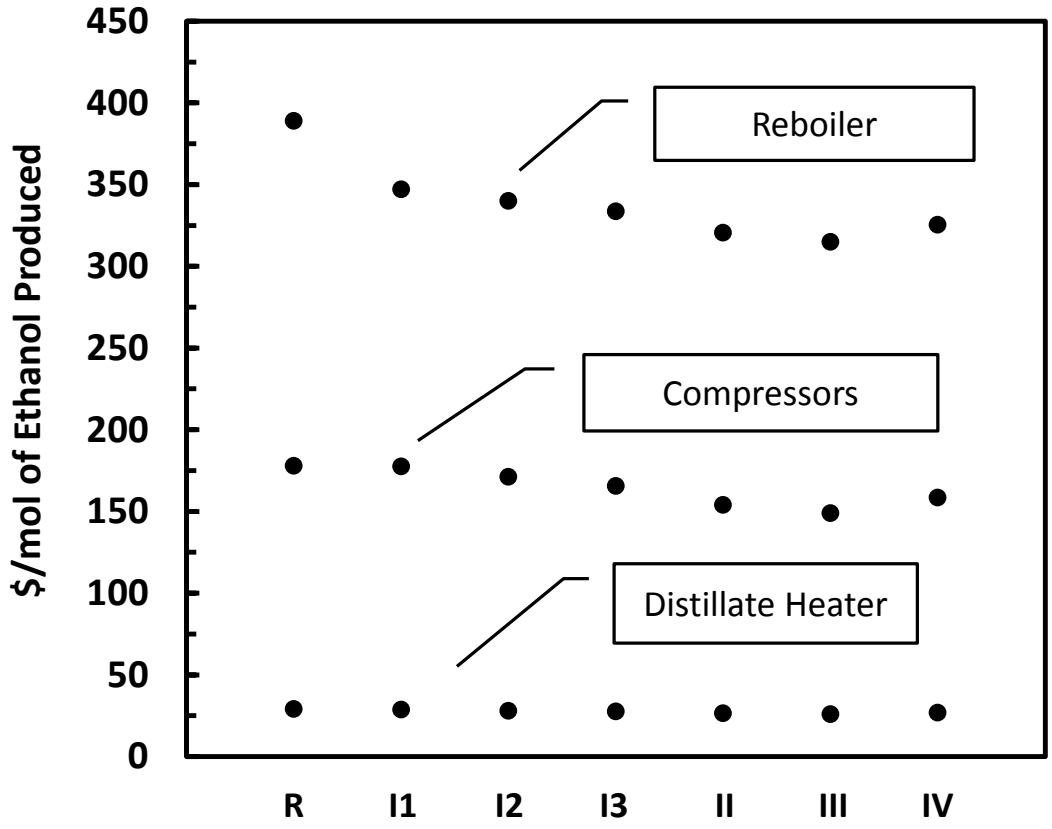

Figure 3.1 Operating costs in the reboiler, compressors and distillate heater of the new hybrid PSA-distillation system for ethanol dehydration.

system, since the recovery of ethanol was lower than that in the hybrid system. In the dual train PSA system, another PSA unit was used to purify water, thus to increase the recovery of ethanol. In the first PSA unit, pure ethanol is produced as light product and the simulating process is the same as that of the PSA unit in the hybrid system. The heavy product stream which is water enriched is sent into the second PSA unit. The light product stream from the second PSA unit is sent back to the first PSA unit. Thus, these two PSA units constitute a "hybrid" PSA system.

3.3 Single PSA System Simulation

3.3.1 Modeling

In the hybrid PSA-distillation process, the feed is the product stream from the beer stripper. When removing the distillation column, as shown in Figure 3.2, the stream is directly fed into the PSA unit in which 98.7 mol% ethanol is produced as a light product and 99.5 mol% water is produced as a heavy product. Before simulation the single PSA process, the operating conditions need to be determined, such as feed flow rate, bed volume, etc. In the hybrid PSA-distillation system, the feed to PSA is 80 mol% ethanol, which is the distillate from distillation. In the single PSA system, the feed to PSA is 40 mol% ethanol. It is assumed that these two systems have the same ethanol product which is expressed by

$$F_1 \times 80\% = F_2 \times 40\% \tag{1}$$

in which F is the feed flow rate. The subscript 1 represents the hybrid PSA-distillation

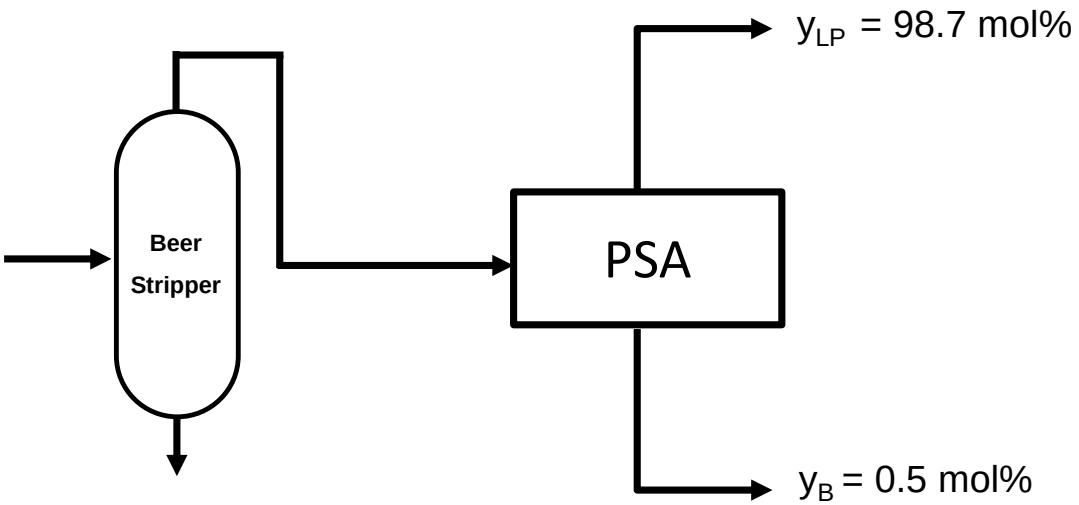

Figure 3.2 Single PSA system for ethanol dehydration. *y* – mole fraction of ethanol in each stream.

system and the subscript 2 represents the single PSA system. Thus, the feed flow rate in the single PSA is twice of that in the hybrid system. From the amount of water to be removed, the bed size of the single PSA system can be calculated.

$$F_{water,1} = F_1 \times (1 - 80\%) \quad (2)$$

$$F_{water,2} = F_2 \times (1 - 40\%) \quad (3)$$

$$F_{water,2} = 6F_{water,1} \quad (4)$$

$$V_{bed,2} = 6V_{bed,1} \quad (5)$$

where F_{water} is the amount of water needs to be removed; V_{bed} is the bed volume. According to the calculation, the bed volume in the single PSA system should be 6 times of that in the hybrid PSA-distillation system. In the simulation, the bed was enlarged by increasing the radius and keeping the height of the bed the same as that in the hybrid system.

The cycles for the single PSA system were the same as those in the hybrid PSA-distillation system, as shown in Figure 3.3. The details of the cycles were introduced in Chapter 2. Case I is a 2-bed 4-step cycle and the steps are feed (F), countercurrent depressurization (CnD), light reflux (LR) and light product pressurization (LPP). Case I is a 3-bed 6-step cycle which has one pair of equalization steps. Case III is a 4-bed 9-step cycle which has two pairs of equalization steps. Case IV is a 4-bed 6-step cycle which also has one pair of equalization steps. Bed length and step time was adjusted proportionally to keep the feed throughput and light reflux throughput the same for all of

Case I: 2-bed 4-step

F	**F**	**F**
CnD	**LR**	**LPP**

Case II: 3-bed 6-step

F	**F**	**F**
EQ	**CnD**	**LR**
EQ'	**LPP**	**LPP**

Case III: 4-bed 9-step

F	**F**	**F**
EQ_1	**EQ_2**	**CnD**
LR	**EQ_2'**	**I**
EQ_1'	**LPP**	**LPP**

Case IV: 4-bed 7-step

F	**F**	**F**
F	**F**	**F**
EQ	**CnD**	**LR**
EQ'	**LPP**	**LPP**

Figure 3.3 Four different PSA cycles for ethanol-water separation are depicted. Each row represents one bed in the cycle, and the unit blocks represent the steps in each cycle.

the four cases with the same operating conditions. The feed flow rate was half of that in the first three cases, but the feed time was doubled. The adsorbent is 4A zeolite and its properties are summarized in Table 3.1 along with the bed properties and operating conditions. Simulations were carried out using dynamic adsorption process simulator (DAPS) with different total cycle time. The feed flow rate was 140000 SLPM in the first three cases and 7000 SLPM for Case IV. The high operating pressure was 125 kPa and the low operating pressure was 13.8 kPa.

3.3.2 Results and Discussion

Table 3.2-3.3 show the PSA performance of all the single PSA simulations with total cycle time ranging from 480s to 3160s for Case I and IV; 150s to 690s for Case II and III. Figure 3.4 shows ethanol and water recovery and purity of all the four cases with different total cycle time. Each curve represents each case and the arrows in the figures show the direction of the total cycle time increasing. When the total cycle time increased, the feed step time increased proportionally. The water front moved closer to the end of the bed. Thus, more ethanol was pushed out of the bed to increase the recovery and some water broke through to contaminate the light product and decreased the purity of ethanol. Meantime, water recovery decreased due to breaking through into the light product. The regions close to the right up corner of the figures represent high PSA performance. As shown in Figure 3.4, Case I obtained the highest product recovery and purity. The purity of fuel ethanol is 98.7 mol%. According to the results shown in Table 3.2, it was very

Table 3.1 PSA process parameters and conditions used in the DAPS.

3A Zeolite-Ethanol Toth Isotherm Parameters:	
n_0 (mol/kg)	16.26
n_1 (K^{-1})	-1.9×10^{-2}
b_0 (kPa^{-1})	1.6×10^{-8}
t_0	1.14
t_1 (K)	-56.42
ΔH (kJ/mol)	57.95
3A Zeolite LDF Mass Transfer Resistance:	
k_{LDF}^{E} (s^{-1})	1.0×10^{-7}
k_{LDF}^{W} (s^{-1})	1.2×10^{-3}
Bed Properties	
length, Z (m)	7.5 or 5.0 or 3.75
outer radius, r_o (m)	3.0254
inner radius, r_i (m)	3.0
porosity, ε_b	0.31
Wall Properties	
density, ρ_w (kg/m^3)	8000
thermal capacity, C_w (kJ/kg/K)	0.5
heat transfer coefficient, h ($kW/m^2/K$)	0.0 (adiabatic)
temperature, T_w (K)	440.15
Operating Conditions	
PSA feed Temperature, T_{PSA} (K)	440.15
high pressure, P_H (kPa)	125.0
low pressure, P_L (kPa)	13.8
feed flow rate (SLPM)	140,000
mole fraction ethanol in feed, y_D	0.40
Total cycle time t_c	variable
3A Zeolite Adsorbent Properties	
radius, r_p (m)	0.005
density, ρ_p (kg/m^3)	1116
porosity, ε_p	0.54
thermal capacity, C_p (kJ/kg/K)	1.045

Table 3.2 PSA performance of single PSA system with four different cycles and different total cycle time: Ethanol recovery (R) and Purity (P)

Ethanol	**Case I**		**Case II**		**Case III**		**Case IV**	
t_c (s)	**R (%)**	**P (%)**	**R (%)**	**P (%)**	**R (%)**	**P (%)**	**R (%)**	**P (%)**
150	-	-	-	-	59.92	99.62	-	-
185	-	-	-	-	64.77	98.76	-	-
225	-	-	-	-	68.41	97.18	-	-
260	-	-	61.33	99.99	71.43	96.01	-	-
335	-	-	66.76	99.90	75.27	93.97	-	-
410	-	-	70.18	99.51	77.75	92.63	-	-
480	54.80	100.00	72.56	98.97	79.38	91.73	59.23	100.00
550	58.67	100.00	74.16	98.43	80.33	91.16	60.77	100.00
621	61.62	100.00	75.46	96.99	81.21	90.65	62.24	100.00
690	63.90	100.00	76.64	96.48	81.91	90.23	63.26	100.00
760	65.85	100.00	-	-	-	-	64.10	100.00
910	69.04	100.00	-	-	-	-	65.44	100.00
985	-	-	-	-	-	-	65.96	100.00
1060	71.29	100.00	-	-	-	-	66.41	100.00
1360	74.16	100.00	-	-	-	-	67.73	99.98
1660	75.95	100.00	-	-	-	-	68.58	99.91
1960	77.09	99.99	-	-	-	-	69.32	99.59
2260	77.87	99.93	-	-	-	-	69.62	98.67
2560	78.47	99.61	-	-	-	-	69.90	96.67
2860	79.18	98.21	-	-	-	-	70.91	92.46
3160	80.04	94.96	-	-	-	-	-	-

Table 3.3 PSA performance of single PSA system with four different cycles and different total cycle time: Water recovery (R) and purity (P)

Water	**Case I**		**Case II**		**Case III**		**Case IV**	
t_c (s)	**R (%)**	**P (%)**	**R (%)**	**P (%)**	**R (%)**	**P (%)**	**R (%)**	**P (%)**
150	-	-	-	-	99.76	78.68	-	-
185	-	-	-	-	99.31	80.57	-	-
225	-	-	-	-	98.53	82.36	-	-
260	-	-	99.99	79.40	97.80	83.60	-	-
335	-	-	99.90	81.69	96.52	85.33	-	-
410	-	-	99.68	83.24	95.56	86.45	-	-
480	100.00	76.57	99.39	84.30	94.87	87.22	100.00	78.33
550	100.00	78.13	99.10	85.04	94.40	87.68	99.99	79.01
621	100.00	38.97	98.50	85.76	93.96	88.11	99.98	79.60
690	100.00	36.61	98.07	86.14	93.59	88.45	99.97	80.06
760	100.00	34.67	-	-	-	-	99.99	80.44
910	100.00	31.53	-	-	-	-	99.99	81.09
985	-	-	-	-	-	-	99.98	81.32
1060	100.00	29.31	-	-	-	-	99.98	81.51
1360	99.98	85.04	-	-	-	-	99.95	82.08
1660	99.96	85.91	-	-	-	-	99.86	82.46
1960	99.93	86.48	-	-	-	-	99.66	82.76
2260	99.86	86.87	-	-	-	-	99.23	82.82
2560	99.65	87.15	-	-	-	-	98.33	82.83
2860	98.85	87.43	-	-	-	-	96.82	83.11
3160	96.70	87.65	-	-	-	-	-	-

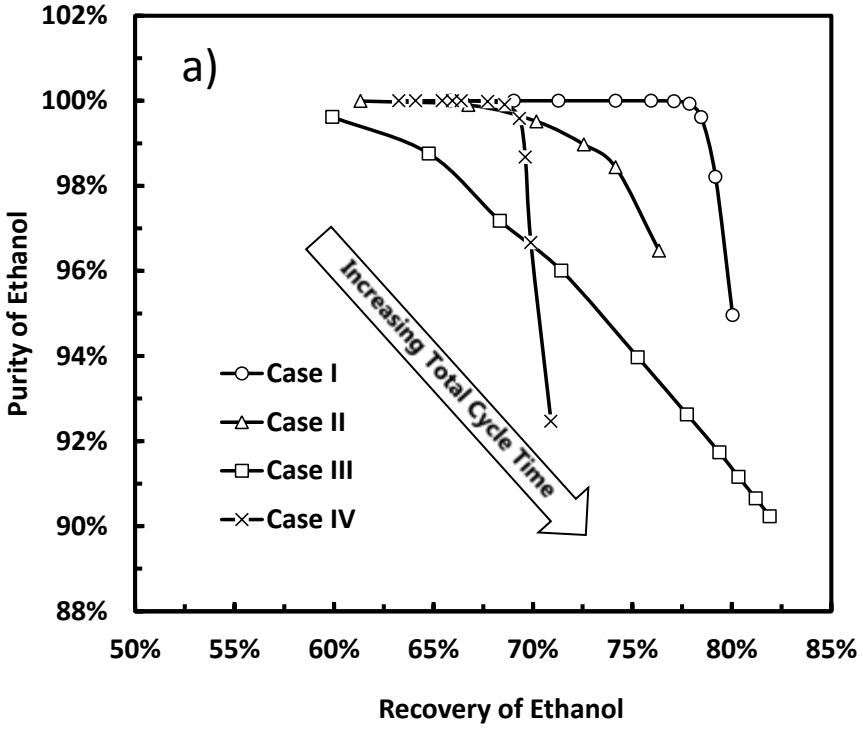

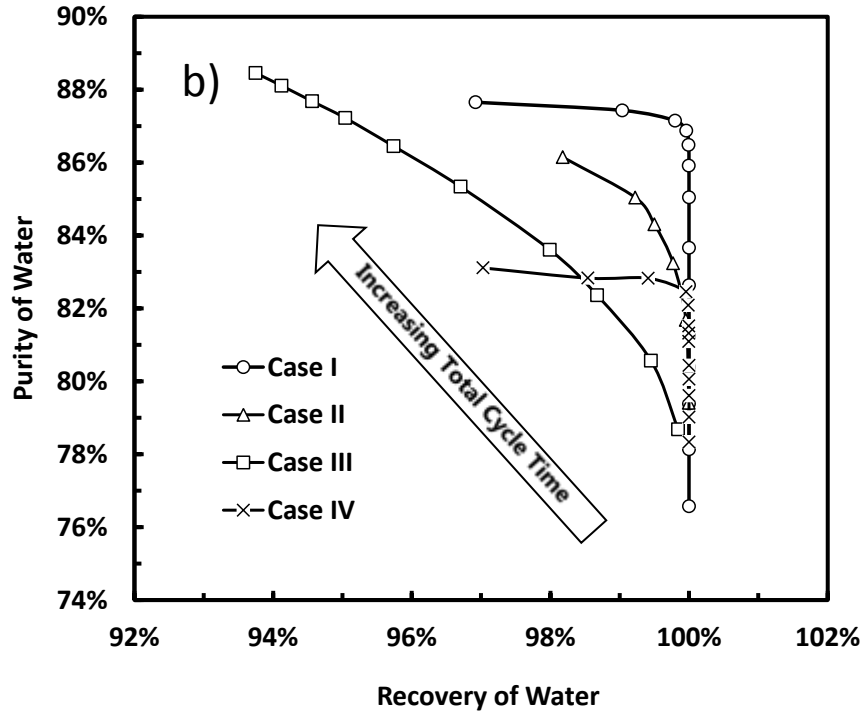

Figure 3.4 a) Water recovery and purity produced in the single PSA system with four different PSA cycles; b) ethanol recovery and purity produced in the single PSA system with four different PSA cycles.

easy to reach the required ethanol purity with these four PSA cycles, and even purer ethanol could be produced. However, compared with the performance of the hybrid PSA-distillation system, the purity of water produced in the single PSA system was much lower. In another word, the recovery of ethanol could not reach the required level. So it was hard to produce both pure heavy product and light product from only one PSA unit. Another separation step is needed to purify water and increase the recovery of ethanol.

3.4 Dual Train PSA System Simulation

3.4.1 Modeling

The dual train PSA system, which is also a hybrid PSA system, is comprised by two PSA units, as shown in Figure 3.5. PSA I was the one in the single PSA system and it was simulated with four different cycles. The simulation with Case I cycle and 2560s total cycle time, which obtained the best performance, was taken as an example of the performance in PSA I. 99.61 mol% ethanol was produced as the light product. The water purity from PSA I was 87.15 mol%, and it was sent into PSA II, in which water was purified to 99.5 mol% as the heavy product. The other stream from PSA II which was ethanol enriched was sent back into PSA I. If ethanol purity from PSA II was about 40 mol%, the stream could be mixed with the feed to PSA I. The flow rates of all the other streams could be calculated from the mass balance. In the actual PSA simulation, the feed flow rate, which was the sum of F_1 and R, was 140000 SLPM, and it was the same as that in the single PSA system simulation. Then the corresponding feed flow rate to PSA II

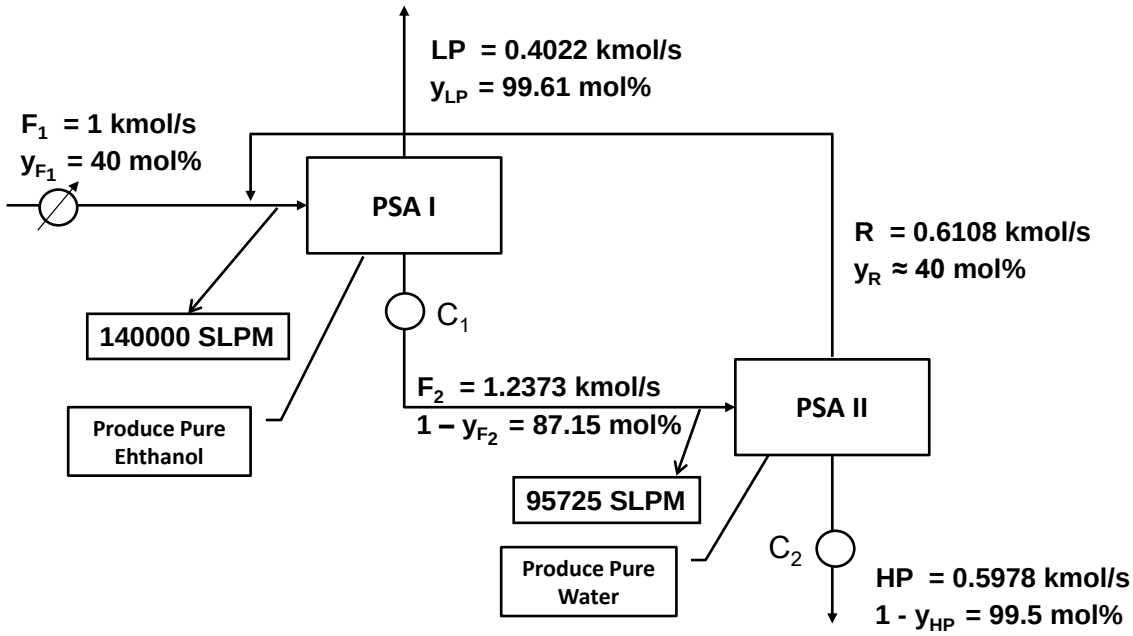

Figure 3.5 Dual Train PSA system. C_1 and C_2 – compressors; F_1 – feed to PSA I; F_2 – feed to PSA II; HP – heavy product (water enriched); LP – light product (ethanol enriched); R – recycled stream from PSA II; y – mole fraction of ethanol.

could be calculated and it was 95725 SLPM. The operating temperature was 440.15 K; high operating pressure was 125 kPa; low operating pressure was 13.8 kPa.

The first three cycles in Figure 3.3 were used to simulate PSA II process. The total cycle time was set to be the same as that of PSA I, which was 2560 s, since PSA I was connected to PSA II and these two units needed to finish each cycle at the same time. The variable was bed size ranging from 0.5 to 1.0 times of the bed sized of PSA I. The heavy product pure water was supposed to be produced from PSA II, and pure ethanol was not required in this process, so water breaking through was allowed to push as much ethanol out of the bed as possible by reducing the bed size. The same adsorbent 3A zeolite was used as PSA I simulation and its properties are summarized in 2.1. The other operating conditions were also the same as those in PSA I simulations.

3.4.2 Results and Discussion

The simulation results of PSA II of the dual train PSA system were summarized in Table 3.4 and Figure 3.6. Figure 3.6a shows water recovery and purity and Figure 3.6b show ethanol recovery and purity. The arrows at the bottom of the figures represent the direction of bed volume decreasing. As the bed volume decreased, the water front moved to the end of the bed and pushed more ethanol out of the bed. Thus, water purity increased, but water recovery decreased due to water breaking through in the feed step. The single circle in the figures was the goal of the performance (water recovery 78.47%; water purity 99.50%; ethanol recovery 97.32%; ethanol purity 40%), which was the ideal

Table 3.4 PSA performance of PSA II of the dual train PSA system with three different cycles: recovery (R) and purity (P)

Water	**Case I**		**Case II**		**Case III**	
Z_2	**R (%)**	**P (%)**	**R (%)**	**P (%)**	**R (%)**	**P (%)**
$1.0 \times Z_1$	100.00	93.97	-	-	80.65	94.89
$0.8 \times Z_1$	100.00	94.71	74.55	98.55	63.58	94.91
$0.7 \times Z_1$	97.30	94.81	65.75	98.59	55.55	95.52
$0.6 \times Z_1$	72.97	97.28	57.84	98.53	-	-
$0.5 \times Z_1$	60.58	97.68	-	-	-	-
Ethanol	**Case I**		**Case II**		**Case III**	
Z_2	**R (%)**	**P (%)**	**R (%)**	**P (%)**	**R (%)**	**P (%)**
$1.0 \times Z_1$	56.19	100.00	-	-	71.72	44.10
$0.8 \times Z_1$	62.12	100.00	94.28	32.82	77.41	28.59
$0.7 \times Z_1$	64.17	85.12	94.73	26.78	82.53	23.96
$0.6 \times Z_1$	86.83	27.54	95.05	23.36	-	-
$0.5 \times Z_1$	90.22	22.64	-	-	-	-

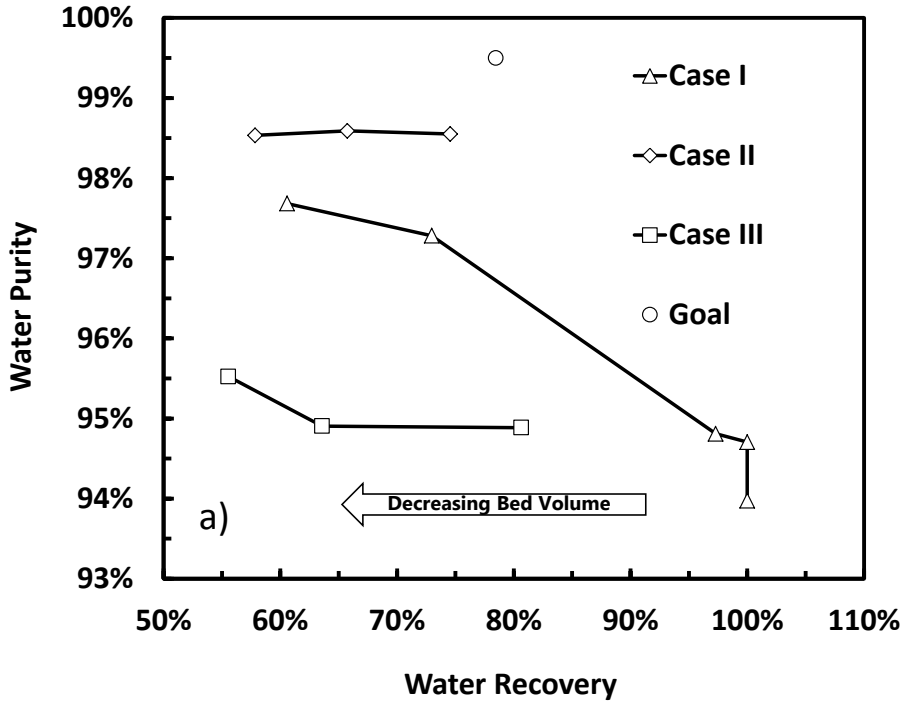

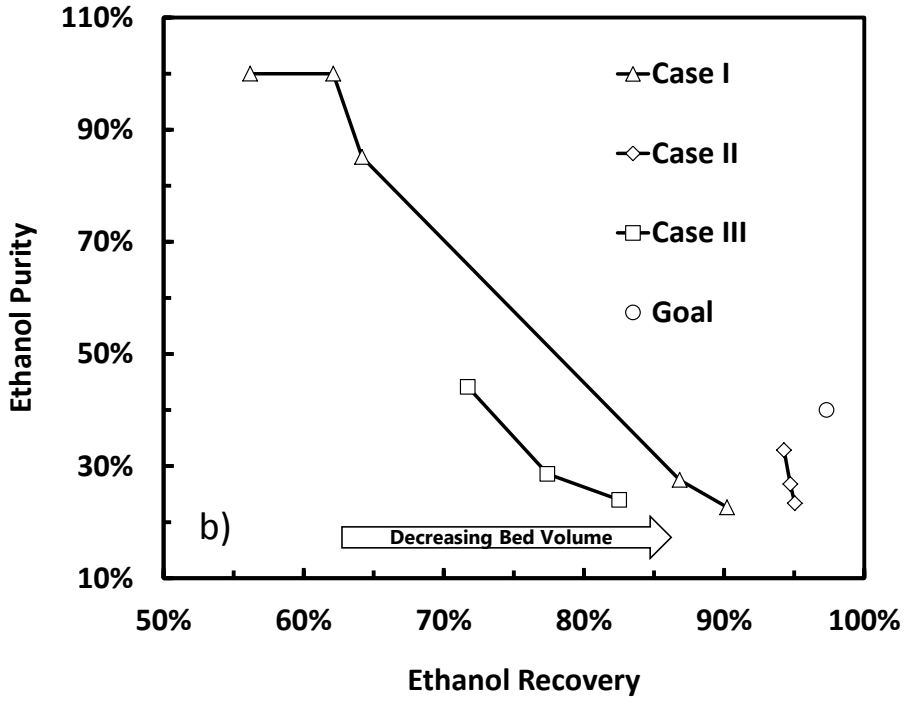

Figure 3.6 a) water recovery and purity in PSA II of the dual train PSA system; b) ethanol recovery and purity of PSA II of the dual train PSA system.

performance of PSA II of the dual train PSA system. As shown in the figures, the cycle with one pair of equalization steps had better performance than the simple 4-bed 4-step cycle. However, none of the simulations could obtain the goal performance. The cycle with two pairs of equalization steps did not have better performance as it did in the hybrid PSA-distillation system.

Details of the cycles were analyzed to understand the relation between the cycles and the performance. Water was produced as heavy product from counter current depressurization (CnD) and light reflux (LR), and water purity depended on the streams coming out of these two steps. Figure 3.7 shows the mass balance in counter current depressurization (CnD) and light reflux (LR) of each cycle. The numbers were the moles of ethanol or water going into or out of each step. The numbers with % were the percentages of water or ethanol in each stream. As shown in the cycle schedule tables in Figure 3.7, LR took the downstream from the feed step (F). During feed, ethanol fraction in the downstream was high in the beginning and then went down as water started to break through. In Case I, the purity of water from CnD was 98.84%. LR took the downstream from the middle part of feed step, in which water purity was 85.46%. Then these two streams were mixed to get the final water purity which was 94.17%. In Case II, during the equalization steps, water front was pushed closer to the end of the bed after feed, and almost all the ethanol was pushed out of the bed. So pure water was produced from CnD. LR was taking the downstream from the last part of feed which contains more

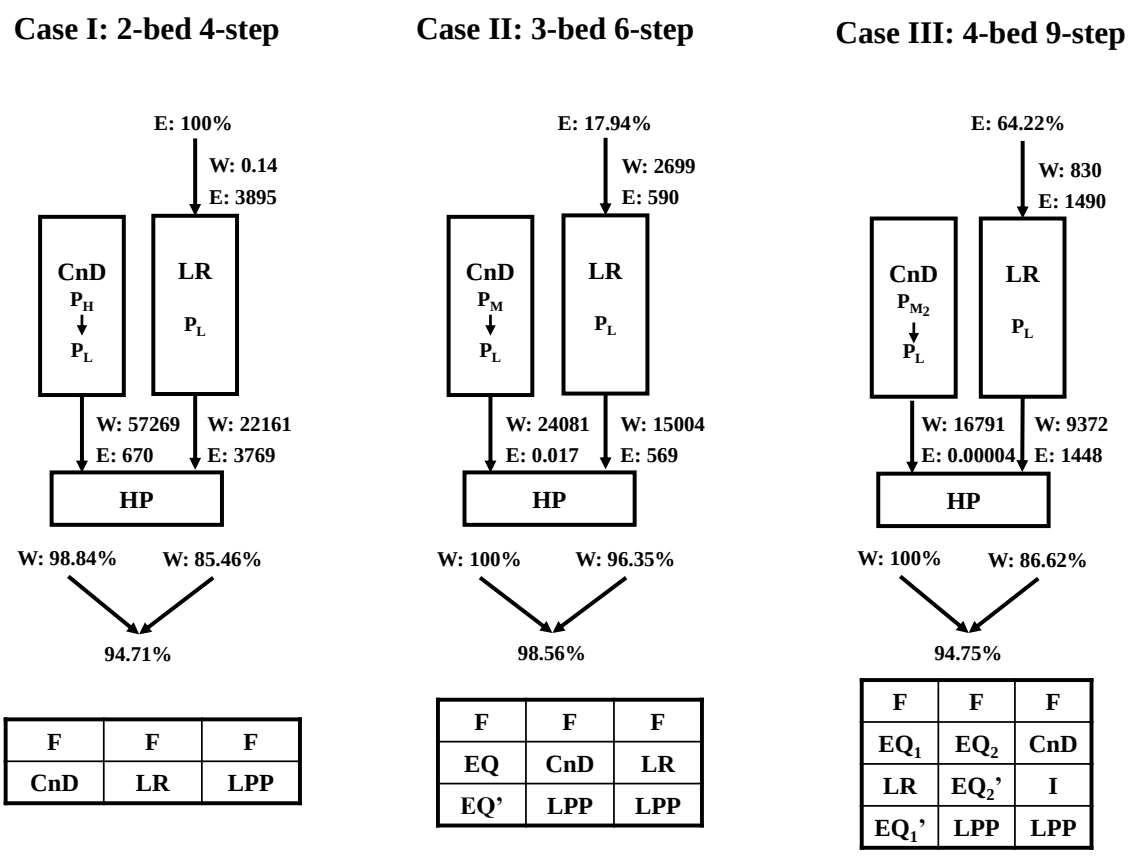

Figure 3.7 Mass balance analysis in counter current depressurization (CnD) and light reflux (LR) steps. W – water; E – ethanol; the numbers represent the moles in each stream in and out the bed; the numbers with % represent water or ethanol purity.

water. So water purity from LR was also very high, which results in high purity final product. In case III, LR took the downstream from the first part of feed which contains more ethanol. Thus, the pure water stream from CnD was diluted by the stream from LR. So the cycle with two pairs of equalization steps did not obtain better performance as the hybrid PSA-distillation system. LR is usually applied when pure light product is required. However, in PSA II of the dual train PSA system, pure heavy product was required. Thus, LR was not as necessary as it was in the hybrid PSA-distillation system, or less mass should be sent into LR. Next, Case II was simulated with less mass going into LR to increase final water purity.

Figure 3.8 and Table 3.5 shows the simulation results including the previous ones and the new ones of Case II with less mass into LR. Much better performance was obtained and the goal performance was reached with new Case II cycle design. The less mass was going into LR, the purer water was produced. The total operating cost of the dual train PSA system were estimated to compare with the hybrid PSA-distillation system, as shown in Table 3.6. Unfortunately, the dual train PSA system requires more total operating cost due to the high compression cost.

3.5 Conclusions

The new hybrid PSA-distillation system could obtain significant cost saving because the PSA unit did some separation work, thus the reboiler cost of the distillation process was reduced. So a single PSA system was developed to replace the hybrid

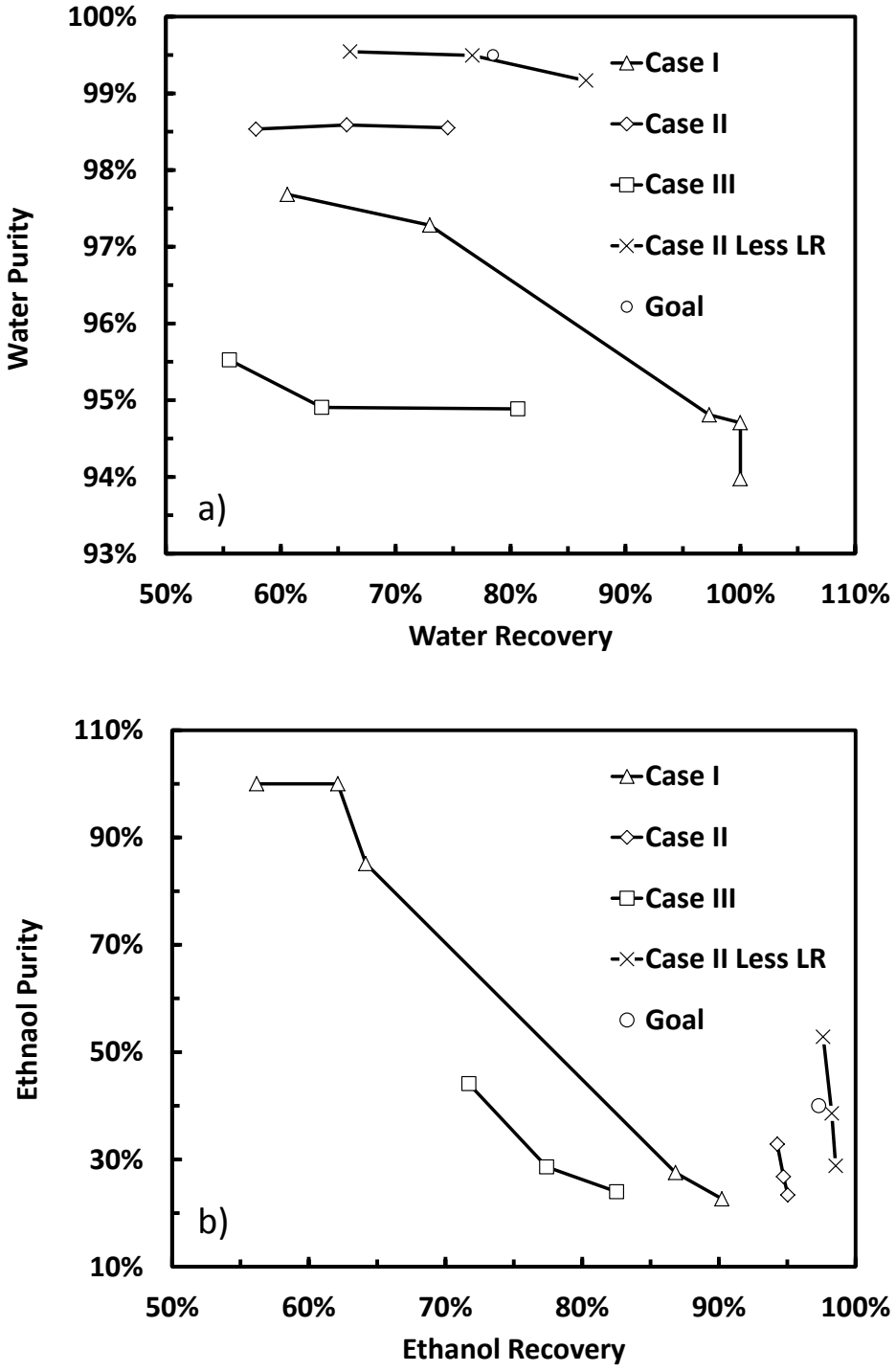

Figure 3.8 PSA performance of PSA II of the dual train PSA system with less LR and Case II cycle.

Table 3.5 PSA performance of PSA II of the dual train PSA system with three different cycles: recovery (R) and purity (P)

Case II (Less LR)	**Water**		**Ethanol**	
Z_2	**R (%)**	**P (%)**	**R (%)**	**P (%)**
$1.0 \times Z_1$	86.57	99.17	97.63	52.84
$0.7 \times Z_1$	76.67	99.50	98.26	38.55
$0.6 \times Z_1$	66.04	99.54	98.55	28.79

Table 3.6 Comparison of the total operating cost ($/Mmol of fuel ethanol) of the hybrid PSA-distillation system (Hybrid) and the dual train PSA system (Dual).

Unit ($)	**Reboiler/ Condenser**	**Heater**	**Compressors**	**Total Operating Cost**
Hybrid	388.94	29.05	177.98	595.96
Dual	-	43.75	837.03	880.77

PSA-distillation system. The feed to the distillation column of the hybrid PSA-distillation system was directly sent into a PSA unit. Several simulations were taken with four different PSA cycles and the effect of the total cycle time was investigated. Shorter cycle time improved in ethanol purity, but decreased water purity and ethanol recovery. According to the simulation results, fuel ethanol could be produced from the single PSA system, however the water purity was much lower than that produced from the hybrid PSA-distillation system. So another PSA unit was applied after to purify water.

The dual train PSA system was comprised by two PSA units, in which PSA I had the same performance as that in the single PSA system. The heavy product stream from PSA I was sent into the second PSA unit, PSA II, from which pure water was produced has heavy product and the light product stream was recycled to PSA I. Three different cycles were used to simulate PSA II process. The analysis of the mass balance of these three cycles and additional simulations proved that less mass into LR could obtain better PSA performance. Total operating cost was estimated for the dual train PSA system and the comparison with the hybrid PSA-distillation system showed that more cost was required due to the high compression cost.

REFERENCES

1. http://www.ethanolrfa.org/pages/annual-industry-outlook: RFA's 2012 Ethanol Industry Outlook.
2. Vane, L. M. Separation Technologies for the Recovery and Dehydration of Alcohols from Fermentation Broths. *Biofuels, Bioprod. Bioref.* **2008**, *2*, 553-588.
3. Collura, M. A.; Luyben, W. L. Energy-Saving Distillation Designs in Ethanol Production. *Ind. Eng. Chem. Res.* **1988**, *27*, 1686-1696.
4. Haelssig, J. B.; Tremblay, A. Y.; Thibault, J. Technical and Economic Considerations for Various Recovery Schemes in Ethanol Production by Fermentation. **2008**, *47*, 6185-6191.
5. Bausa, J.; Marquardt, W. Shortcut Design Methods for Hybrid Membrane/Distillation Processes for the Separation of Nonideal Multicomponent Mixtures. *Ind. Eng. Chem. Res.* **2000**, *39*, 1658-1672.
6. Hoch, P. M.; Espinosa, J. Design of a Hybrid Distillation-Pervaporation Bio-Ethanol Purification Process Using Conceptual Design and Rigorous Simulation Tools. *AIChE Annual Meeting* **2008**, 316a.
7. Quintero, J. A.; Montoya, M. I.; Sanchez, O. J; Giraldo, O. H.; Cardona, C. A. Fuel

Ethanol Production from Sugarcane and Corn: Comparative Analysis for a Colombian Case. *Energy*, **2008**, *33*, 385-399.

8. Ritter, J. A.; Wu, F.; Ebner, A. D. New Approach for Modeling Hybrid PSA-Distillation Processes. *Ind. Eng. Chem. Res.* **2012,** *51,* 9343-9355
9. Wu, F.; Ebner, A. D.; Ritter, J. A. Improved PSA Cycles of Hybrid Pressure Swing Adsorption-Distillation Process for Ethanol Dehydration. To be submitted.

CHAPTER 4: MODELING OF HYBRID PRESSURE SWING ADSORPTION-DISTILLATION PROCESS FOR PROPANE/PROPYLENE SEPARATION

4.1 Summary

A new configuration, hybrid PSA-distillation process, was introduced for propane/propylene separation. Different PSA cycles were developed and examined to determine if a hybrid PSA-distillation process can be more energy efficient than the commercial distillation alone. First, a simple procedure using a "black-box" PSA process was used to find more energy efficient hybrid configurations for propane/propylene separation. Then, the dynamic adsorption process simulator (DAPS) was used to search for an "actual" PSA process with the same or similar performance as that of the "black-box" PSA process. The total operating cost for each hybrid system was calculated and compared with the commercial distillation process.

4.2 Introduction

Polymer grade propylene is important and widely used in the manufacture of many chemicals and plastics, especially used as monomer feedstock for polypropylene elastomer production. Its purity cannot be less than 99.5 mol%. Propane/propylene mixture is one of the products from the thermal or catalytic cracking of hydrocarbons, and then separated in a C_3 splitter. In the traditional distillation, the relative volatility for

this system is between 1.05 and 1.22 at the temperature in the range of 100-160 ℉ and at the pressure in the range of 189-454 psia.[1] The separation is commonly performed in columns with more than 200 trays with reflux ratios about 13, and a high operating pressure 14.4 atm is needed.[2] Thus, propane/propylene separation is one of the most energy consuming chemical process in industry. New processes must be developed to replace the traditional distillation and to substantially reduce the current use of energy. Pressure swing adsorption (PSA) is one of the options.

Jarvelin and Fair studied the adsorption equilibria and Kinetics of propane and propylene in zeolite 4A, 5A, 13X and activated carbon.[3] Huang et al. constructed the mathematical models based on their experimental adsorption and desorption rate for pure propylene, pure propane, and propane/propylene mixtures on 13X zeolite at different temperatures and compositions.[4] Da Silva and Rodrigues investigated propane/propylene single-adsorption equilibrium isotherms and mass transfer kinetics over 13X. They also designed a vacuum swing adsorption process (VSA) with five steps to split an equimolar mixture of propane and propylene. Propylene was enriched to 98 mol%, however the recovery is only 19 mol% with a productivity of 0.785 mol/kg/h.[5-6] Carbon molecular sieve has a selectivity of 2.3 at 343 K and 1.7 at 423 K in the low-pressure range, and a five-step cycle could produce 83 mol% propylene with 84% recovery.[7-9] Several literatures offered adsorption kinetics and experimental data on the isotherms of propane and propylene in silica gel.[10-12] 4A zeolite is a popular adsorbent for propane/propylene

separation, and Rodrigues has done a lot of study on it including kinetics and PSA cycles.[13-16] Single vacuum pressure swing (VPSA) could produce propylene with purity higher than 99.6%, but only 67% recovery. A dual VPSA system could increase propylene recovery significantly; however its energy consumption was higher than that of the traditional distillation.[17] So replacing distillation with PSA process is not a way to reduce the current use of energy in propane/propylene separation. Ritter et al published their work on the methodology of modeling hybrid PSA-distillation system for ethanol dehydration and proved that significant savings were obtained using the new hybrid system with new designed PSA cycles.[18] Hybrid PSA-distillation process combines the features and strengths of both PSA and distillation and has big potential on energy saving. In this work, hybrid PSA-distillation configuration was developed for propane/propylene separation to replace the traditional distillation. A 10-step 6-bed PSA cycle was applied and simulated with 4A zeolite as the adsorbent and with different operating conditions. Costs were calculated and compared with the traditional distillation to investigate the potential saving.

4.3 Modeling

4.3.1 "Black-Box" PSA Simulation

Figure 4.1a depicts the flow sheet of the commercial distillation system[19] used in industry for propane propylene separation. It is a fractional distillation column with 232

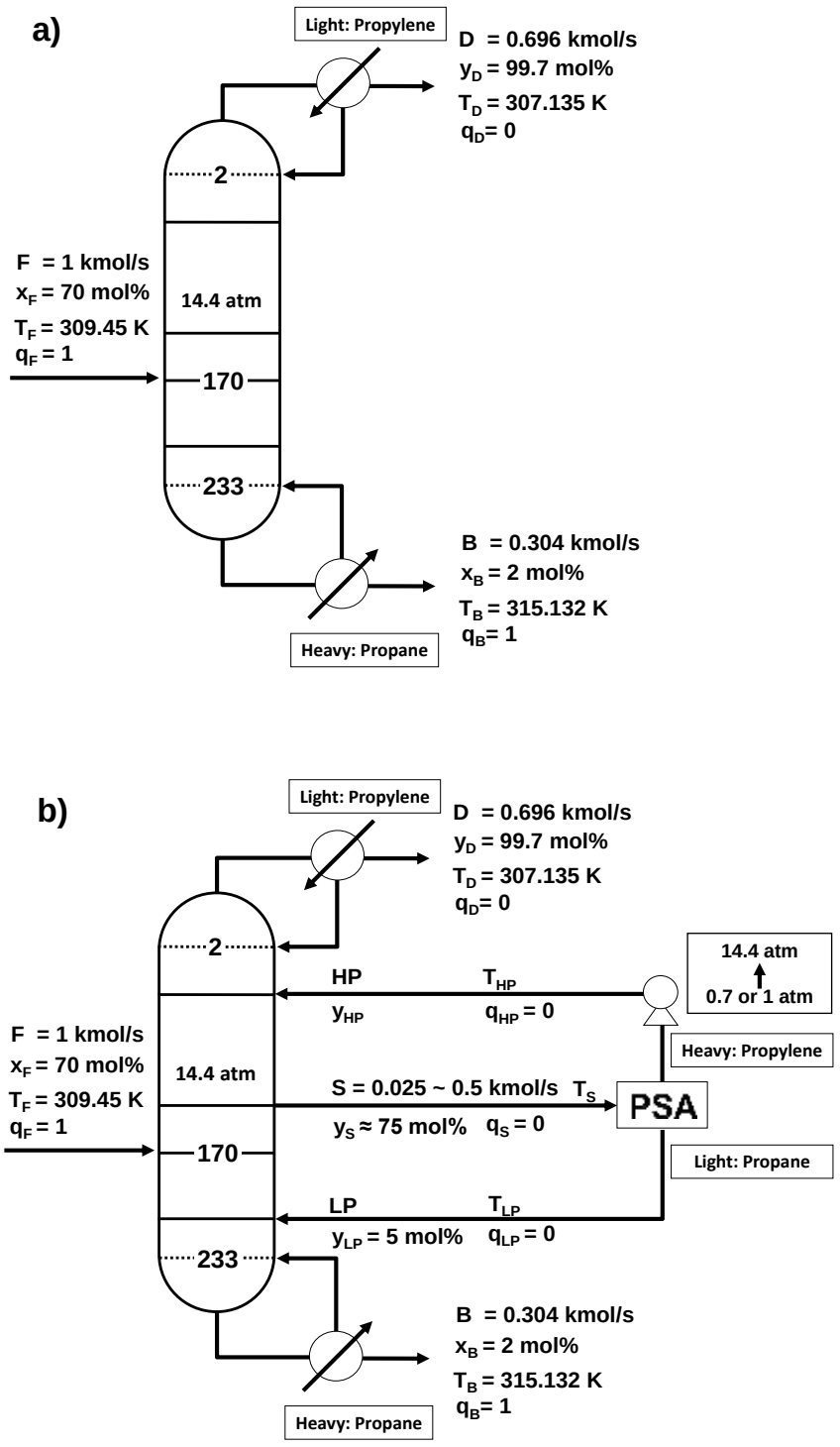

Figure 4.1 a) Commercial distillation system for propane propylene separation. b) Hybrid PSA-distillation system for propane propylene separation. *x* and *y* represents mole fraction of propylene in each stream.

trays plus one partial condenser and one reboiler. The partial condenser is counted as the 1st tray, and the reboiler is counted as the 234th tray. Saturated liquid containing 70 mol% propylene (x_F = 0.70) is fed into the 147th tray, and the flow rate is assumed to be 1 kmol/s. 99.7 mol% propylene (y_D = 0.997) is produced as distillate, and 98 mol% propane (x_B = 0.02) is produced as the bottom product. The column pressure is 14.4 atm. This commercial distillation process was considered as a reference in this study. In the PSA-distillation process, as shown in Figure 4.1b, a PSA unit is connected to the middle of distillation column. A gas phase side stream *S* which contains 75 mol% propylene (y_S = 0.75) is taken from the distillation column and sent into the PSA unit. Propylene is produced as heavy product in PSA and the gas phase product stream (*HP)* is returned to the upper part of the distillation column; propane is produced as light product and the gas phase product stream (*LP)* is returned to the lower part of the distillation column. The high operating pressure in PSA is 14.4 atm, which is the same as that in the distillation column. The low operating pressure is 0.7 or 1 atm. So a compressor is used to bring the pressure of the heavy product stream from 0.7 or 1 atm up to 14.4 atm. Light product (propane) purity (y_{LP}) from PSA was assumed to be 95 mol% and the recovery (R_L) was assumed to range from 80 to 95%. With this assumed process performance, the PSA unit is considered as a "black box". The feed stream PSA is the side stream from the distillation column, and the flow rate ratio of the feed to PSA and distillation *S/F* was considered as a variable, ranged from 0.025 to 0.5. The overall mass balance is given by

Eq. 1 and 2

$$F = B + D \tag{1}$$

$$Fy_F = Bx_B + Dy_D \tag{2}$$

from which the flow rates of the distillate (*D*) and the bottom product (*B*) are calculated

$$D = F\frac{y_F - x_B}{y_D - x_B} \tag{3}$$

$$B = F\frac{x_F - y_D}{x_B - y_D} \tag{4}$$

Propane recovery in PSA is given by Eq. 5

$$R_L = \frac{R(1-y_R)}{S(1-y_S)} \tag{5}$$

Combining with PSA mass balance Eq. 6 and 7, product stream flow rates (*HP* and *LP*) and composition (y_{HP}) can be calculated.

$$S = HP + LP \tag{6}$$

$$Sy_S = HPy_{HP} + LPy_{LP} \tag{7}$$

$$LP = R_L S\frac{(1-y_S)}{(1-y_{LP})} \tag{8}$$

$$HP = S - LP \tag{9}$$

$$y_{HP} = \frac{Sy_S - LPy_{LP}}{HP} \tag{10}$$

The distillation process was simulated in Chemsep™ to obtain the partial condenser and reboiler duties. In Chemsep™, *S* was considered as a side stream and *HP* and *LP* were considered as two extra feed streams to the distillation column. The compressor duty was calculated from Eq. 11.

$$Q_C = \frac{\gamma}{\gamma-1} RT \left[\left(\frac{P_H}{P_L} \right)^{\frac{\gamma}{\gamma-1}} - 1 \right] \frac{1}{\eta} \dot{n} \quad (11)$$

where γ is the isentropic constant, which is 1.4; η = 0.8, which is the efficiency of the compressors; n is the flow rate of a stream, mol/s; and T is the absolute temperature of a stream. The total operating cost was calculated according to the utility prices listed in Table 2.3. Then, the total operating cost of the hybrid processes was compared to that of the reference case.

4.3.2 "Actual" PSA Simulation

The "black-box" PSA analyses that resulted in energy savings (and thus internal flow reductions in the distillation column) relative to the reference case provided PSA performance targets for an "actual" PSA process. DAPS (Dynamic Adsorption Process Simulator) was used to simulated the actual PSA process. The adsorbent was 4A zeolite. Figure 4.2 shows the adsorption isotherms of propane and propylene on 4A zeolite. The upper three curves are the loadings of propylene at three different temperatures (373, 423 and 473 K). The other two curves are the loadings of propane at two different temperatures (423 and 473 K). The circles and squares are experimental data[17] and the lines are results obtained by fitting the experimental data to the Two-Process Langmuir model[20], which is given by Eqs. 12 to 14.

$$q = \frac{q_{SA} b_A P}{1 + b_A P} + \frac{q_{SB} b_B P}{1 + b_B P} \quad (12)$$

$$b_A = b_{0A} \exp\left(\frac{\Delta H_A}{RT}\right) \quad (13)$$

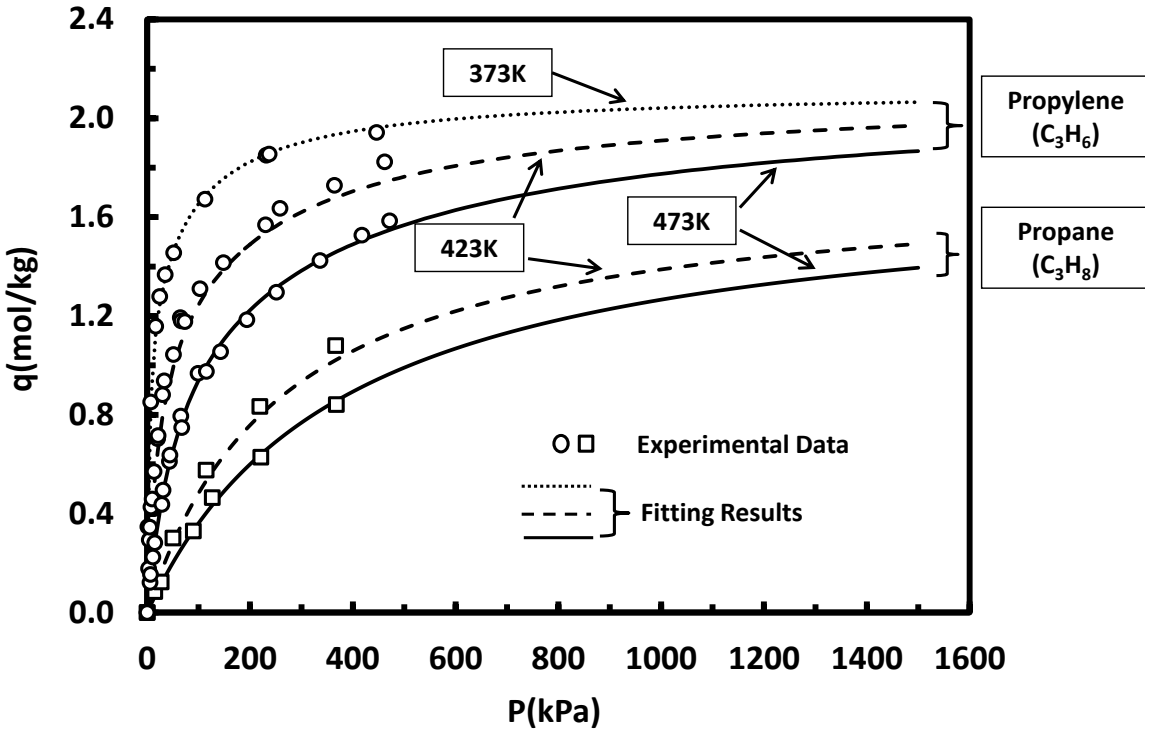

Figure 4.2 Adsorption isotherms of propane and propylene in 4A zeolite at different temperatures. Circles and squares represent experimental data and lines represent fits to the two-process Langmuir model.

$$b_B = b_{0B}\exp(\frac{\Delta H_B}{RT}) \quad (14)$$

where q is the equilibrium loading (mol/kg); q_s is the saturation loading (mol/kg); b_0 is the pre-exponential factor (1/kPa); ΔH is the isosteric heat of adsorption (kJ/mol). The values of these parameters are summarized in Table 4.1. The mass transfer coefficients of propane and propylene on 4A zeolite are shown in Table 4.2. The higher the temperature is, the larger the value of the mass transfer coefficients. As shown in Figure 4.2, there is no large difference in the loading of propane and propylene on 4A zeolite at the same temperature. However, the mass transfer coefficient of propane is much smaller than that of propylene. So when the gas mixture of propane and propylene is passed through the PSA bed packed with 4A zeolite, propylene diffuses much faster than propane into the pores, leaving relatively more propane in the gas phase. In the "actual" PSA simulation, the bed was isolated and the temperature was not constant. In order to include the temperature effect, the values of mass transfer coefficients k were expressed by Eq. 5 and 6.[15]

$$D_c = D_c^0\exp(\frac{-E_a}{RT}) \quad (15)$$

$$k = \frac{15D_c}{r_c^2} \quad (16)$$

where D_c is the crystal diffusivity; D_c^0 is the limiting diffusivity at high temperatures; E_a is the activation energy; r_c is the crystal radius.

Figure 4.3 shows the 6-bed 10-step PSA cycle for propane propylene separation. The steps are feed (F), equalization one and two (EQ_1 and EQ_2), concurrent depressurization

Table 4.1 PSA process simulation parameters and conditions used in the DAPS

2-P Langmuir Isotherm Parameters	C_3H_8	C_3H_6
q_{SA} (mol/kg)	1.69	1.13
q_{SB} (mol/kg)	0.54	0.98
b_{0A} (1/kPa)	1.39×10^{-5}	2.55×10^{-7}
b_{0B} (1/kPa)	1.95×10^{-12}	6.42×10^{-6}
ΔH_A (kJ/mol)	-20.733	-44.42
ΔH_B (kJ/mol)	-65.24	-23.74
Bed Properties		
length, Z (m)	0.87	
outer radius, r_o (m)	0.0106	
inner radius, r_i (m)	0.0105	
porosity, ε_b	0.37	
Wall Properties		
density, ρ_w (kg/m^3)	8238	
thermal capacity, C_w (kJ/kg/K)	0.5	
heat transfer coefficient, h (kW/m^2/K)	0 (adiabatic)	
temperature, T_w (K)	418;428;433;438	
Operating Conditions		
feed temperature, T_{PSA} (K)	418;428;433;438	
high pressure, P_H (atm)	14.4	
low pressure, P_L (atm)	0.7 or 1.0	
feed flow rate F_{PSA} (SLPM)	0.55;0.60;0.65;1.00	
mole fraction of propylene in feed, y_S	0.75	
Adsorbent Properties		
crystal radius, r_c (m)	1.9×10^{-6}	
pellet radius, r_p (m)	0.0008	
density, ρ_p (kg/m^3)	1210	
porosity, ε_p	0.34	
thermal capacity, C_p (kJ/kg/K)	0.92	
Kinetic Properties	C_3H_8	C_3H_6
activation energy, E_a (kJ/mol)	23.67	15.61
limiting diffusivity, D_c^0(m^2/s)	2.26×10^{-15}	4.66×10^{-14}

Table 4.2 Mass transfer coefficients (1/s) of propane and propylene in 4A zeolite.

	373K	**423K**	**473K**	**433K**
C_3H_6	1.26E-03	2.29E-03	3.66E-03	2.53E-03
C_3H_8	4.55E-06	1.12E-05	2.28E-05	1.31E-05

(CoD), countercurrent depressurization (CnD), light reflux (LR), idle (I),light product pressurization (LPP). During F step, 75 mol% propylene was fed into the bed at a constant pressure, which was the high operating pressure. Then the bed was connected to another bed to release some gas and equalize the pressure to the first intermediate pressure, followed by the second equalization step in which the bed was depressurized to the second intermediate pressure. The bed was again depressurized through the light end to a lower pressure during CoD step, and then depressurized through the heavy end to the low operating pressure during CnD step. The mass from CoD step was sent into LR step to purge the bed. All the valves were closed and the pressure was constant in I step, since it was used to make the cycle schedule reasonable and complete. Part of the light gas from F steps was sent into LPP step to pressurize the bed again to the high operating pressure. This cycle scheduled was designed based on the cycles reported in the literatures.[16] The bed properties, adsorbent properties and operating conditions were summarized in Table 4.1.

4.4 Results and Discussion

4.4.1 "Black-Box" PSA Simulation

Figure 4.4 shows the partial condenser and reboiler costs of the hybrid systems in which the PSA unit was considered as a black box. The x-axis is the flow rate ratio of the feed to the PSA unit and distillation column. The y-axis is the cost calculated as dollars per mega mole of propylene finally produced. Each curve represents a different assumed

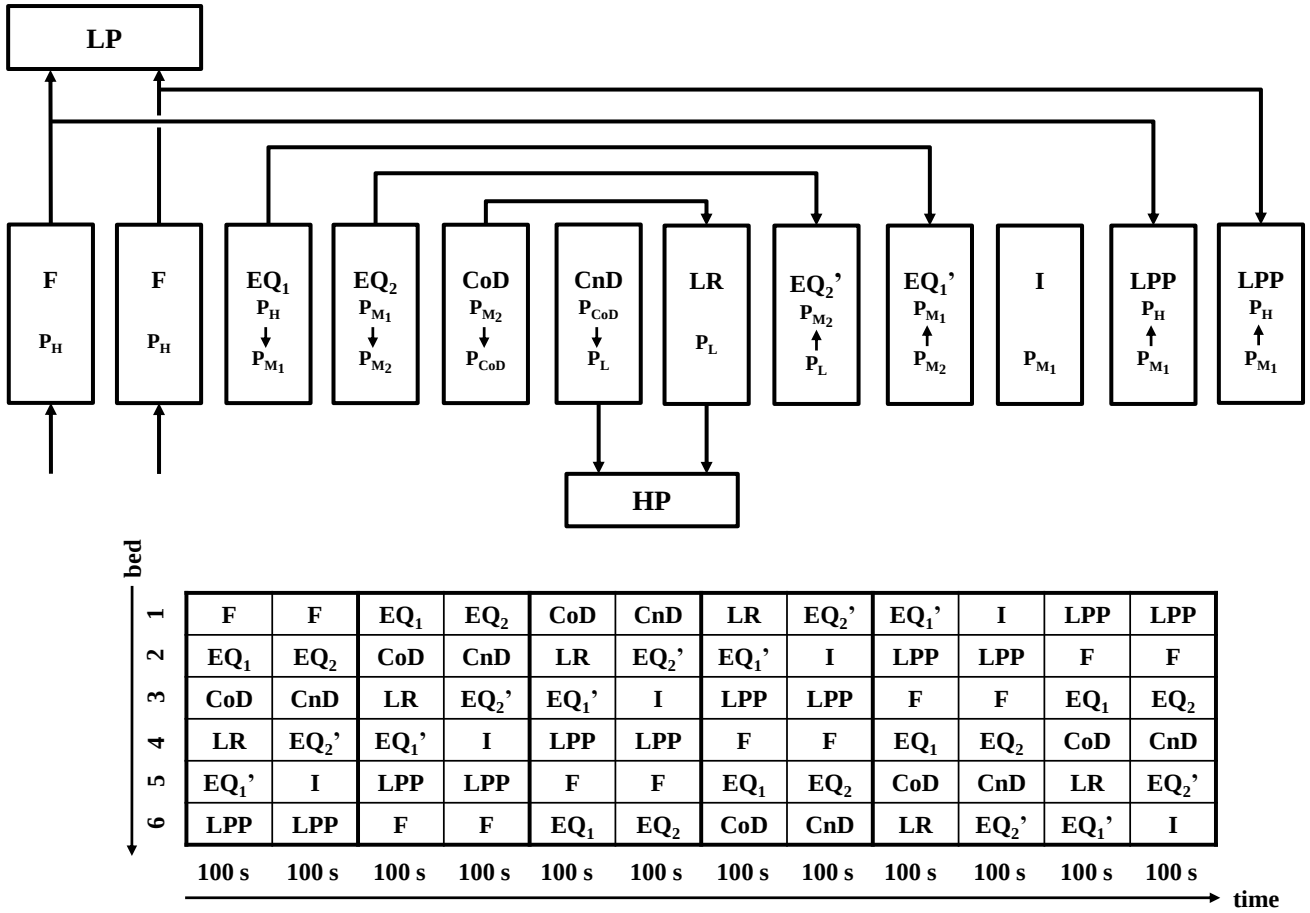

bed												
1	F	F	EQ_1	EQ_2	CoD	CnD	LR	EQ_2'	EQ_1'	I	LPP	LPP
2	EQ_1	EQ_2	CoD	CnD	LR	EQ_2'	EQ_1'	I	LPP	LPP	F	F
3	CoD	CnD	LR	EQ_2'	EQ_1'	I	LPP	LPP	F	F	EQ_1	EQ_2
4	LR	EQ_2'	EQ_1'	I	LPP	LPP	F	F	EQ_1	EQ_2	CoD	CnD
5	EQ_1'	I	LPP	LPP	F	F	EQ_1	EQ_2	CoD	CnD	LR	EQ_2'
6	LPP	LPP	F	F	EQ_1	EQ_2	CoD	CnD	LR	EQ_2'	EQ_1'	I
	100 s	100 s	100 s	100 s	100 s	100 s	100 s	100 s	100 s	100 s	100 s	100 s

Figure 4.3 6-bed 10-step cycle schematic and schedule for propane propylene separation. F: feed step; EQ: equalization step; CoD: concurrent depressurization step; CnD: countercurrent depressurization step; LR: light reflux step; I: idle step; LPP: light product pressurization step.

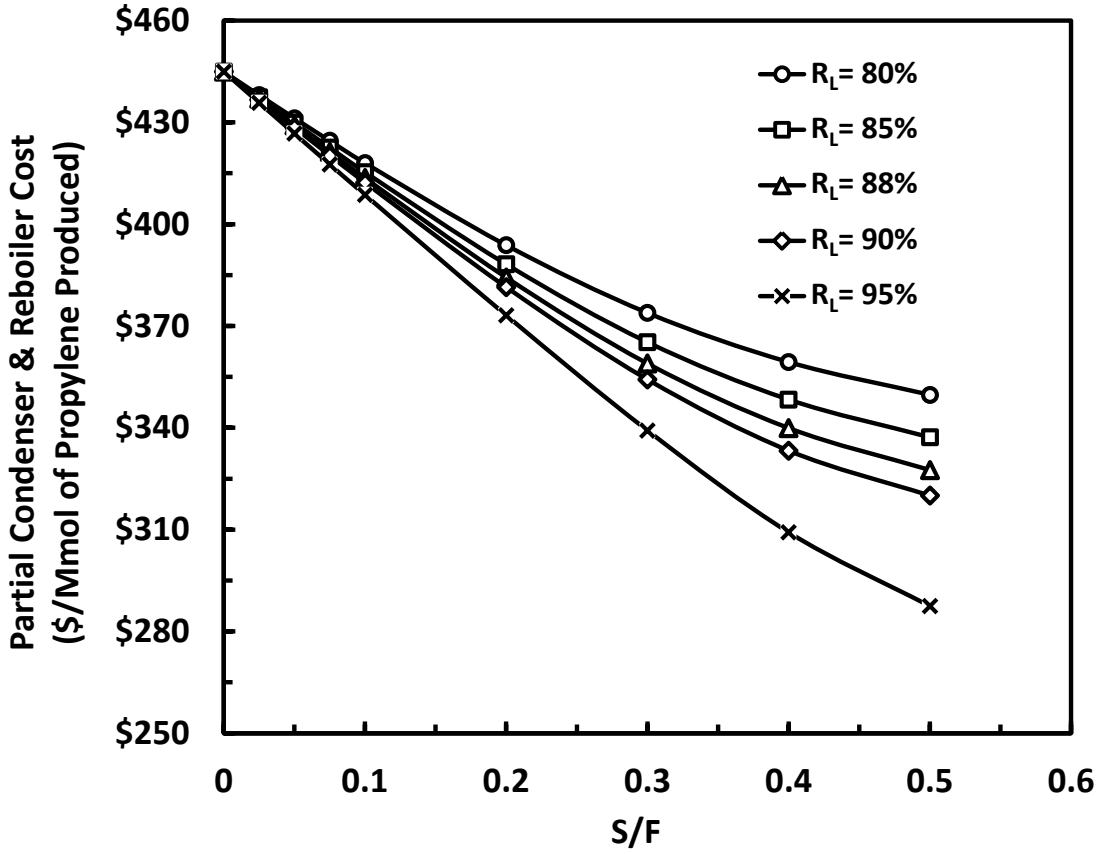

Figure 4.4 Partial condenser and reboiler cost for different feed flow rate ratios to PSA and distillation (*S/F*) units for different propane recoveries (R_L) in the PSA unit.

propane recovery in the PSA unit. The point at *S/F* = 0 represents the cost of the reference process which is the simple distillation. Two different low operating pressures were tested in the hybrid process; however, the low pressure did not affect the partial condenser and reboiler costs. Both the feed flow rate ratio *S/F* and propane recovery in PSA R_L had strong effects on the partial condenser and reboiler costs. As shown in Figure 4.4, both larger feed flow rate ratio *S/F* and higher propane recovery R_L helped in reducing partial condenser and reboiler costs. Larger feed flow rate ratio *S/F* means more mass was taken from the distillation column and sent into the PSA unit, so more separation work was done in the PSA unit, resulting in the reduction of distillation work and energy consumption in both the partial condenser and reboiler.

The heavy product stream (*HP*) was at the low operating pressure of PSA, so a compressor was used to compress this stream to the operating pressure of the distillation column, which was 14.4 atm. Two different PSA low operating pressures were tested in the cost calculation. Figure 4.5 shows the compression cost when the low operating pressure in PSA was 0.7 atm (Figure 4.5a) and 1.0 atm (Figure 4.5b) respectively. Each curve represents the compression cost with certain propane recovery (R_L) in PSA. Obviously, more compression cost was required with a lower low operating pressure because of the larger pressure difference between the distillation column and the PSA unit. When the feed flow rate ratio *S/F* was larger, more mass was sent into the PSA unit, resulting in more mass in the product streams. So more compression cost was required.

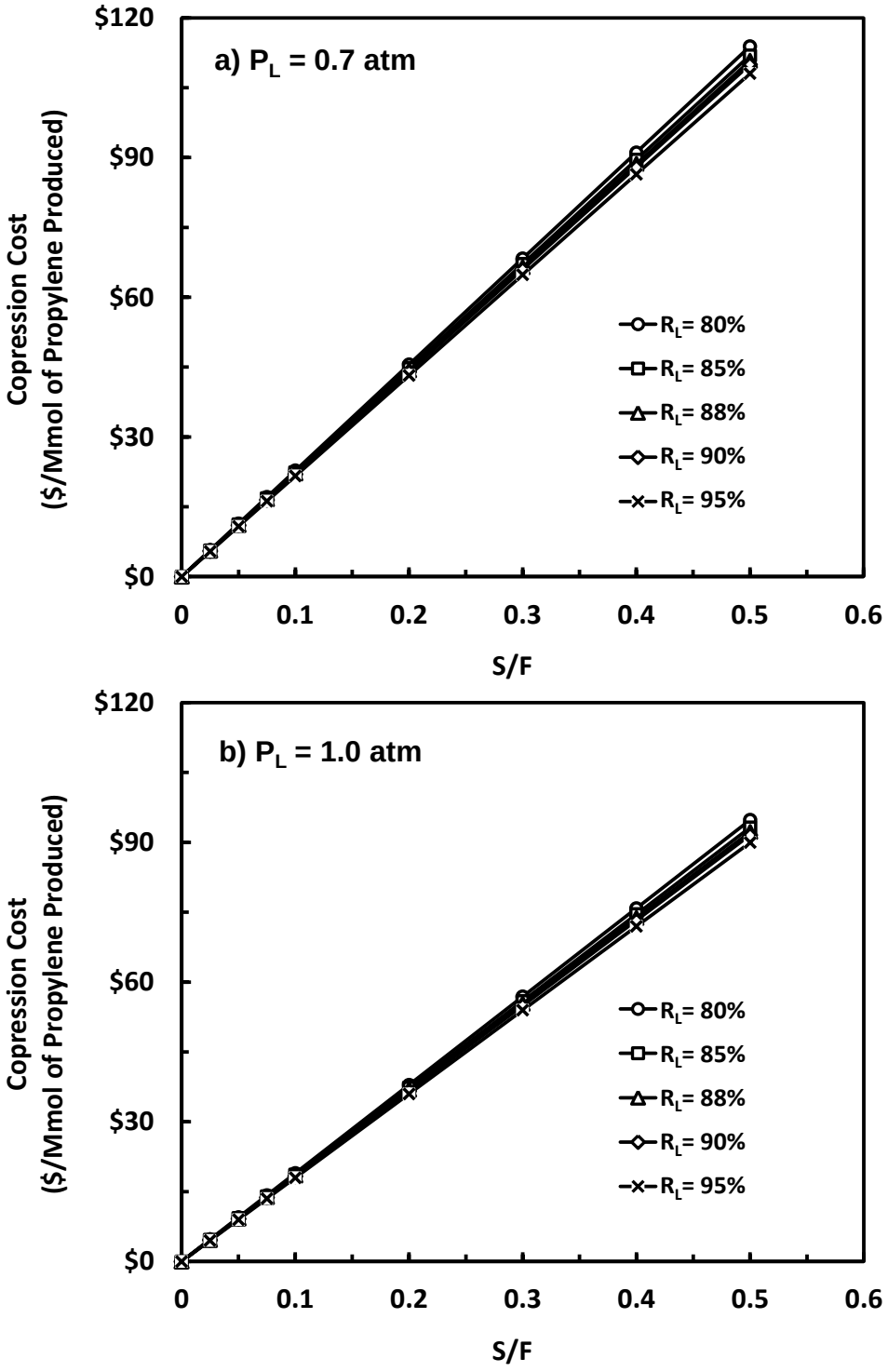

Figure 4.5 Compression cost for two different low operating pressures in the PSA unit. a) P_L = 0.7 atm; b) P_L = 1.0 atm.

However, there was almost no effect of propane recovery (R_L) on compression cost, which means the PSA performance did not affect the compression cost much. Thus, the mass in the product streams from the PSA unit plays a more important role than the PSA performance in affecting compression cost.

All the costs were added together to obtain the total operating cost, including the cost of the partial condenser, reboiler and PSA product compressor. It should be noticed that the temperature difference existed between the distillation column and the PSA unit. So both heaters and condensers were needed to change the temperature of the streams connected these two units. However, heat integration is usually utilized in industry. So the cost in the stream heaters and condensers were not considered in the total operating cost. Figure 4.6 shows the total operating cost savings compared to the reference case for the two different low operating pressures in the PSA unit (0.7 atm, Figure 4.6a; 1.0 atm, Figure 4.6b). The savings reached a maximum, and then decreased with increasing feed flow rate ratio *S/F*. When *S/F* was small, the partial condenser and reboiler costs decreased, and the compression cost was little. So there was some savings in the total operating cost. However, when *S/F* was larger than a certain value, the total operating cost was higher than the reference case due to the higher compression cost overwhelming any cost savings associated with the partial condenser and reboiler. A higher low operating pressure in the PSA unit also resulted in more total operating cost savings due to less compression cost.

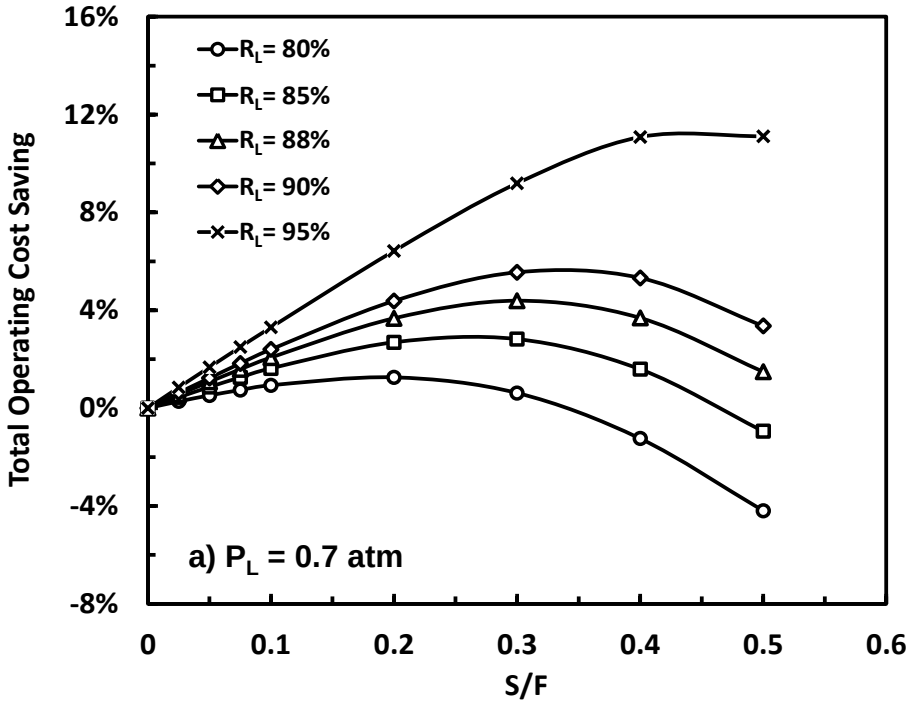

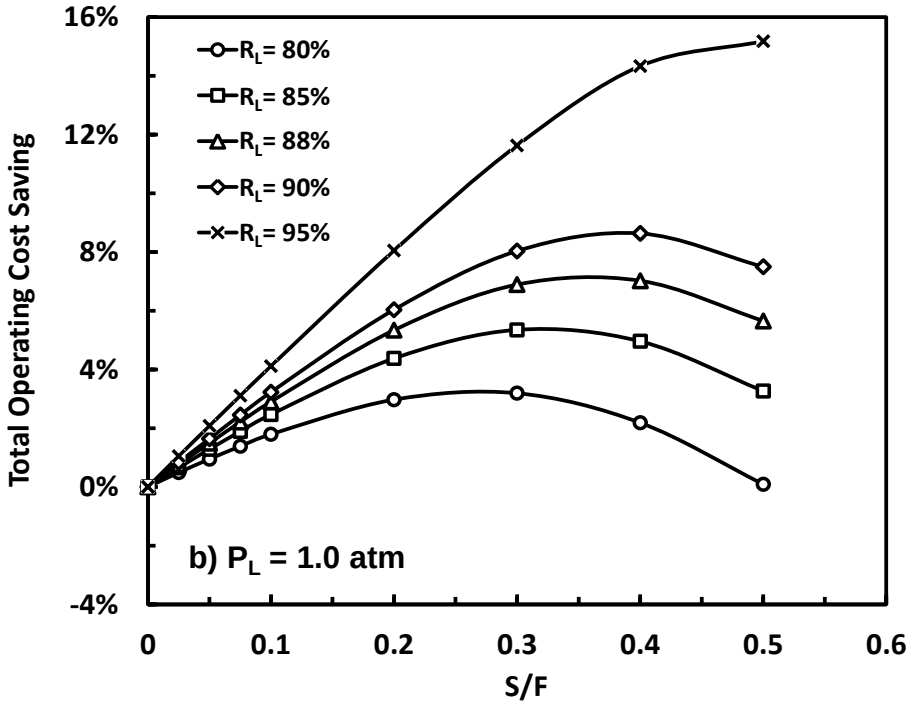

Figure 4.6 Total operating cost saving for two different low operating pressures in PSA. a) P_L = 0.7 atm; b) P_L = 1.0 atm.

4.4.2 "Actual" PSA Simulation

The "actual PSA" simulations were carried out at different operating conditions which are summarized in Table 4.1. The PSA performances are shown in Table 4.3. Four different temperatures, two different low operating pressures and four different feed flow rates were investigated. High temperature improved mass transfer of gas into the adsorbent; low operating pressure helped in regenerating the adsorbent. Thus, both of these two conditions resulted in better PSA performance. Bigger feed flow rate helped in increasing the purity of heavy product (C_3H_6), however it caused more heavy product breaking through, resulting in lower propylene recovery and propane purity. Thus, smaller feed flow rate would be used. Four of these runs were chosen as the PSA process in the hybrid system, which were italicized in Table 4.3. The product streams information from the PSA unit was collected and put into Chemsep^{TM} to simulate the distillation process. In Chemsep^{TM}, the feed stream to PSA was considered as a side stream of distillation; its concentration was the same as the feed concentration to PSA and its flow rate was determined by the feed flow rate ratio *S/F* ranged from 0.1 to 0.5. The two product streams from PSA were considered as two extra feed streams to distillation; their concentration was determined by the PSA simulation results and flow rates were calculated based on mass balance for each corresponding feed flow rate ratio *S/F*. After simulating the distillation process in Chemsep^{TM}, the energy information in partial condenser and reboiler was collected to calculate the cost. Also, the compression cost was

Table 4.3 PSA performance for propane/propylene separation with different operating conditions.

	Operating Conditions			**Propylene (C_3H_6)**		**Propane (C_3H_8)**	
Run No.	**T_{PSA} (K)**	**P_L (atm)**	**F_{PSA} (SLPM)**	**Recovery (%)**	**Purity (%)**	**Recovery (%)**	**Purity (%)**
1	*433*	*0.7*	*0.55*	*91.38*	*91.97*	*76.08*	*75.53*
2	433	0.7	1.00	57.33	93.01	86.91	49.23
3	438	0.7	1.00	59.44	93.47	87.48	50.67
4	438	0.7	0.55	92.66	91.90	75.23	78.09
5	428	0.7	0.55	90.34	91.54	74.95	73.69
6	418	0.7	0.55	86.44	90.84	73.57	68.24
7	*438*	*0.7*	*0.60*	*89.61*	*92.75*	*78.86*	*73.61*
8	*438*	*0.7*	*0.65*	*85.07*	*93.07*	*80.69*	*69.26*
9	*438*	*1.0*	*0.65*	*78.39*	*92.03*	*79.34*	*61.79*
10	438	1.0	0.55	88.20	91.52	75.46	70.21

calculated from Eq. 11 based on the simulation results of both PSA and distillation. The total operating cost was then calculated for each "actual" PSA simulation and each feed flow rate ratio *S/F*, and then compared with that of the reference case which is the simple distillation. The heating and cooling cost for the streams between PSA and distillation was not included in the total operating cost, because usually heat integration was utilized in industry.

Figure 4.7 shows the partial condenser and reobiler costs in the hybrid systems with these four PSA units. The costs dropped immediately as a stream was drawn from the distillation column and sent into a PSA unit. The point at *S/F* = 0 shows the cost of the reference case. Similar to the "black-box" PSA simulations, a larger feed flow rate ratio *S/F* resulted in less partial condenser and reboiler costs. The runs with higher temperature and lower low operating pressure had lower partial condenser and reboiler cost. However, the cost difference was not much among these four hybrid simulations. Figure 4.8 shows compression cost, and as shown in the figure, a large amount of compression cost was required in these four hybrid systems. Run 9 required less compression cost than the other three because of its higher low operating pressure in PSA. Then all the costs were summed to get total operating cost and compared with the reference to get the total operating cost saving, as shown in Figure 4.9. The total operating cost saving increased with the elevation of feed flow rate ratio *S/F*, and then decreased to negative number. *S/F* represented how much mass was drawn from the

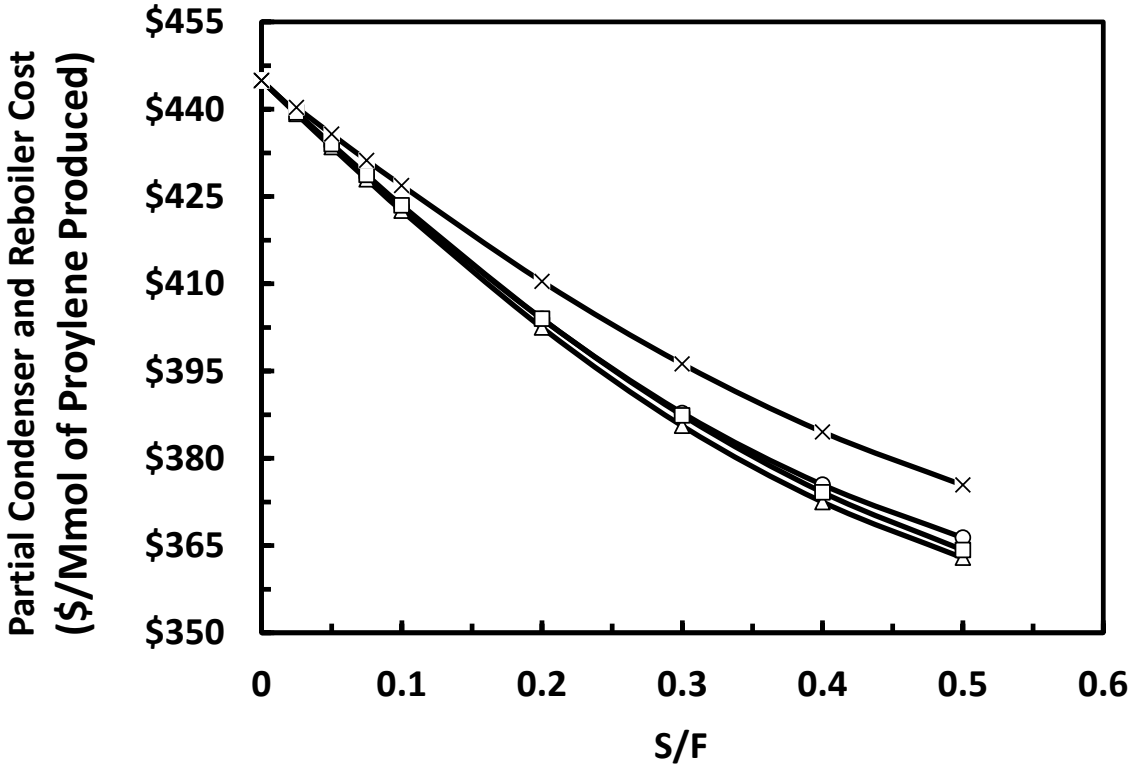

Figure 4.7 Partial condenser and reboiler cost of the hybrid PSA-distillation system based on “actual” PSA simulations.

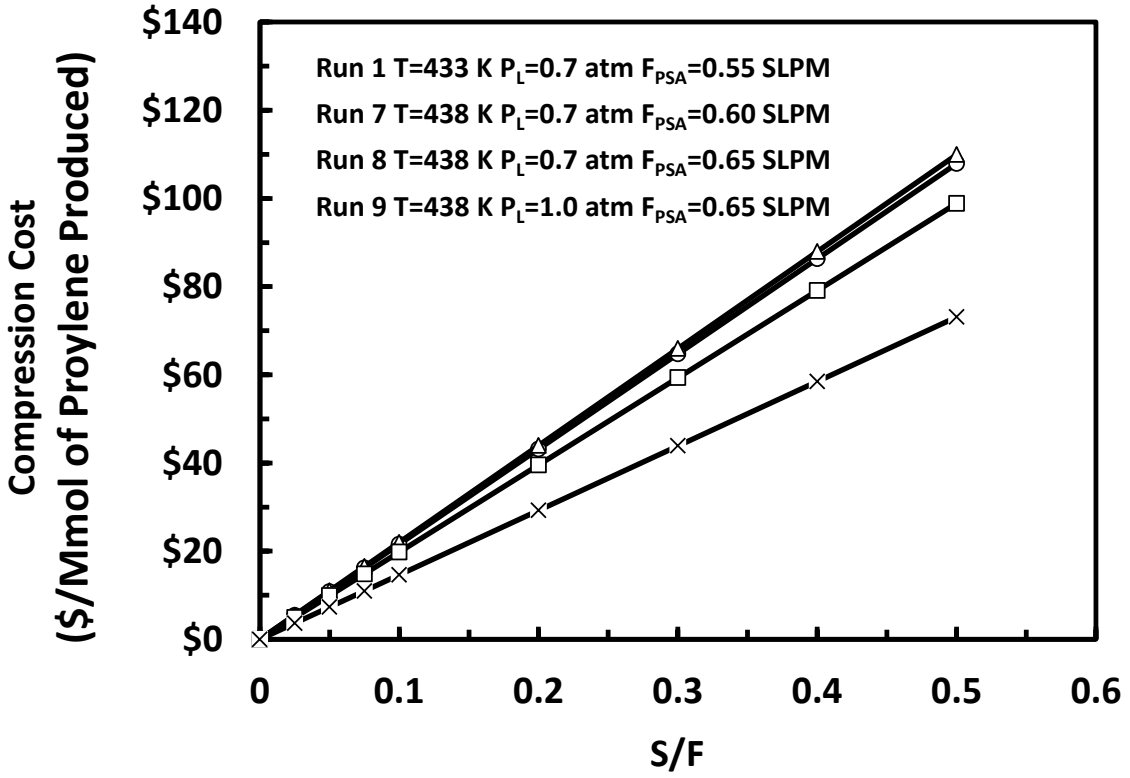

Figure 4.8 Compressor cost in the hybrid PSA-distillation system based on "actual" PSA simulations.

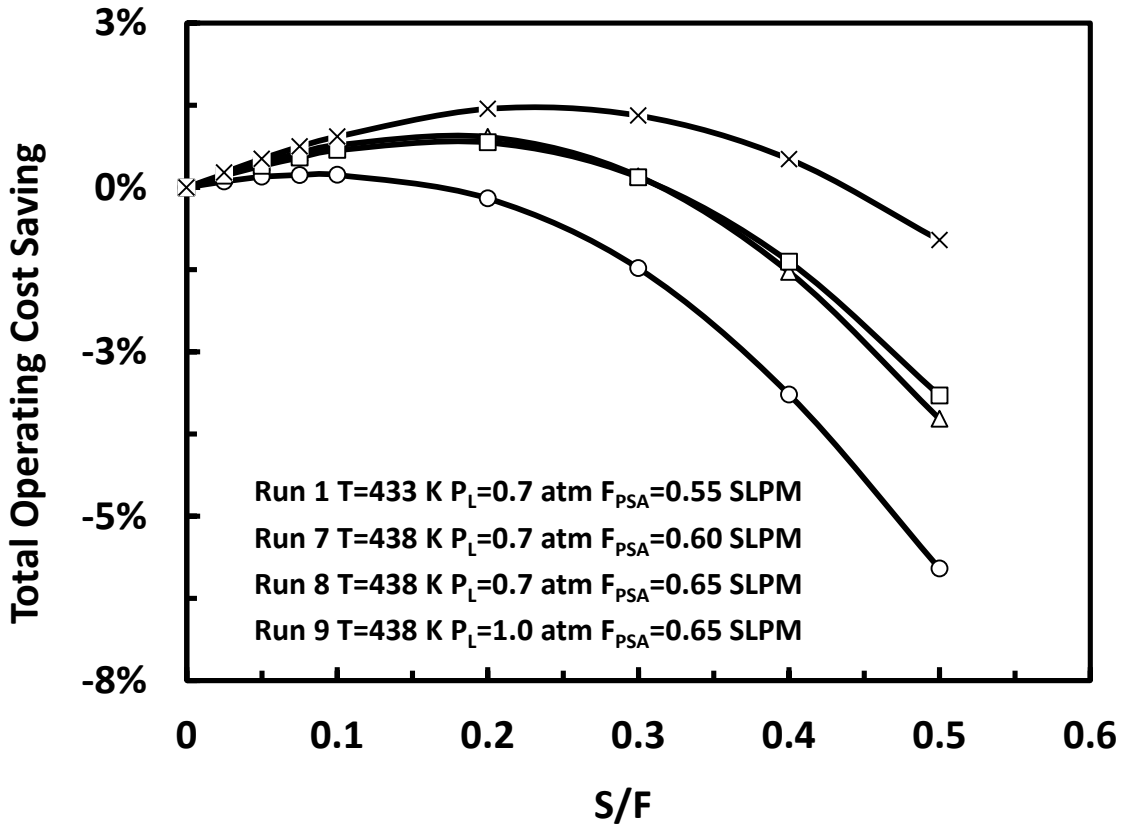

Figure 4.9 Total operating cost saving in hybrid PSA-distillation system based on "actual" PSA simulations compared with commercial distillation system.

distillation column and sent into the PSA unit, or how much separation work was done in the PSA unit. Separation in PSA helped in saving cost in distillation process, however, when certain amount of separation was done in PSA, the requirement of cost in the compressors exceeded the saving in distillation. So the saving was negative when more mass was sent into the PSA unit. The runs with 0.7 atm low operating pressure cost more due to lager pressure ratio. The maximum saving was 1.19% which was obtained with 438 K operating temperature, 1.0 atm low operating pressure and 0.65 SLPM feed flow rate to PSA. The saving was not as significant as that predicted in the "black box" PSA simulations, because the PSA performance was not so good due to the very low selectivity between propane and propylene on 4A zeolite. In the "black-box" PSA simulations, propane purity was assumed to be 95%. However, in the "actual" PSA simulations, propane purity was less than 82%. Apparently, the differences in the mass transfer rates in 4A zeolite were not enough to provide a good separation between these two species. Other commercial adsorbents are even worse. A better adsorbent is needed that exhibits better equilibrium and/or kinetic selectivities between these two very similar molecules coupled with more sophisticated PSA cycles.

4.5 Conclusions

In this work, a hybrid PSA-distillation system was introduced to replace the commercial distillation system for propane/propylene separation. A side stream was drawn from the distillation column and sent into a PSA unit. Then two product streams

from the PSA unit were sent back into the distillation column. In the first part of the simulation work, the PSA unit was considered as a black box, and its performance was assumed. Only distillation process was simulated by considering the product streams from PSA as two additional feeds to distillation. Different simulations were done by varying the feed flow rate ratio to PSA and distillation *S/F* with different PSA performances. Compression cost was calculated based on the assumption of the operating pressures in the PSA unit, and total operating cost for each case was calculated and compared with the traditional distillation process. Both PSA performance and feed flow rate ratio *S/F* had strong effect on the total operating cost of hybrid systems. The results show savings in partial condenser and reboiler, providing potential for expansion of distillation capacity. Significant saving in total operating cost could be achieved by applying these hybrid PSA-distillation systems with those assumptions. Then in the second part of the simulation work, "black-box" PSA processes were replaced with "actual" ones. PSA processes were simulated with real adsorbent properties, bed properties and operating conditions. 4A zeolite was the adsorbent and several simulations was done with different operating conditions, including temperature, low operating pressure and feed flow rate to PSA. Four runs with better performance were chosen to be applied in the hybrid system. Costs were calculated and compared with the traditional distillation. The low operating pressure in PSA determined the compression cost. The higher the low operating pressure was, the less compression cost was required. The total

operating cost saving was not as expected because the PSA performance was not as good as the assumptions in the “black-box” PSA simulations. Better performance would be achieved to save the cost if an adsorbent with better selectivities was used and/or more sophisticated PSA cycles were designed.

REFERENCES

1. Laurance, D. R; Swift, G. W. Relative Volatility of Propane-Propylene System from 100-160. deg. F. *J. Chem. Eng. Data.* **1972**, *17*, 333-337
2. Lewis, W. K.; Gilliland, E. R.; Chertow, B.; Hoffman, W. H. Vapor-Adsorbate Equilibrium. I. Propane-Propylene on Activated Carbon and on Silica Gel. *J. Am. Chme. Soc.* **1950,** *72,* 1153-1157
3. Jarvelin, H.; Fair. J. R. Adsorptive Separation of Propylene-Propane Mixtures. *Ind. Eng. Chem. Res.* **1993,** *32,* 2201-2207
4. Huang, Y. H.; Liapis, A. I.; Xu, Y.; Crosser, O. K.; Johnson, J. W. Binary Adsorption and Desorption Rates of Propylene-Propane Mixtures on 13X Molecular Sieves. *Separations Technology*. **1995**, *5,* 1-11
5. Da Silva, F. A.; Rodrigues, A. E. Adsorption Equilibria and Kinetids for Propylene and Propane over 13 X and 4A Zeolite Pellets. *Ind. Eng. Chem. Res.* **1999,** *38*, 2051-2057
6. Da Silva, F. A.; Rodrigues, A. E. Propylene/Propane Separation by Vacuum Swing Adsorption Using 13X Zeolite. *AIChE Journal*. **2001,** *47,* 341-357

7. Grande, C. A.; Silva, V. M. T. M.; Gigola, C.; Rodrigues, A. E. Adsorption of Propane and Propylene onto Carbon Molecular Sieve. *Carbon.* **2003,** *41,* 2533-2545

8. Grande, C. A.; Rodridues, A. E. Adsorption of Binary Mixtures of Propane-Propylene in Carbon Molecular Sieve 4A. *Ind. Eng. Chm. Res.* **2004,** *43,* 8057-8065

9. Grande, C. A.; Cavenati, S.; Da Silva, F. A.; Rodrigues, E. Carbon Molecular Sieves for Hydrocarbon Separations by Adsorption. *Ind. Eng. Chem. Res.* **2005,** *44,* 7218-7227

10. Lewis, E. K.; Gilliland, E. R.; Chertow, B.; Hoffman, W. H. Vapor-Adsorbate Equilibrium. I. Propane-Propylene on Activated Carbon and on Silica Gel. *J. Am. Chme. Soc.* **1950,** *72,* 1153-1157

11. Maslan, F.; Aberth, E. R. Adsorption of Propane and Propylene on Silica Gel at Low Temperatures. *Journal of Chemical and Engineering Data,* **1972,** *17,* 286-287

12. Grande, C. A.; Rodrigues, A. E. Adsorption Equilibria and Kinetics of Propane and Propylene in Silica Gel. *Ind. Eng. Chem. Res.* **2001,** *40,* 1686-1693

13. Grande, C. A.; Rodrigues, A. E. Adsorption Kinetics of Propane and Propylene in Zeolite 4A. *Chemical Engineering Research and Design* **2004,** *82,* 1604-1612

14. Patino, I. M. E.; Aguilar, A. G.; Jimenez, L. A.; Rodriguez, C. E. Kinetics of the Total and Reversible Adsorption of Propylene and Propane on Zeolite 4A (CECA) at Different Temperatures. *Colloids and Surfaces A: Physicochem. Eng. Aspects.* **2004,** *237,* 73-77

15. Grande, C. A.; Rodrigues, A. E. Propane/Propylene Separation by Pressure Swing Adsorption Using Zeolite 4A. *Ind. Eng. Chem. Res.* **2005**, *44,* 8815-8829

16. Da Silva, F. A.; Rodrigues, A. E. Vacuum Swing Adsorption for Propylene/Propane Separation with 4A Zeolite. *Ind. Eng. Chem. Res.* **2001,** *40,* 5758-5774

17. Grande, C. A.; Gigola, C; Rodrigues, A. E. Propane-Propylene Binary Adsorption on Zeolite 4A. *Adsorption*, **2003**, *9,* 321-329

18. Ritter, J. A.; Wu, F.; Ebner, A. D. New Approach for Modeling Hybrid PSA-Distillation Processes. *Ind. Eng. Chem. Res.* **2012,** *51,* 9343-9355

19. Gokhale, V.; Hurowitz, S.; Riggs, J. B. A Comparison of Advanced Distillation Control Techniques for a Propylene/Propane Splitter. *Ind. Eng. Chem. Res.* **1995**, *34,* 4413-4419

20. Bhadra, S. J.; Ebner, A. D. ;Ritter, J. A. On the Use of the Dual-Process Langmuir Model for Correlating Unary Equilibria and Predicting Mixed-Gas Adsorption Equilibira. *Langmuir*, **2012**, *28*, 6935-6941

CHAPTER 5: MODELING OF HYBRID PSA-DISTILLATION PROCESS FOR PROPANE/PROPYLENE SEPARATION WITH HYPOTHETICAL ADSORBENT

5.1 Summary

A hybrid PSA-distillation process has been designed to replace the traditional simple distillation process. Several PSA simulations were carried out with 4A zeolite as the adsorbent and the total operating cost was calculated to compare with the simple distillation process. The results showed that the maximum saving was less than 2% and the saving was negative for most cases. Thus a hypothetical adsorbent was proposed to replace the commercial adsorbents, which is silica gel particle coated with 4A zeolite powder. 4A zeolite forms a very thin film on the surface of the silica gel particle, so its working capacity is negligible. PSA processes were simulated with the hypothetical adsorbent to investigate the total operating cost and to compare with the reference. Much better performance was obtained and the maximum of 13.22% total operating cost was saved compared with the traditional distillation.

5.2 Introduction

Propane/propylene separation is one of the most energy consuming chemical processes in industry, because of the low relative volatility and high reflux ratio in the

simple distillation process. Several pressure swing adsorption (PSA) processes have been developed in an attempt to replace the traditional process, Because PSA requires less energy. Several different adsorbents have been tested with these PSA processes, such as 13X zeolite,[1-3] 4A zeolite,[4-11] carbon molecular sieve,[12-14] and silica gel.[15-17] However, the performance of a single PSA unit is not comparable with the traditional distillation. This stems from it being difficult to produce two pure products from a single PSA process.

The objective of last chapter has been to develop a hybrid PSA-distillation process for propane/propylene separation. 4A zeolite was used as the adsorbent. Simulations were carried out with different operating temperature, pressures and different feed flow rates. The total operating cost, including the cost in the partial condenser, reboiler, compressors, product stream condensers and PSA heater, was calculated and compared with the reference case. To compete with traditional distillation, the energy required by adding a PSA unit must be less than the resulting energy reduction in the distillation unit. However, the results showed that the energy savings could not be achieved, since none of the aforementioned commercial adsorbents work well, even in a hybrid process. The goal of this chapter is to show via hybrid PSA-distillation process simulation that a hypothetical adsorbent that somehow combines the equilibrium properties of silica gel with the kinetic properties of 4A zeolite may work.

5.3 Experiments and Modeling

The hybrid PSA-distillation configuration for propane/propylene separation was

introduced in the last chapter and the details were also explained. Figure 4.1 depicts both the traditional industrial distillation and hybrid PSA-distillation process for propane/propylene separation with 4A zeolite as the adsorbent. Figure 5.1 shows the hybrid system with the hypothetical adsorbent in the PSA process. In the hybrid process, a PSA unit was connected to the middle part of the distillation column. The feed to PSA was a gas phase side stream of the distillation column, and the two product streams were sent back to distillation at different trays according to their compositions. In the PSA unit, 4A zeolite was used as the adsorbent, and simulations were done with different operating conditions. The distillation part of the hybrid process was simulated using Chemsep^{TM}, so was the traditional distillation. The total operating cost, including the cost in the partial condenser, reboiler and compressors, was calculated to see if the hybrid process could achieve some saving compared to the traditional distillation. The results showed that the saving was not significant due to average performance in the PSA unit. Thus, a more efficient adsorbent rather than 4A zeolite is needed to improve PSA performance. As mentioned in the introduction, several commercial adsorbents have been tested for propane/propylene separation. However, all of them require a high operating pressure ratio in the PSA unit due to low selectivity or working capacity, which results in the high compression costs. For this purpose, a hypothetical adsorbent was introduced which comprises the desirable properties of two commercial adsorbents, i.e., the kinetics of 4A zeolite and the equilibrium isotherms of silica gel.

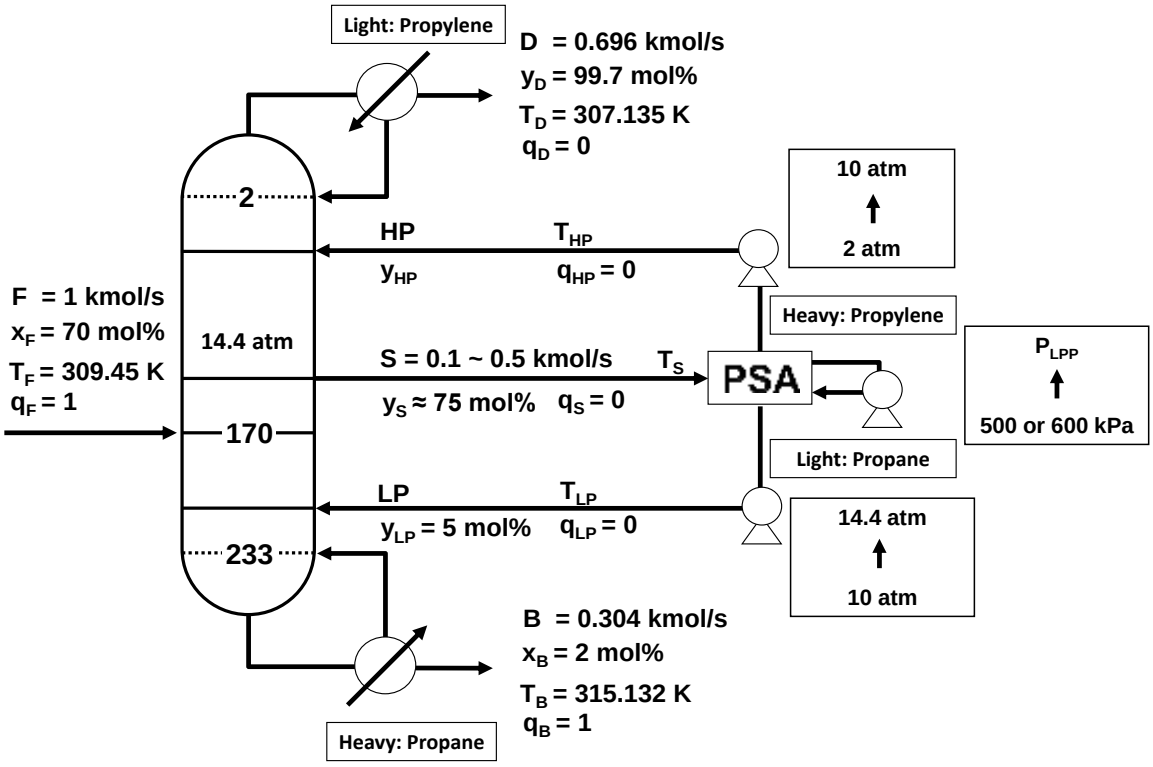

Figure 5.1 Hybrid PSA-distillation system for propane/propylene separation with the hypothetical adsorbent. *x* and *y* represents mole fraction of propylene in each stream.

The isotherms of propane and propylene on silica gel (40 grade provided by Grace Davison) were measured in the lab using microbalance. The experiment system is shown in Figure 5.2. The MK2-M5 pressure head was provided by Precision. The sample was put in the left goblet in the bed and glass beads were put in the right goblet for the balance. The bed was generated under vacuum overnight using a turbo pump at the operating temperature. Helium was used as inert gas and sent into the bed through the valves TV-3 and V-3. Several weight points were recorded by the data acquisition system in the pressure range from 0 kPa to about 330 kPa. The results were used as base to calculate the isotherms. The bed was vacuumed again and the runs were repeated at the same temperature with the working gas pure propane or propylene which was sent into the bed through the valves TV-2 and V-2. The weight points were recorded and the corresponding loadings were calculated. The isotherms were taken at three different temperatures, 80 C °, 100 C °and 120 C °, respectively for propane and propylene.

The experimental data were fitted to the 2-P Langmuir model, which is given by Eqs. 1 and 2.

$$q = \frac{q_{SA} b_A P}{1+b_A P} + \frac{q_{SB} b_B P}{1+b_B P} \quad (1)$$

$$b_A = b_{0A} \exp\left(\frac{\Delta H_A}{RT}\right) \quad (2)$$

where q is the equilibrium loading (mol/kg); q_s is the saturation loading (mol/kg); b_0 is the pre-exponential factor (1/kPa); ΔH is the isosteric heat of adsorption (kJ/mol). The values of these parameters are summarized in Table 5.1 and the results are shown in

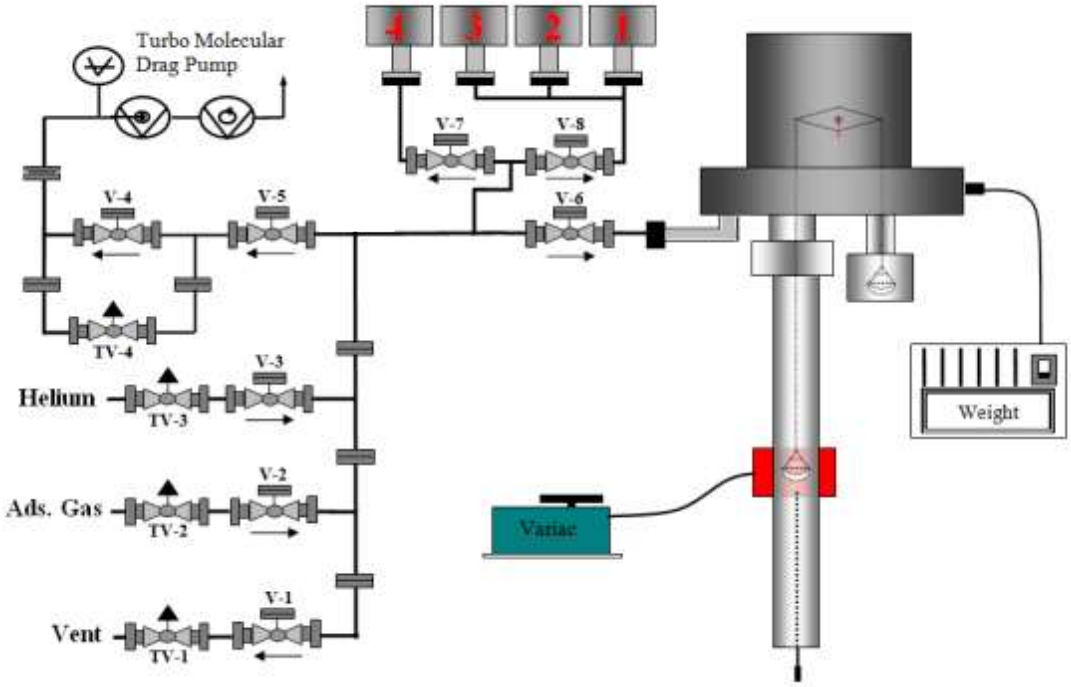

Figure 5.2 Microbalance system for measuring the isotherms of propane and propylene on silica gel at different temperatures.

Table 5.1 Isotherm parameters for propane and propylene on silica gel.

2-P Langmuir Isotherm Parameters	C_3H_8	C_3H_6
q_{SA} (mol/kg)	5.39	4.33
q_{SB} (mol/kg)	0.67	0.76
b_{0A} (1/kPa)	2.93×10^{-7}	4.06×10^{-7}
b_{0B} (1/kPa)	2.67×10^{-7}	9.95×10^{-8}
ΔH_A (kJ/mol)	-21.11	-21.81
ΔH_B (kJ/mol)	-28.00	-33.33

Figure 5.3. The circles, squares and triangles are experimental data and the lines are results obtained by fitting the experimental data to the 2-P Langmuir model. As shown in the figure, there is no big difference between the equilibrium loadings of propane and propylene in silica gel, thus the selectivity is small. So silica gel alone is not ideal adsorbent for propane/propylene separation. 4A zeolite also has very small selectivity; but propylene molecule diffuses into 4A zeolite faster than propane molecule, and the kinetic property difference results in the separation. However, it has very small working capacity, as shown in Figure 4.2. So the bed needs to be vacuumed to regenerate the adsorbent, requiring much compression cost. A hypothetical adsorbent is silica gel particle coated with a very thin film of 4A zeolite and its simple structure is depicted in Figure 5.4. The theory is to use 4A zeolite film to control the diffusion of propane and propylene and to utilize the working capacity of silica gel. The adsorption in 4A silica gel is negligible since the thickness of the film is less than 10μ.

In the pressure region of interest (200-1000kPa), 4A zeolite has a small working capacity, so a PSA unit requires vacuum for regeneration and thus higher compression costs. In contrast, the modified SG has a much larger working capacity in this pressure range. As a result, a PSA unit requires a smaller operating pressure ratio thus reducing compression costs. In the PSA process simulations, the hypothetical adsorbent has the adsorption properties of silica gel and kinetic properties of 4A zeolites. The mass transfer coefficients are given by

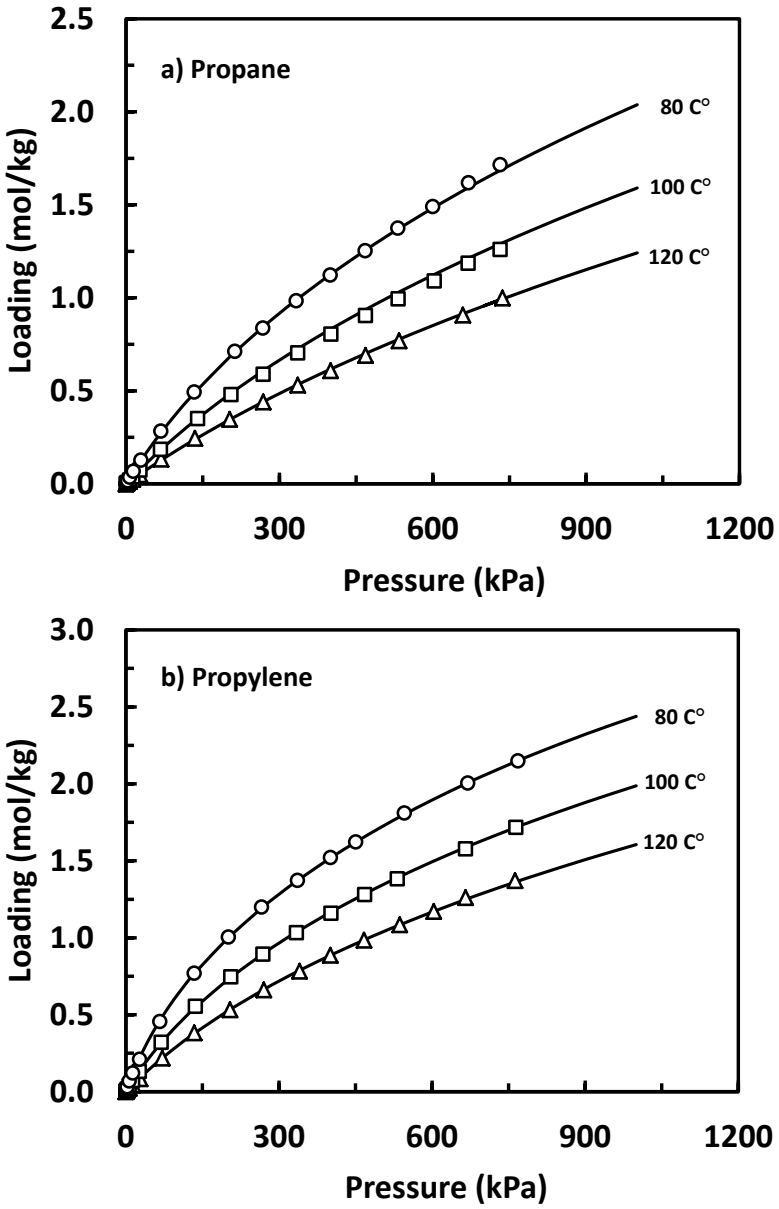

Figure 5.3 Adsorption isotherms of propane and propylene on silica gel at different temperatures. Circles, squares and triangles represent experimental data, and lines represent fits to 2-P Langmuir model.

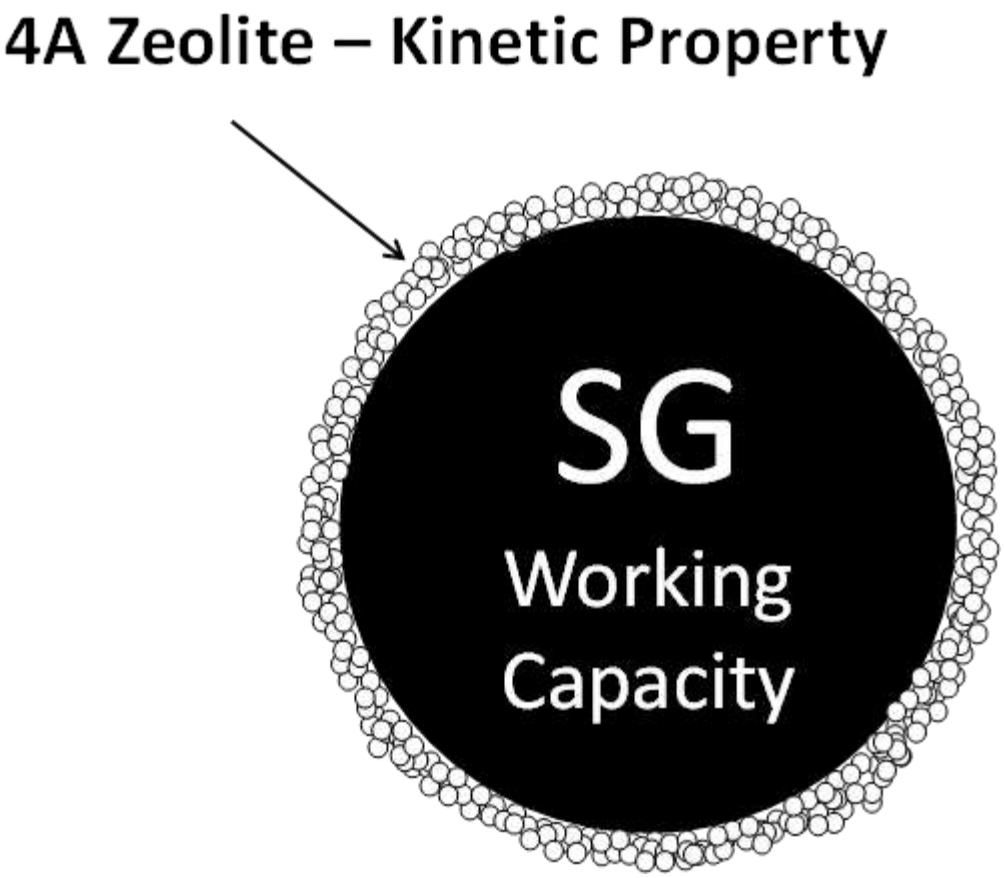

Figure 5.4 Structure of hypothetical adsorbent: silica gel particle coated with a film of 4A zeolite. Combination of silica gel's working capacity and 4A zeolite's kinetic property.

$$D_c = D_c^0 \exp(\frac{-E_a}{RT}) \quad (5)$$

$$k = \frac{15D_c}{r_c^2} \quad (6)$$

where D_c is the crystal diffusivity; D_c^0 is the limiting diffusivity at high temperatures; E_a is the activation energy; r_c is the crystal radius.

The PSA cycle used in the hybrid process is shown in Figure 5.5, which is a 5-bed 8-step cycle. The steps are feed (F), cocurrent depressurization (CoD), equalization one and two (EQ_1 and EQ_2), countercurrent depressurization (CnD) and light product pressurization (LPP). During F step, the high pressure flow was sent into the bed, and a downstream was coming out of the bed at the same time to keep the bed pressure constant. Then during CoD step, the valve at the feed end was closed and the bed was depressurized from the other end to a certain pressure. Light product was produced from the downstreams of F. Next, the bed was connected with low pressure beds at the light end to equalized the pressure twice, followed by CnD step from which heavy product was produced and the bed was depressurized through the heavy end to the low operating pressure. After equalized with high pressure beds, the bed was pressurized through the light end with some light product to the high operating pressure. The feed to the PSA unit was a vapor phase side stream of distillation containing 75 mol% propylene, and was at the high operating pressure. The high operating pressure was 10 atm and the low operating pressure was 2 atm, which was the pressure of the heavy product. Different operating temperatures, CoD end pressures and feed flow rates were investigated with

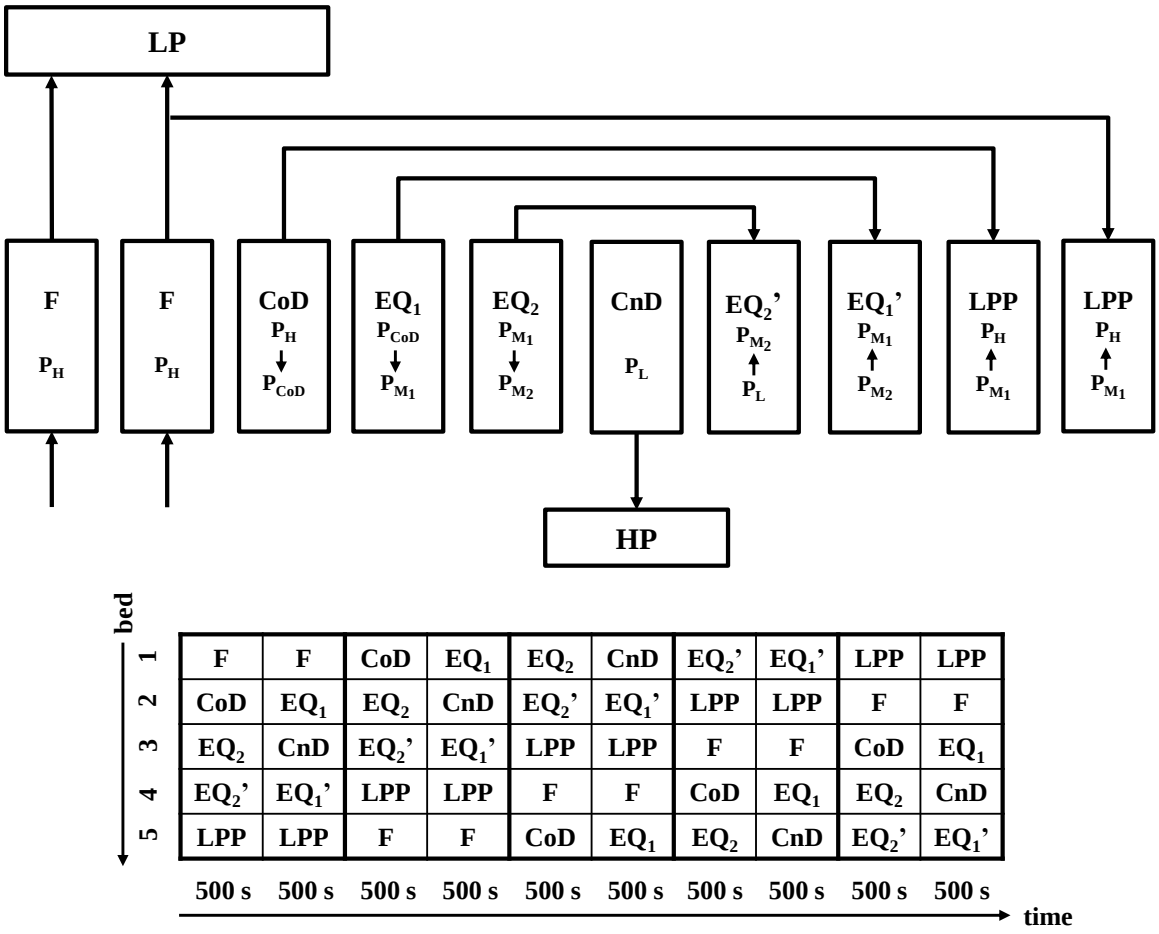

Figure 5.5 5-bed 8-step cycle schematic and schedule for propane propylene separation. F: feed step; EQ: equalization step; CoD: concurrent depressurization step; CnD: countercurrent depressurization step; LR: light reflux step; I: idle step; LPP: light product pressurization step.

12 PSA process simulations with silica gel as the adsorbent. The bed property, silica gel adsorbent property and operating conditions are summarized in Table 5.2. And 6 more simulations with 4A zeolite as the adsorbent were carried out as references. The adsorbent property is summarized in Table 4.1 in Chapter 4. The operating pressure in distillation was 14.4 atm, thus two compressors were used between the distillation column and the PSA unit. One was for compressing the heavy product stream from CnD from 2 to 14.4 atm, and the other was for compressing the light product steam from 10 to 14.4 atm. Another compressor was used to compress the downstream from CoD from the CoD end pressure to the pressure of the first part of LPP.

After getting the results from PSA simulations, the distillation process of the hybrid system was simulated using Chemsep^{TM} by considering the feed to PSA as a side stream and the product streams from PSA as two additional feed streams to the distillation column. The flow rates and compositions of these two additional feeds were obtained from the PSA simulation results. The flow rate of the side stream was determined by the feed flow rate ratio to PSA and distillation *S/F*, which represented the mass taken from distillation and sent to PSA, and also represented how much separation work was done by the PSA unit. The flow rate ratio *S/F* ranged from 0.1 to 0.5. Five distillation simulations were done respectively with each PSA simulation. Partial condenser and reboiler duties were obtained from distillation simulations and converted to operating cost according to the steam and cooling water prices in Table 2.3.

Table 5.2 PSA process simulation parameters and conditions used in the DAPS

Bed Properties		
length, Z (m)		0.87
outer radius, r_o (m)		0.0106
inner radius, r_i (m)		0.0105
porosity, ε_b		0.41
Wall Properties		
density, ρ_w (kg/m^3)		8238
thermal capacity, C_w (kJ/kg/K)		0.5
heat transfer coefficient, h (kW/m^2/K)		0 (adiabatic)
temperature, T_w (K)		353.15 or 393.15
Operating Conditions		
feed temperature, T_{PSA} (K)		353.15 or 393.15
high pressure, P_H (atm)		10
low pressure, P_L (atm)		2
CoD end pressure, P_{CoD} (kPa)		500 or 600
feed flow rate F_{PSA} (SLPM)		0.04;0.05;0.06
mole fraction of propylene in feed, y_S		0.75
Silica Gel Adsorbent Properties		
silica gel pellet radius, r_p (m)		0.0012
density, ρ_p (kg/m^3)		1260
porosity, ε_p		0.4
thermal capacity, C_p (kJ/kg/K)		1.13
4A Zeolite Kinetic Properties	C_3H_8	C_3H_6
activation energy, E_a (kJ/mol)	23.67	15.61
limiting diffusivity, D_c^0(m^2/s)	2.26×10^{-15}	4.66×10^{-14}

The compression duty was calculated from Eq. 7.

$$Q_C = \frac{\gamma}{\gamma-1} RT \left[\left(\frac{P_H}{P_L} \right)^{\frac{\gamma}{\gamma-1}} - 1 \right] \frac{1}{\eta} \dot{n} \tag{7}$$

where γ is the isentropic constant, which is 1.4; η = 0.8, which is the efficiency of the compressors; n is the flow rate of a stream, mol/s; and T is the absolute temperature of a stream. Electricity was assumed to be used in the compressors and the compression cost was calculated. The total operating cost was calculated by adding all the costs, however, the cost for heating and cooling the streams between distillation and PSA was not included, because heat integration is usually used in industry to save energy. Then the operating cost of the hybrid process was compared to that of the traditional distillation to study the potential of cost saving.

5.4 Results and Discussion

The simulation results are summarized in Table 5.3. Figure 5.6a shows the recovery and purity of propylene, and Figure 5.6b shows the recovery and purity of propane of all the simulations. The arrows at the bottom of the figures represent the direction of feed flow rate increasing (from 0.04 to 0.06 SLPM). The four curves in the upper right corner represent the results with the hypothetical adsorbent and the other two curves at the bottom represent the results with 4A zeolite. Larger feed flow rates and higher temperatures resulted in higher purity propylene, but lower propylene recovery. Reducing the CoD end pressure resulted in significant improvement in propylene purity while sacrificing some of

Table 5.3 PSA performance for propane/propylene separation with different operating conditions. Run 1-12: hypothetical adsorbent; Run 13-18: 4A zeolite.

	Operating Conditions			**Propylene (C_3H_6)**		**Propane (C_3H_8)**	
Run No.	**T_{PSA} (K)**	**P_{CoD} (kPa)**	**F_{PSA} (SLPM)**	**Recovery (%)**	**Purity (%)**	**Recovery (%)**	**Purity (%)**
1	353.15	600	0.04	98.80	84.76	47.73	91.71
2	353.15	600	0.05	98.22	88.59	62.41	91.51
3	353.15	600	0.06	94.90	92.26	76.81	81.64
4	353.15	500	0.04	98.77	86.18	52.38	93.66
5	*353.15*	*500*	*0.05*	*94.07*	*93.10*	*79.51*	*79.22*
6	353.15	500	0.06	89.29	95.94	88.41	70.45
7	393.15	600	0.04	98.77	86.18	52.38	93.66
8	393.15	600	0.05	97.25	90.67	70.31	88.59
9	*393.15*	*600*	*0.06*	*94.30*	*94.05*	*82.74*	*81.19*
10	393.15	500	0.04	96.98	90.77	70.27	87.53
11	*393.15*	*500*	*0.05*	*93.96*	*94.81*	*84.84*	*80.32*
12	393.15	500	0.06	88.08	97.30	92.53	70.33
13(4A)	353.15	600	0.04	57.50	78.38	52.47	32.64
14(4A)	353.15	600	0.05	46.37	78.40	61.54	28.12
15(4A)	353.15	600	0.06	38.55	78.35	68.31	26.45
16(4A)	393.15	600	0.04	67.92	83.29	58.94	39.27
17(4A)	393.15	600	0.05	55.04	83.31	66.80	32.63
18(4A)	393.15	600	0.06	46.08	83.32	72.33	29.25

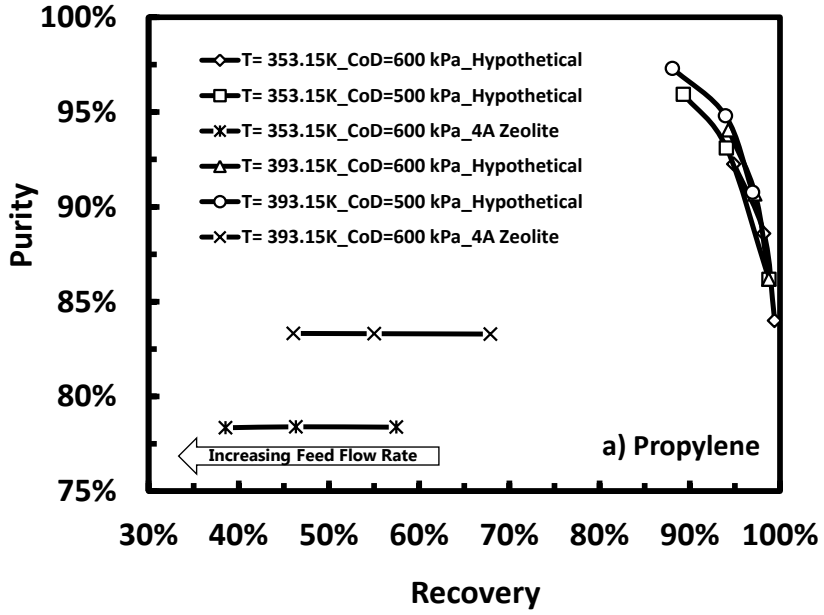

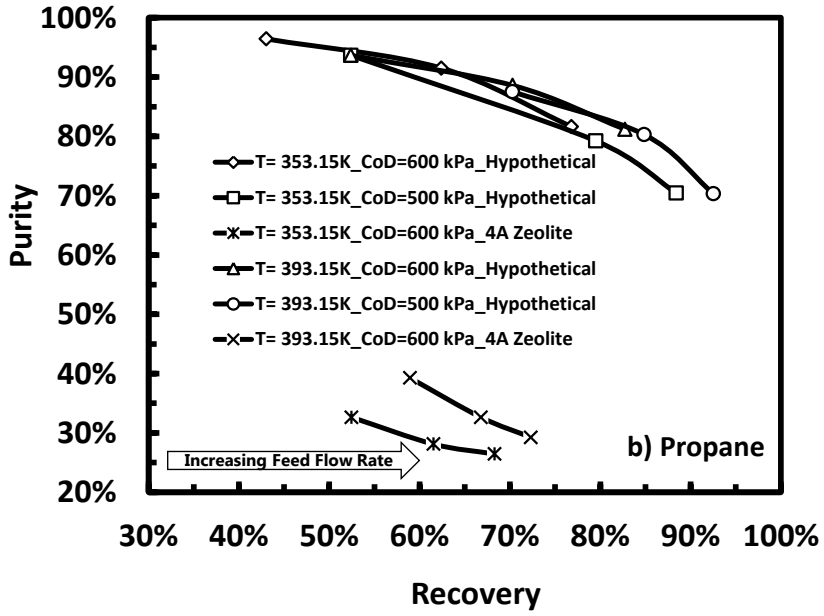

Figure 5.6 PSA simulation results with 4A zeolite and hypothetical adsorbent at different operating conditions.

its recovery. It is obvious that the simulations with the hypothetical silica gel resulted in much better performances than 4A zeolite, and the points close to the top right corner are the best ones. Three of the best results, which are italicized in Table 5.3, were selected for the hybrid PSA-distillation system. Another two cases with 4A zeolite as the adsorbent were selected to be as the references to be compared with the hypothetical adsorbent cases.

Twenty five distillation simulations, five for each PSA simulation, were carried out to get the duties in the partial condenser and reboiler, and the costs are shown in Figure 5.7. The x axil is the value of *S/F* and the zero point is for the reference case which is simple distillation. A larger value of *S/F* means that more separation is done by the PSA unit, which reduced the partial condenser and reboiler costs in the distillation unit. Operating temperature, CoD end pressure and PSA feed flow rate did not affect these costs in the cases with the hypothetical adsorbent. Not much cost difference was observed between the reference case and the cases with 4A zeolite as the adsorbent. Figure 5.8 shows the compression costs of the hybrid PSA-distillation processes with the hypothetical adsorbent and 4A zeolite as the adsorbent. Larger values of *S/F* required more costs because more mass was needed to be compressed. There were only minimal effects of the PSA operating conditions on these costs. No compression cost was required in the reference case which was shown as the zero point in the figure.

All these costs were combined and compared to the reference case in terms of the total operating cost savings. The results are shown in Figure 5.9. Figure 5.9a shows the

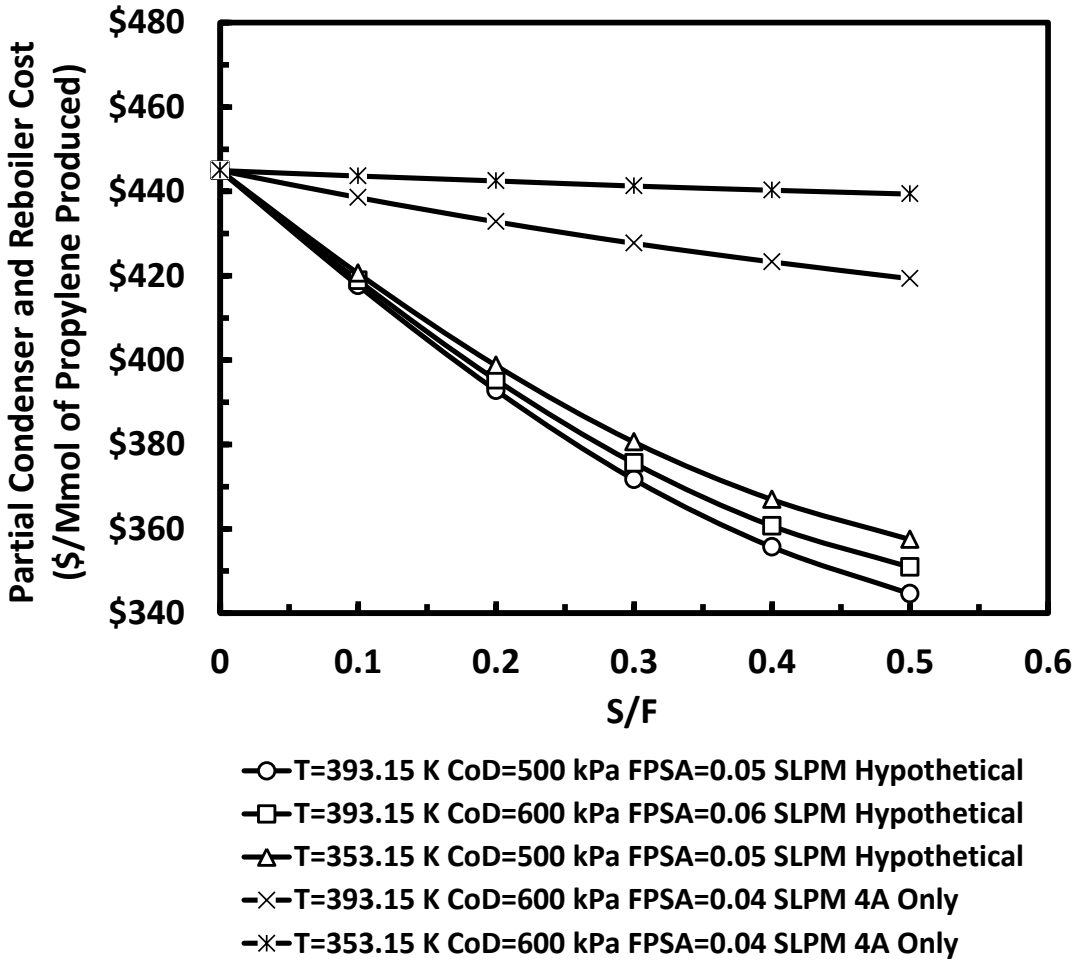

Figure 5.7 Partial condenser and reboiler costs of the hybrid PSA-distillation processes with hypothetical adsorbent or 4A zeolite as the adsorbent.

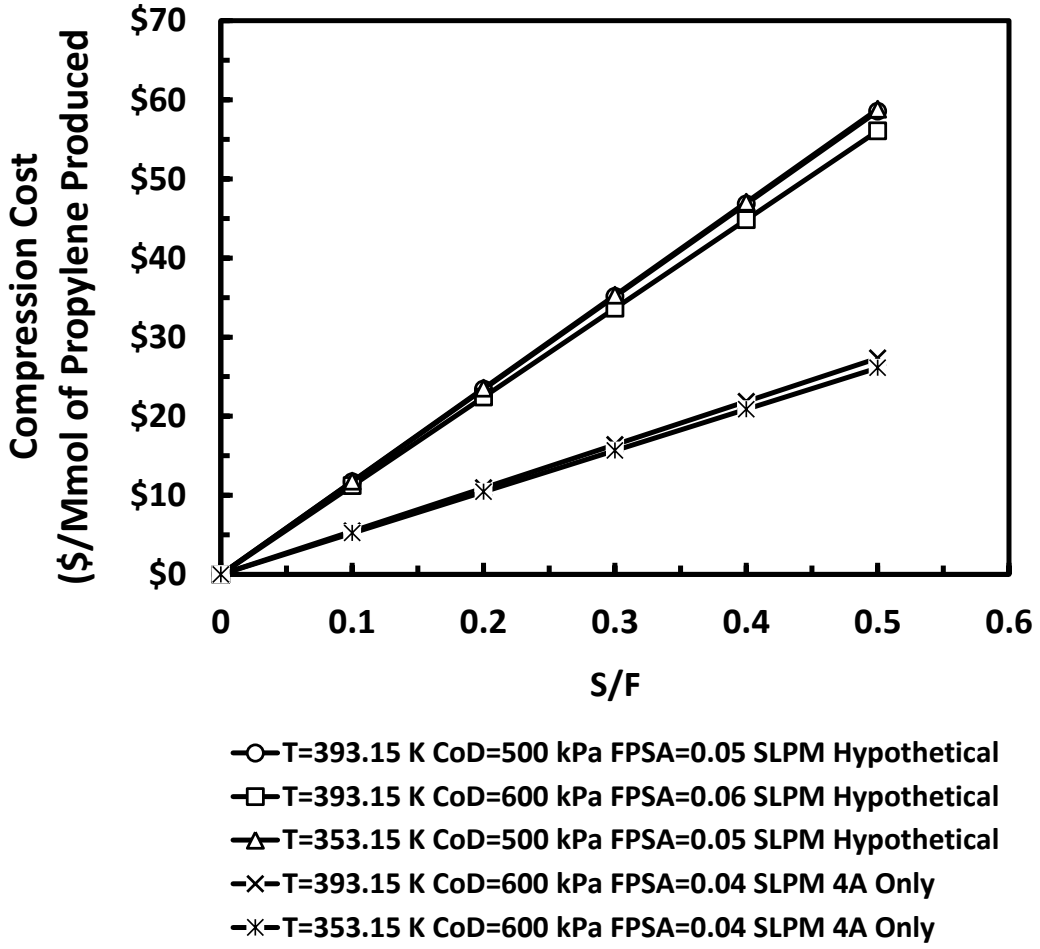

Figure 5.8 Compression costs of the hybrid PSA-distillation processes with hypothetical adsorbent or 4A zeolite as the adsorbent.

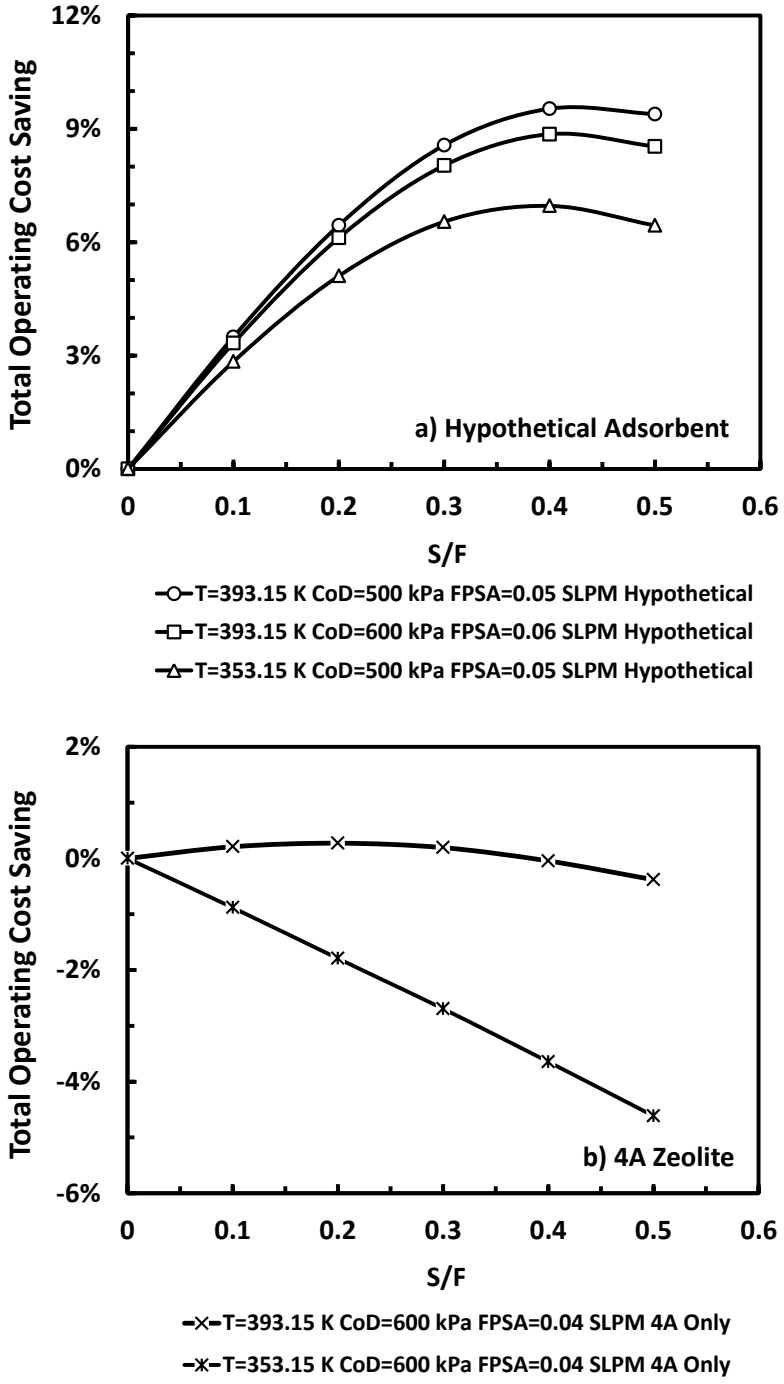

Figure 5.9 Total operating cost savings compared to the commercial distillation system for propane/propylene separation. a) cost savings in the cases with hypothetical adsorbent; b) cost savings in the cases with 4A zeolite as the adsorbent.

cost saving for the cases with hypothetical adsorbent in the PSA unit. The maximum saving was 9.53% at 393.15 K, 500 kPa CoD end pressure and 0.05 SLPM PSA feed flow rate with hypothetical adsorbent in the PSA unit. The cost savings increased with larger *S/F* value. Figure 5.9b shows the cost saving for the cases with 4A zeolite as the adsorbent in the PSA unit. The cost savings were little and even negative for most cases due to bad PSA performance.

5.5 Conclusion

A hypothetical adsorbent, which is silica gel particle coated with a thin film of 4A zeolite, was proposed and tested by simulating the PSA process. The isotherm of the hypothetical adsorbent was predicted from the silica gel experimental data and the mass transfer coefficients relations of 4A zeolite were used in the simulation. PSA simulations were done under different operating conditions, such as operating temperature, CoD end pressure and feed flow rate. Both hypothetical adsorbent and 4A zeolite was used in the simulations to compare the performance. The results showed that better PSA performance could be obtained with the hypothetical adsorbent. Also, because of the bigger working capacity of the hypothetical adsorbent than 4A zeolite, a smaller operating pressure ratio was used in the simulations compared to the ones in Chapter 4. Thus less compression cost was required. The PSA processes with the best performance were chosen to connect with a distillation column to build a hybrid system, and the distillation processes were simulated with different feed flow rate ratios to PSA and distillation. Two cases with 4A

zeolite as the adsorbent were also simulated to compare with the hypothetical adsorbent cases. The costs in the partial condenser, reboiler of distillation and compressors were calculated for all the hybrid systems with the selected PSA processes. The total operating cost was compared with the reference which is the commercial distillation and the results showed that this hypothetical adsorbent appears to do the job that commercial silica gel, 4A zeolite, 13X zeolite and carbon molecular sieve could not do. When combined with an efficient PSA cycle, this hypothetical adsorbent can be used in a PSA-distillation process to reduce energy costs by about 10%.

REFERENCES

1. Huang, Y. H.; Liapis, A. I.; Xu, Y.; Crosser, O. K.; Johnson, J. W. Binary Adsorption and Desorption Rates of Propylene-Propane Mixtures on 13X Molecular Sieves. *Separations Technology*. **1995**, *5*, 1-11
2. Da Silva, F. A.; Rodrigues, A. E. Adsorption Equilibria and Kinetids for Propylene and Propane over 13 X and 4A Zeolite Pellets. *Ind. Eng. Chem. Res.* **1999,** *38*, 2051-2057
3. Da Silva, F. A.; Rodrigues, A. E. Propylene/Propane Separation by Vacuum Swing Adsorption Using 13X Zeolite. *AIChE Journal*. **2001,** *47*, 341-357
4. Da Silva, F. A.; Rodrigues, A. E. Vacuum Swing Adsorption for Propylene/Propane Separation with 4A Zeolite. *Ind. Eng. Chem. Res.* **2001,** *40,* 5758-5774
5. Grande, C. A.; Gigola, C; Rodrigues, A. E. Propane-Propylene Binary Adsorption on Zeolite 4A. *Adsorption*, **2003**, *9*, 321-329
6. Grande, C. A.; Rodrigues, A. E. Adsorption Kinetics of Propane and Propylene in Zeolite 4A. *Chemical Engineering Research and Design.* **2004,** *82,* 1604-1612
7. Grande, C. A.; Basaldella, E.; Rodrigues, A. E. Crystal Size Effect in Vacuum Pressure-Swing Adsorption for Propane/Propylene Separation, *Ind. Eng. Chem. Res.*

2004, *43*, 7557-7565

8. Patino, I. M. E.; Aguilar, A. G.; Jimenez, L. A.; Rodriguez, C. E. Kinetics of the Total and Reversible Adsorption of Propylene and Propane on Zeolite 4A (CECA) at Different Temperatures. *Colloids and Surfaces A: Physicochem. Eng. Aspects.* **2004,** *237*, 73-77
9. Grande, C. A.; Cavenati, S.; Barcia, P.; Hammer, J.; Fritz, H. G.; Rodrigues, A. E. Adsorption of Propane and Propylene in Zeolite 4A Honeycomb Monolith. *Chemical Engineering Science* **2006,** *61*, 3053-3067
10. Granato, M. A.; Vlugt, T. J. H.; Rodrigues, A. E. Molecular Simulation of Propane-Propylene Binary Adsorption Equilibrium in Zeolite 4A. *Ind. Eng. Chem. Res.* **2007,** *46*, 32-328
11. Grande, C. A.; Poplow, F.; Rodrigues, A. E. Vacuum Pressure SWING Adsorption to Produce Polymer-Grade Propylene. *Separation Science and Technology* **2010,** *45*, 1252-1259
12. Grande, C. A.; Silva, V. M. T. M.; Gigola, C.; Rodrigues, A. E. Adsorption of Propane and Propylene onto Carbon Molecular. *Carbon* **2003,** *41*, 2533-2545
13. Grande, C. A.; Rodrigues, A. E. Adsorption of Binary Mixtures of Propane-Propylene in Carbon Molecular Sieve 4A. *Ind. Eng. Chem. Res.* **2004,** *43*, 8057-8065
14. Grande, C. A.; Cavenati, S.; Da Silva, F. A.; Rodrigues, A. E. Carbon Molecular Sieves for Hydrocarbon Separations by Adsorption. *Ind. Eng. Chem. Res.* **2005**, *44*,

7218-7227

15. Lewis, W. K.; Gilliland, E. R.; Chertow, B.; Hoffman, W. H. Vapor-Adsorbate Equilibrium. I. Propane-Propylene on Activated Carbon on Silica Gel. *J. Am. Chem. Soc.* **1950,** *72,* 1153-1157
16. Maslan, F.; Aberth, E. R.; Adsorption of Propane and Propylene on Silica Gel at Low Temperatures. *Journal of Chemical and Engineering Data* **1972,** *17,* 286-287
17. Jarvelin, H.; Fair, J. R. Adsorptive Separation of Propylene-Propane Mixtures. *Ind. Eng. Chem. Res.* **1993,** *32,* 2201-2207
18. Grande, C. A.; Rodrigues, A. E. Adsorption Equilibria and Kinetics of Propane and Propylene in Silica Gel. *Ind. Eng. Chem. Res.* **2001,** *40,* 1686-1693
19. Olivier, M. G.; Jadot, R. Adsorption of Light Hydrocarbons and Carbon Dioxide on Silica Gel. *J. Chem. Eng. Data* **1997,** *42,* 230-233

BIBLIOGRAPHY

Aspen Adsim 2004.1; Adsorption Reference Guide; Aspen Technology: Cambridge, MA, 2005.

Ausitakis, J. P.; Garg, D. R. Adsorption Separation Cycle. U. S. Patent **1983,** 4,373,935 .

Bausa, J.; Marquardt, W. Shortcut Design Methods for Hybrid Membrane/Distillation Processes for the Separation of Nonideal Multicomponent Mixtures. *Ind. Eng. Chem. Res.* **2000**, *39*, 1658-1672.

Bhadra, S. J.; Ebner, A. D. ;Ritter, J. A. On the Use of the Dual-Process Langmuir Model for Correlating Unary Equilibria and Predicting Mixed-Gas Adsorption Equilibira. *Langmuir*, **2012**, *28*, 6935-6941

Boonfung, C.; Rattanaphanee, P. Pressure Swing Adsorption with Cassava Adsorbent for Dehydration of Ethanol Vapor. *World Academy of Science, Engineering and Technology* **2010**, *71*, 637-640.

Bryan, P. F. Removal of Propylene from Fuel-Grade Propane. *Sep. Purif. Rev.* **2004,** *33*, 157-182.

Caputo, D.; Iucolano, F.; Pepe, F.; Colella, C. Modeling of Water and Ethanol Adsorption Data on a Commercial Zeolite-Rich Tuff and Prediction of the Relevant Binary Isotherms. *Microporous and Mesoporous Materials*, **2007**, *105*, 260-267.

Carmo, M. J.; Gubulin, J. C. Ethanol-Water Separation in the PSA Process. *Adsorption* **2002**, *8*, 235-248.

Collura, M. A.; Luyben, W. L. Energy-Saving Distillation Designs in Ethanol Production. *Ind. Eng. Chem. Res.* **1988**, *27*, 1686-1696.

Da Silva, F. A.; Rodrigues, A. E. Adsorption Equilibria and Kinetids for Propylene and Propane over 13 X and 4A Zeolite Pellets. *Ind. Eng. Chem. Res.* **1999,** *38*, 2051-2057

Da Silva, F. A.; Rodrigues, A. E. Propylene/Propane Separation by Vacuum Swing Adsorption Using 13X Zeolite. *AIChE Journal*. **2001,** *47*, 341-357

Da Silva, F. A.; Rodrigues, A. E. Vacuum Swing Adsorption for Propylene/Propane Separation with 4A Zeolite. *Ind. Eng. Chem. Res.* **2001,** *40*, 5758-5774

El-Bourawi, M. S.; Ding, Z.; and Ma, R.; Khayel, M. A Framework for Better Understanding Membrane Distillation Separation Process. *J. Mem. Sci.* **2006**, *285*, 4-29.

Eldridge, R. B. Olefin Paraffin Separation Technology: A Review. *Ind. Eng. Chem. Res.* **1993,** *32*, 2208-2212.

Eldridge, R. B.; Seibert, A. F.; Robinson, S. Hybrid Separations/Distillation Technology: Research Opportunities for Energy and Emissions Reduction. Work Performed Under Contract, U.S. Department of Energy, DOE Report, April 2005.

Esteves, I. A. A. C.; Mota, J. P. B. Simulation of a New Hybrid Membrane/Pressure Swing Adsorption Process for Gas Separation. *Desalination* **2002**, *148*, 275-280. Fan, Z. L.; Lynd L. R. Conversion of Paper Sludge to Ethanol, II: Process Design and Economic Analysis. *Biopro. Biosyst. Eng.* **2007**, *30*, 35-45.

Ethanol Production Process. *Comp. Chem. Eng.* **2008**, *32*, 1635-1649

Feng, X. S.; Pan, C. Y.; Ivory, J. Pressure Swing Permeation: Novel Process for Gas Separation by Membranes. *AIChE J.* **2000**, *46*, 724-733.

Feng, X. S.; Pan, C. Y.; Ivory, J.; Ghosh, D. Integrated Membrane/Adsorption Process for Gas Separation. *Chem. Eng. Sci.* **1998**, *53*, 1689-1698.

Fukada, S. Tritium Isotope Separation by Water Distillation Column Packed with Silica-Gel Beads. *J. Nuclear Sci. Technol.* **2004**, *41*, 619-623.

Ghosh, T. K.; Lin, H. D.; Hines, A. l. Hybrid Adsorption Distillation Process for Separating Propane and Propylene. *Ind. Eng. Chem. Res.* **1993**, *32*, 2390-2399.

Ginder, W. F. Method of Removing Water from Ethanol. U. S. Patent **1983,** 4,407,662.

Gokhale, V.; Hurowitz, S.; Riggs, J. B. A Comparison of Advanced Distillation Control Techniques for a Propylene/Propane Splitter. *Ind. Eng. Chem. Res.* **1995**, *34*, 4413-4419

Granato, M. A.; Vlugt, T. J. H.; Rodrigues, A. E. Molecular Simulation of Propane-Propylene Binary Adsorption Equilibrium in Zeolite 4A. *Ind. Eng. Chem. Res.* **2007,** *46*, 32-328

Grande, C. A.; Basaldella, E.; Rodrigues, A. E. Crystal Size Effect in Vacuum Pressure-Swing Adsorption for Propane/Propylene Separation, *Ind. Eng. Chem. Res.* **2004**,

43, 7557-7565

Grande, C. A.; Cavenati, S.; Barcia, P.; Hammer, J.; Fritz, H. G.; Rodrigues, A. E. Adsorption of Propane and Propylene in Zeolite 4A Honeycomb Monolith. *Chemical Engineering Science* **2006,** *61*, 3053-3067

Grande, C. A.; Cavenati, S.; Da Silva, F. A.; Rodrigues, E. Carbon Molecular Sieves for Hydrocarbon Separations by Adsorption. *Ind. Eng. Chem. Res.* **2005,** *44*, 7218-7227

Grande, C. A.; Gigola, C; Rodrigues, A. E. Propane-Propylene Binary Adsorption on Zeolite 4A. *Adsorption*, **2003**, *9*, 321-329

Grande, C. A.; Poplow, F.; Rodrigues, A. E. Vacuum Pressure SWING Adsorption to Produce Polymer-Grade Propylene. *Separation Science and Technology* **2010,** *45*, 1252-1259

Grande, C. A.; Rodridues, A. E. Adsorption of Binary Mixtures of Propane-Propylene in Carbon Molecular Sieve 4A. *Ind. Eng. Chm. Res.* **2004,** *43*, 8057-8065

Grande, C. A.; Rodrigues, A. E. Adsorption Equilibria and Kinetics of Propane and Propylene in Silica Gel. *Ind. Eng. Chem. Res.* **2001,** *40*, 1686-1693

Grande, C. A.; Rodrigues, A. E. Adsorption Kinetics of Propane and Propylene in Zeolite 4A. *Chemical Engineering Research and Design* **2004,** *82*, 1604-1612

Grande, C. A.; Rodrigues, A. E. Propane/Propylene Separation by Pressure Swing Adsorption Using Zeolite 4A. *Ind. Eng. Chem. Res.* **2005**, *44*, 8815-8829

Grande, C. A.; Silva, V. M. T. M.; Gigola, C.; Rodrigues, A. E. Adsorption of Propane and Propylene onto Carbon Molecular Sieve. *Carbon.* **2003,** *41*, 2533-2545

Guan, J.; Hu, X. Simulation and Analysis of Pressure Swing Adsorption: Ethanol Drying Processes by the Electrical Analogue. *Separation and Purification Technology* **2003**, *31*, 31-35.

Haelssig, J. B.; Tremblay, A. Y.; Thibault, J. Technical and Economic Considerations for Various Recovery Schemes in Ethanol Production by Fermentation. **2008**, *47*, 6185-6191.

Hoch, P. M.; Espinosa, J. Design of a Hybrid Distillation-Pervaporation Bio-Ethanol Purification Process Using Conceptual Design and Rigorous Simulation Tools. *AIChE Annual Meeting* **2008**, 316a.

Huang, Y. H.; Liapis, A. I.; Xu, Y.; Crosser, O. K.; Johnson, J. W. Binary Adsorption and Desorption Rates of Propylene-Propane Mixtures on 13X Molecular Sieves. *Separations Technology*. **1995**, *5*, 1-11

Huang, Z.; Shi, Y.; Wen, R.; Guo, Y. H.; Su, J. F.; Matsuura, T. Multilayer Poly(Vinyl Alcohol)-Zeolite 4A Composite Membranes for Ethanol Dehydration by Means of Pervaporation. *Sep. Purif. Technol.* **2006,** *51*, 126-136.

Humphrey, J. L.; Koort, R.; Seibert, A. F. Separation Technologies-Advances and Priorities. Work Performed Under Contract No. AC07-90ID12920, U.S. Department of Energy, DOE Report, February 1991.

Jarvelin, H.; Fair. J. R. Adsorptive Separation of Propylene-Propane Mixtures. *Ind. Eng. Chem. Res.* **1993,** *32*, 2201-2207

Jeong, J. S.; Jang, B. U.; Kim, Y. R.; Chung, B. W.; Choi, G. W. Production of Dehydrated Fuel Ethanol by Pressure Swing Adsorption Process in the Pilot Plant. *Korean J. Chem. Eng.* **2009**, *26*, 1308-1312.

Knaebel, K. S.; Reinhold, H. E. Landfill Gas: From Rubbish to Resource. *Adsorption-J. Inter. Adsorption Soc.* **2003**, *9*, 87-94.

Krishnamurthy R.; Maclean, D. L. Method and Apparatus of Producing Carbon Dioxide in High Yields from Low Concentration Carbon Dioxide Feeds. U. S. Patent **1990**, 4,952,223.

Kumar, R.; Golden, T.C.; White, T.R.; Rokicki, A. Novel Adsorption Distillation Hybrid Scheme for Propane Propylene Separation. *Sep. Sci. Technol.* **1992,** *27*, 2157-2170.

Kumar R.; Kleinberg W. T. Integrated Adsorption/Cryogenic Distillation Process for the Separation of an Air Feed. *U. S. Patent* **1995**, 5,463,869.

Kumins, L, Parker L.; Yacobucci, B. Refining capacity-challenges and opportunities facing the U.S. industry. Report, Petroleum Industry Research Foundation, Inc," 2004.

Laurance, D. R; Swift, G. W. Relative Volatility of Propane-Propylene System from 100-160. deg. F. *J. Chem. Eng. Data.* **1972**, *17*, 333-337

Lee, C. H.; and Hong, W. H. Effect of Operating Variables on the Flux and Selectivity in Sweep Gas Membrane Distillation for Dilute Aqueous Isopropanol. *J. Mem. Sci.* **2001**, *188*, 79-86.

Lei, Z. G.; Li, C. Y.; Chen, B. H. Extractive Distillation: A Review. *Sep. Purif. Rev.* **2003**,

32, 121-213.

Lewis, W. K.; Gilliland, E. R.; Chertow, B.; Hoffman, W. H. Vapor-Adsorbate Equilibrium. I. Propane-Propylene on Activated Carbon and on Silica Gel. *J. Am. Chme. Soc.* **1950,** *72*, 1153-1157

Lewis, W. K.; Gilliland, E. R.; Chertow, B.; Hoffman, W. H. Vapor-Adsorbate Equilibrium. I. Propane-Propylene on Activated Carbon on Silica Gel. *J. Am. Chem. Soc.* **1950,** *72*, 1153-1157

Madson, P. W.; Monceaux, D. A. Fuel Ethanol Production. *KATZEN International, Inc.* **2003**.

Maslan, F.; Aberth, E. R. Adsorption of Propane and Propylene on Silica Gel at Low Temperatures. *Journal of Chemical and Engineering Data*, **1972,** *17*, 286-287

Mehrotra, A.; Ebner, A. D.; Ritter, J. A. Arithmetic Approach for Complex PSA Cycle Scheduling. *Adsorption*, **2010**, 16, 113-116.

Moganti, S.; Noble, R. D.; Koval, C. A. Analysis of a Membrane Distillation Column Hybrid Process. *J. Mem. Sci.* **1994**, *93*, 31-44.

Mujiburohman, M.; Sediawan, W. B.; Sulistyo, H. A Preliminary STudy: Distillation of Isopropanol-Water Mixture Using Fixed Adsorptive Distillation Method. *Sep. Purif. Technol.* **2006**, *48*, 85-92.

Nguyen, T. C.; Baksh, M. S. A.; Bonaquist, D. P.; Weber, J. A. Cryogenic Hybrid System for Producing High Purity Argon. U. S. Patent **1998**, 5,730,003.

Nomura, M.; Yamaguchi, T.; Nakao, S. Ethanol/Water Transport through Silicalite Membranes. *J. Mem. Sci.* **1998,** *144*, 161-171.

Olivier, M. G.; Jadot, R. Adsorption of Light Hydrocarbons and Carbon Dioxide on Silica Gel. *J. Chem. Eng. Data* **1997,** *42*, 230-233

Parthan, W.; Noble, R. D.; Koval, C. A. Design Methodology for a Membrane Distillation Column Hybrid Process. *J. Mem. Sci.* **1995**, *99*, 259-272.

Patino, I. M. E.; Aguilar, A. G.; Jimenez, L. A.; Rodriguez, C. E. Kinetics of the Total and Reversible Adsorption of Propylene and Propane on Zeolite 4A (CECA) at Different Temperatures. *Colloids and Surfaces A: Physicochem. Eng. Aspects.* **2004,** *237*, 73-77

Pettersen, T.; Argo, A.; Noble, R. D.; Koval, C. A. Design of Combined Membrane and

Distillation Processes. *Sep. Technol.* **1996**, *6*, 175-187.

Pressly, T. G.; and Ng, K. M. A Break-Even Analysis of Distillation-Membrane Hybrids. *AIChE J.* **1998**, *44*, 93-105.

Pruksathorn, P.; Vitidsant, T. Production of Pure Ethanol from Azeotropic Solution by Pressure Swing Adsorption. *American J. of Engineering and Applied Sciences* **2009**, *2*, 1-7.

Qariouh, H.; Schue, R.; Schue, F.; Bailly, C. Sorption, Diffusion and Pervaporation of Water/Ethanol Mixtures in Polyetherimide Membranes. *Polym. Inter.* **1999,** *48*, 171-180.

Quintero, J. A.; Montoya, M. I.; Sanchez, O. J.; Giraldo, O. H.; Cardona, C. A. Fuel Ethanol Production from Sugarcane and Corn: Comparative Analysis for a Columbian Case. *Energy* **2008**, *33*, 383-399.

Ramachandran R.; Dao L. H. Method of Producing Unsaturated Hydrocarbons and Separating the Same from Saturated Hydrocarbons. U. S. Patent **1994**, 5,365,011.

Reynolds, S. P.; Ebner, A.D.; Ritter, J.A. Stripping PSA Cycles for CO_2 Recovery from Flue Gas at High Temperature Using a HTlc Adsorbent. *Ind. Eng. Chem. Res.* **2006**, *45*, 4278-4294.

Ritter, J. A.; Wu, F.; Ebner, A. D. New Approach for Modeling Hybrid PSA-Distillation Processes. *Ind. Eng. Chem. Res.* **2012,** *51*, 9343-9355

Robinson, S.; Jubin, R. Materials for Separation Technologies: Energy and Emission Reduction Opportunities. Work Performed Under Contract No. DE-AC05-00OR22725, U.S. Department of Energy, DOE Report, May 2005.

Sano, T.; Yanagishita, H.; Kiyozumi, Y.; Mizukami, F.; Haraya, K. Separation of Ethanol-Water Mixture by Silicalite Membrane on Pervaporation. *J. Mem. Sci.* **1994**, *95*, 221-228.

Simo, M.; Brown, C. J.; Hlavacek, V. Simulation of Pressure Swing Adsorption in Fuel Ethanol Production Process. *Computers and Chemical Engineering* **2008**, *32*, 1635-1649.

Simo, M.; Sivashanmugam, S. Brown, C. J.; Hlavacek, V. Adsorption/Desorption of Water and Ethanol on 3A Zeolite in Near-Adiabatic Fixed Bed. **2009**, *48*, 9247-9260.

Sircar, S.; Waldron, W.E.; Rao, M. B.; Anand, M. Hydrogen Production by Hybrid SMR-PSA-SSF Membrane System. *Sep. Purif. Technol.* **1999**, *17*, 11-20.

Skarstrom, C. W. Combination Process Comprising Distillation Operation in Conjunction with a Heatless Fractionator. U. S. Patent **1964**, 3,122,486.

Smitha, B.; Suhanya, D.; Sridhar, S.; and Ramakrishna M. Separation of Organic-Organic Mixtures by Pervaporation – A Review. *J. Mem. Sci.* **2004,** *241*, 1-21.

Suk, D. E.; and Matsuura, T. Membrane-Based Hybrid Processes: A Review. *Sep. Sci. Technol.* **2006**, *41*, 595-626.

Szitkai, Z.; Lelkes, Z.; Rev, E.; Fonyo, Z. Optimization of Hybrid Ethanol Dehydration Systems. *Chem. Eng. Process.* **2002,** *41*, 631-646.

Vane, L. M. Separation Technologies for the Recovery and Dehydration of Alcohols from Fermentation Broths. *Biofuels, Bioprod. Bioref.* **2008**, *2*, 553-588.

Van Hoof, V.; Dotremont, C.; Buekenhoudt, A. Performance of Mitsui NaA Type Zeolite Membranes for the Dehydration of Organic Solvents in Comparison with Commercial Polymeric Pervaporation Membranes. *Sep. Purif. Technol.* **2006,** *48*, 304-309.

Van Hoof, V.; Van den Abeele, L.; Buekenhoudt, A.; Dortemont, C.; Leysen, R. Economic Comparison Between Azeotropic Distillation and Different Hybrid Systems Combining Distillation with Pervaporation for the Dehydration of Isopropanol. *Sep. Purif. Technol.* **2004,** *37*, 33-49.

Westphal.; K. G. G. Combined Adsorption-Rectification Method for Separating a Liquid Mixtures. International Patent. DE3 **2007**, 712,291.

Wu, F.; Ebner, A. D.; Ritter, J. A. Improved PSA Cycles of Hybrid Pressure Swing Adsorption-Distillation Process for Ethanol Dehydration. To be submitted.

http://tonto.eia.doe.gov/dnav/pet/pet_pnp_top.asp: Data, Energy Information Administration.

http://www.eia.doe.gov/pub/oil_gas/petroleum/analysis_publications/oil_market_basics/refining_text.htm: Refining, Annual Energy Review.

http://www.ethanolrfa.org/pages/annual-industry-outlook: RFA's 2012 Ethanol Industry Outlook.